VOLUME 37 JANUARY 1959 NUMBER 1

Canadian Journal of Physics

Published by THE NATIONAL RESEARCH COUNCIL

OTTAWA CANADA

CANADIAN JOURNAL OF PHYSICS

Under the authority of the Chairman of the Committee of the Privy Council on Scientific and Industrial Research, the National Research Council issues THE CANADIAN JOURNAL OF PHYSICS and five other journals devoted to the publication, in English or French, of the results of original scientific research. Matters of general policy concerning these journals are the responsibility of a joint Editorial Board consisting of: members representing the National Research Council of Canada; the Editors of the Journals; and members representing the Royal Society of Canada and four other scientific societies.

Manuscripts for publication should be submitted to Dr. H. E. Duckworth, Editor, Canadian Journal of Physics, Hamilton College, McMaster University, Hamilton, Ontario.
For instructions on preparation of copy, see **NOTES TO CONTRIBUTORS** (back cover).

Proof, correspondence concerning proof, and orders for reprints should be sent to the Manager, Editorial Office (Research Journals), Division of Administration and Awards, National Research Council, Ottawa 2, Canada.

Subscriptions, renewals, requests for single or back numbers, and all remittances should be sent to Division of Administration and Awards, National Research Council, Ottawa 2, Canada. Remittances should be made payable to the Receiver General of Canada, credit National Research Council.

The journals published, frequency of publication, and prices are:

Canadian Journal of Biochemistry and Physiology	Monthly	$9.00 a year
Canadian Journal of Botany	Bimonthly	$6.00 a year
Canadian Journal of Chemistry	Monthly	$12.00 a year
Canadian Journal of Microbiology	Bimonthly	$6.00 a year
Canadian Journal of Physics	Monthly	$9.00 a year
Canadian Journal of Zoology	Bimonthly	$5.00 a year

The price of regular single numbers of all journals is $2.00.

VOLUME 37 1959

Canadian Journal of Physics

Published by THE NATIONAL RESEARCH COUNCIL

OTTAWA CANADA

Canadian Journal of Physics

Issued by THE NATIONAL RESEARCH COUNCIL OF CANADA

VOLUME 37 JANUARY 1959 NUMBER 1

GENETIC MEASUREMENT OF THE HALF LIFE OF Bi^{207} [1]

J. SOSNIAK[2] AND R. E. BELL

ABSTRACT

The half life of Bi^{207} has been measured by the genetic method, using the parent–daughter pair Po^{207} and Bi^{207}. Both activities are electron capturers, and the measured half life depends only on the activity ratio between them. The value found, $T_{1/2} = 28 \pm 3$ years, agrees with one of three previous determinations of this half life.

INTRODUCTION

It is necessary to know the half life of Bi^{207} in order to make measurements of activation cross sections of reactions leading to Bi^{207}, such as Pb^{208} $(p, 2n)$. Previous measurements of this half life by different workers had led to discordant values. We now report the result of a measurement by a genetic method, leading to the result $T_{1/2} = 28 \pm 3$ years.

In the first detailed work on Bi^{207}, Neumann and Perlman (1951) estimated the half life both by a genetic method involving the α-decay of At^{211}, and by Geiger counting sources of Bi^{207} over a period of 2.75 years. The first method yielded a value of 50 years, and the second, showing no perceptible decay, suggested a lower limit of 40 years. Neumann and Perlman therefore quoted the value 50 years without assigning a probable error.

Harbottle (1955 and private communication) used a balanced double ionization chamber, standardized with radium, to observe the decay of Bi^{207} over a period of 3 months. His value for the half life was $27 \pm (2 \text{ or } 3)$ years.

Cheng *et al.* (1955) observed the decay of a sample of long lived bismuth activity for a period of 11 years, and found a half life of 8.0 ± 0.6 years. A scintillation spectrum of this source appeared to be "identical with that of the 50 year Bi^{207}". This result clearly disagrees with the results of the other investigators.

EXPERIMENTAL METHOD

The present measurement emerges from a study of the radioactive chain

$$Po^{207}\text{—EC}\rightarrow Bi^{207}\text{—EC}\rightarrow Pb^{207} \text{ (stable)}.$$

[1]Manuscript received August 18, 1958.
Contribution from the Radiation Laboratory, Department of Physics, McGill University, Montreal, Canada.

[2]Now at Department of Physics, University of Western Ontario, London, Canada.

A measured amount of pure Po^{207} is allowed to decay completely ($T_{1/2} = 5.7$ hours), and the amount of Bi^{207} activity that grows from it is measured. The ratio of the two activities is equal to the inverse ratio of their half lives, and the half life of Bi^{207} is thus determined. The essence of the experiment is just the measurement of the ratio of two similar electron capture activities. In the actual experiment the K X-rays emitted by the two activities were counted with a sodium iodide crystal and a 28-channel analyzer. The K X-rays form a very clean peak (actually two peaks because of the escape effect in NaI) in the scintillation spectrum, easily separable from the effects of any gamma rays.

The intrinsic efficiency of the sodium iodide counter is close to unity for the K X-rays, and it only remains to estimate the number of K X-rays emitted per disintegration of Po^{207} and Bi^{207}. This question has been discussed for a number of electron capturers, including Po^{207}, by Bell and Skarsgard (1956). Their conclusion was that the ratio of K capture to total electron capture from all shells could not be far from 1:1.33. This conclusion could be upset only for an electron capturer whose decay energy was low enough to be comparable with the K electron binding energy of the atom, but in the case of Po^{207} an estimate exists for the total decay energy, 2.80 ± 0.45 Mev (Gray 1955). We thus conclude that there are 0.75 K shell vacancies per electron capture process in Po^{207}. Additional K shell vacancies may arise from K conversion of gamma rays following the electron capture process. If a complete table of gamma ray intensities and conversion coefficients were at hand, this contribution could be worked out. Alternatively, as shown by Bell and Skarsgard, the contribution may be measured by detecting K–K X-ray coincidences from the source by detecting the "sum peak" in the scintillation spectrum of a weak source placed close to the counter. Their measurement for Po^{207} showed that the number of K X-rays was increased by 9% owing to internal conversion. The total number of K shell vacancies per disintegration of Po^{207} therefore becomes 0.82.

For Bi^{207}, a complete disintegration scheme is available from the work of Alburger and Sunyar (1955), including a close estimate of the decay energy; for one of the electron capture branches this energy is so low that only L and higher shell capture occurs. With the help of the compilation of Brysk and Rose (1955), the ratio of K to total electron capture is found to be 1:1.54 for the sum of all the electron capture branches, leading to the figure of 0.65 K vacancies per disintegration. The effect of K conversion of gamma rays is computed from Alburger and Sunyar's work to add 0.11 to this figure, giving a total of 0.76 K vacancies per disintegration. The counting efficiencies for Bi^{207} and Po^{207} are therefore very nearly equal, being in the ratio 0.76:0.82. Effects of Auger transitions cancel between the two activities, and absorption within the sources is eliminated from consideration by making the sources of Bi^{207} and Po^{207} physically identical.

The Po^{207} parent material was produced by the reaction Bi^{209} $(p, 3n)$ in the McGill synchrocyclotron. Bismuth trioxide powder was wrapped in 0.0005 in. aluminum foil to form a strip-like target 0.007 in. thick, and bombarded in

the circulating beam with about 1 microampere-hour of 24 Mev protons. According to the cross-section curves of Bell and Skarsgard (1956), the maximum yield would have occurred at about 30 Mev, but the lower energy was preferred in order to minimize the formation of 9-day Po^{206} by the $(p, 4n)$ reaction. The bombardment also produces some Bi^{207} directly by the $(p, p2n)$ reaction; the chemical procedure described below removed this component. In addition, there would be appreciable production of the 2.9-year Po^{208} by the $(p, 2n)$ reaction; fortunately, however, Po^{208} emits relatively few X-rays and its presence does not affect our measurements.

A few minutes after the end of the bombardment, the Po^{207} was separated from the active bismuth trioxide powder by a simple chemical procedure. The objects of this separation were to get rid of the bulk of the bombarded material, and to avoid the Bi^{207} formed during the bombardment either by the $(p, p2n)$ reaction or by the decay of Po^{207}. The active powder was dissolved in hydrochloric acid to which a few milligrams of tellurium carrier had been added. The addition of a few drops of stannous chloride precipitated the tellurium, carrying the Po^{207} activity with it. The Po^{207} separation was considered to have taken place at the moment of formation of this precipitate. The precipitate was then centrifuged off and redissolved in hydrochloric acid. This simple procedure sufficed for the purpose because most of the detectable active atoms present in the target were Po^{207} in the first place.

On account of the large ratio of the half lives, about 40,000:1, the initial Po^{207} sample was much too strong to be counted in direct comparison with the eventual Bi^{207} daughter. Instead, the Po^{207} solution was diluted three times by successive factors of 10, producing a nominal dilution factor of 1000. Polonium activity is notorious for its tendency to adhere to glass surfaces, and in the dilution procedure polyethylene utensils were used, except for glass graduated pipettes. Each step in the dilution was checked by counting the Po^{207} activities, and the counting results, rather than the volumetric measurements, were always accepted as representing the true dilution. The discrepancy was sometimes as high as 16%. The result of the dilution procedure was a set of four identical polyethylene bottles each holding 5 ml of solution, the first one containing 0.9 of the original amount of Po^{207}, and the last (nominally) 10^{-3} of the original amount. The actual counting comparison then involved the Po^{207} in the weakest sample and the Bi^{207} formed by the decay of the strongest sample; the activity ratio between these two samples was about 40:1, so that they could be counted in the same geometry.

The weakest Po^{207} sample was counted at once in direct contact with a 1.5 in. $\times$ 1 in. sodium iodide crystal. Its 5.7-hour decay was followed for a few hours, and the counting rate was extrapolated back to the moment of chemical separation. The strong source was allowed to stand for several days to allow the Po^{207} to decay to Bi^{207}, and then counted in the same manner as the Po^{207}. The Bi^{207} sample was checked for the absence of the 9-day Po^{206} over a period of some days, and checked again after some weeks or months to show that the Bi^{207} sample was not showing any decay faster than that expected for a half life of several years.

RESULTS

Three complete experiments were performed giving three numerical values for the half life of Bi^{207}, viz. 24.3, 29.7, and 29.2 years. The average of the three values is 27.7 years with a root mean square deviation in the average of ± 1.4 years. This deviation is of little value as an estimate of the real error in the result. We have considered the errors in the various factors entering into the experiment, and estimate a probable error of about 10% for them all. This error would be higher if it were not for the way in which many uncertain factors cancel for the two sources being compared. We therefore give for the result of the experiment,

$$T_{1/2}\,(Bi^{207}) = 28 \pm 3 \text{ years.}$$

This result agrees very well with that of Harbottle (1955), and is not in strong contradiction with the early work of Neumann and Perlman (1951). The value of Cheng *et al.* for the half life, 8 years, remains as before, unexplained.

REFERENCES

BELL, R. E. and SKARSGARD, H. M. 1956. Can. J. Phys. **34**, 745.
BRYSK, H. and ROSE, M. E. 1955. Oak Ridge National Laboratory Report 1830.
CHENG, L. S., RIDOLFO, V. C., POOL, M. L., and KUNDU, D. N. 1955. Phys. Rev. **98**, 231.
GRAY, P. R. 1955. University of California Radiation Laboratory Report 3104.
HARBOTTLE, G. 1955. *Quoted by* ALBURGER, D. E. and SUNYAR, A. W. Phys. Rev. **99**, 695.
NEUMANN, H. M. and PERLMAN, I. 1951. Phys. Rev. **81**, 958.

POISSON BRACKETS IN FIELD THEORY[1]

HANS FREISTADT

ABSTRACT

Poisson brackets for covariant field theory are defined in such a way as to demonstrate the close connection and ready transition between the classical brackets and the corresponding commutators of quantum theory. The approach of Good is followed in general; but the questions of tensor algebra are handled differently, requiring the introduction of a family of space-like surfaces and their normals. As an illustration, the free Klein-Gordon and Dirac fields are worked out.

INTRODUCTION

It is our purpose in this paper to develop a Poisson bracket (P.B.) formalism for classical covariant field theory, in such a way as to permit ready passage to quantum theory. Hamiltonian formalisms for classical field theory have been much neglected, except for the work of Bergmann (1949) and his disciples, and that of Good (1954). Treatises on quantum field theory (e.g. Wentzel 1943; Schweber, Bethe, DeHoffmann 1955) rarely go beyond the Lagrangian formalism; then they recall that in quantum mechanics, commutation relations between momenta and co-ordinates are introduced, and proceed to do likewise for the fields. The P.B., the classical source of the commutation relations, are usually not even mentioned, let alone developed. More recent approaches (Jauch and Rohrlich 1955) forsake the Hamiltonian formalism altogether, deriving commutation relations from an action principle. However, if one wishes to write out explicitly the (functional) Schrödinger equation for the quantized field system, from there to pass to the Hamilton-Jacobi formulation and to the non-linear modification of the original field equations (Freistadt 1956), the development of a covariant Hamiltonian formalism is rather necessary. The recovery of the field equations from the equations of motion in quantum mechanical P.B. form is usually the only method available for ascertaining whether a proposed Hamiltonian density deserves confidence as a description of the system under consideration. This is especially so in those cases in which the Hamiltonian does not follow from the Lagrangian in the elementary way, as in the Dirac field.

Bergmann (1949) does treat P.B. in detail; but his approach is based on a "parameter formalism", the effect of which is that field momentum densities are of the same tensor rank as the field variables to which they are conjugate. Without implying any criticism of Bergmann's approach, we do not follow it here; rather, we let our momentum densities be of one higher tensor rank than the corresponding field variables (four momentum symbols for every field variable), following in this respect the procedure first introduced by Born (1934) and Weyl (1934), and subsequently used by Schwinger (for

[1]Manuscript received August 20, 1958.

Contribution from the Faculty of Medicine, The University of British Columbia. Author's postal address: 5507 Fairview Avenue, Vancouver 8, B.C. Presented to the American Physical Society meeting at Vancouver, August 26, 1958 (Bull. Am. Phys. Soc. Ser. II, **3**, 317 (1958)).

which see Jauch and Rohrlich 1955) and Good (1954). The latter's purely classical Hamiltonian formalism is entirely adequate, and is, in fact, somewhat more elegant than ours. However, Good's formalism is not a convenient starting point for Hamiltonian quantization, in which P.B. are replaced by commutators (or anticommutators). To begin with, Good's P.B., unlike commutators, are not antisymmetric, i.e. $(u, v)_\mu \neq -(v, u)_\mu$. Another difficulty derives from the tensor rank of Good's P.B., $(u, v)_\mu$, which, unlike the commutator, is one higher than the product of the variables involved, because of differentiation with respect to the momentum densities. This is avoided here by a contraction with the normal unit vector to a family of space-like surfaces, assumed to be given. In our procedure, the P.B. (say, of field variables and their conjugate momenta) have the usual values of quantum mechanical commutators (except for trivial factors); this permits almost automatic quantization.

Our definition of P.B. is thus dependent on the particular family of space-like surfaces chosen. However, measurements (at least in flat space-time—very little is known about measurements in curved space) always involve quantities (such as momentum, energy) which are the result of an integration over a space-like surface. This is especially true in the quantized theory, in which measurements pertain to a system of particles. In the course of such an integration, the explicit dependence on the family of space-like surfaces disappears. This is the usual state of affairs in quantum theory. Good's formalism is not tied to such a family of space-like surfaces; that is perhaps the reason which renders it unsuitable for quantization.

Our formalism is entirely covariant and couched in the language of geometrical objects in space–time; the latter is not assumed to be flat. However, the components of the metric tensor are not treated as field variables; our treatment therefore does not cover the theory of gravitation.

An earlier attempt (Freistadt 1957) based on a tensor Hamiltonian density, appears to be less satisfactory than the present modification of Good's approach.

NOTATION AND REVIEW OF EARLIER WORK

As in our earlier papers (1955, hereafter quoted as CFHJ, and 1956, quoted as QFHJ), the field variables are denoted by y^A; they are functions of the space–time co-ordinates ξ^μ, which are not required to be Cartesian. The metric $g_{\mu\nu}$ is assumed to be given. The dynamical behavior of the fields is obtained, as usual, from a variational principle, $\delta W = 0$, where $W = (1/c)\int L\, d\omega$, and $d\omega$ is a scalar volume element of integration in space–time. The Lagrangian density $L(y^A, y^B{}_\mu, \xi^\nu)$ is a scalar function. The symbol $y^A{}_\mu$ means $\nabla_\mu y^A$, the covariant derivative of the field variables. There is assumed to be given a continuous family of non-intersecting, but not necessarily plane, space-like surfaces. The symbol $d\sigma_\mu$ is an element of integration on one such surface. The unit normal at each space–time point to the space-like surface passing through that point is indicated by n^μ. The momentum densities are defined by $\pi_A{}^\mu = \partial L/\partial y^A{}_\mu$, and the Hamiltonian density by

$$H(y, \pi) = L - y^A{}_\alpha \pi_A{}^\alpha, \tag{1}$$

provided the elimination of the $y^A{}_\mu$ is possible. (Hereafter, as in eq. (1), the indices are omitted where y, π, ξ appear as arguments.)

The Hamiltonian equations of motion are those of Good,

$$\begin{aligned} y^A{}_\mu &= -\partial H/\partial \pi_A{}^\mu, \\ \nabla_\alpha \pi_A{}^\alpha &= \partial H/\partial y^A \end{aligned} \tag{2}$$

(except for a trivial change in sign, traceable to the definition of the Hamiltonian, and consistent with earlier papers).

CLASSICAL POISSON BRACKETS

The classical P.B. of two variables, $u\,(y, \pi)$ and $v\,(y, \pi)$, at the same space–time point, is defined by

$$(u, v) = n^\alpha [(\partial u/\partial \pi_C{}^\alpha)(\partial v/\partial y^C) - (\partial u/\partial y^C)(\partial v/\partial \pi_C{}^\alpha)]. \tag{3}$$

For instance,

$$(\pi_A{}^\mu, y^B) = n^\mu \delta_A{}^B. \tag{4}$$

The P.B. so defined has all the usual algebraic properties (see, for example, Dirac 1947); in particular, $(u, v) = -(v, u)$, a result which is useful when passing to quantum theory.

In the definition of P.B. of quantities at different points on a space-like surface, a functional derivative is used. It is defined as

$$\delta u(\xi)/\delta v(\xi') = \partial u/\partial v\, \delta(\xi - \xi') \tag{5}$$

where $\partial u/\partial v$ is the formal derivative, and $\delta(\xi - \xi')$ is a three-dimensional delta function, meant to be integrated over a space-like surface. Note that, as usual, the functional derivative does not have the same dimensions as the formal derivative.

We now introduce

$$\begin{aligned} (u(\xi), v(\xi')) &= \int n^\alpha \left(\frac{\delta u(\xi)}{\delta \pi_C{}^\alpha(\xi'')} \frac{\delta v(\xi')}{\delta y^C(\xi'')} - \frac{\delta u(\xi)}{\delta y^C(\xi'')} \frac{\delta v(\xi')}{\delta \pi_C{}^\alpha(\xi'')} \right) n^\beta(\xi'')\, d\sigma_\beta(\xi''), \\ &= \int (u, v)\, \delta(\xi - \xi'')\, \delta(\xi' - \xi'')\, n^\beta(\xi'')\, d\sigma_\beta(\xi''), \\ &= (u, v)\, \delta(\xi - \xi'). \end{aligned} \tag{6}$$

For instance,

$$(\pi_A{}^\mu(\xi),\ y^B(\xi')) = \delta_A{}^B \delta^\mu(\xi - \xi') \tag{7}$$

where

$$\delta^\mu(\xi - \xi') = n^\mu \delta(\xi - \xi'),$$

i.e.

$$\int f(\xi')\, \delta^\alpha(\xi - \xi')\, d\sigma_\alpha(\xi') = f(\xi),$$

as defined in QFHJ and also in Jauch and Rohrlich (1955).

EQUATIONS OF MOTION

Proceeding as in Good (1954), one verifies directly that, $K(y, \pi)$ being a dynamical field variable,

$$\begin{aligned} \partial K/\partial y^A &= n_\alpha(\pi_A{}^\alpha, K) \\ n^\alpha(\partial K/\partial \pi_A{}^\alpha) &= -(y^A, K) \end{aligned} \tag{8}$$

from which it follows (by letting $K = H$, and referring to eq. (2)) that the Hamiltonian equations of motion can be written in the form

$$\begin{aligned} n^\alpha y^A{}_\alpha &= (y^A, H) \\ \nabla_\alpha \pi_A{}^\alpha &= n_\alpha (\pi_A{}^\alpha, H). \end{aligned} \tag{9}$$

The first of these equations is formally a contraction with n^μ of the first of eqs. (2); but it is identical with it, in view of the completely arbitrary choice of the family of space-like surfaces. Equations (9), in the quantum mechanical form (eqs. (12) below) are used in quantum field theory to test whether a Hamiltonian is the correct one to use. Equations analogous to (9) and (12) are well known in the literature of quantum field theory, though nowhere, as far as we know, do they appear in this completely covariant form.

QUANTIZATION

Passage to quantum theory is now effected in the usual Hamiltonian way by defining the quantum mechanical P.B.

$$i\hbar c(u, v)_{\text{qm}} = [u, v]_\pm \tag{10}$$

where the brackets on the right-hand side mean, as usual, the commutator $[\ ]_-$ or the anticommutator $[\ ]_+$, to be used depending on the spin of the field in question, except that in the equations of motion (9) the quantum mechanical P.B., as is well known, is always the commutator. The quantum mechanical P.B. are then assigned exactly the same values as the classical P.B., which gives, for instance, for the commutator (or anticommutator)

$$[\pi_A{}^\mu(\xi), y^B(\xi')] = i\hbar c \delta_A{}^B \delta^\mu(\xi - \xi'), \tag{11}$$

that is, the expression used in Jauch and Rohrlich (1955) and in QFHJ.

Then the test for the suitability of a Hamiltonian density in quantum field theory consists in verifying whether eq. (9) in quantum mechanical form, i.e.

$$\begin{aligned} n^\alpha y^A{}_\alpha &= (i\hbar c)^{-1}[y^A, H]_- \\ \nabla_\alpha \pi_A{}^\alpha &= (i\hbar c)^{-1} n_\alpha [\pi_A{}^\alpha, H]_- \end{aligned} \tag{12}$$

reproduce the field equations of the theory in question. As is well known, in applying the usual algebraic identities to the quantum mechanical P.B., the order of the factors, which are now quantum mechanical operators, must be kept in mind. In the two examples below, each term in the Hamiltonian density H consists of two factors, and the right hand side of eq. (12) is expanded by the familiar identity $[a, bc]_- = [a, b]_\pm c - b[c, a]_\pm$.

THE FREE KLEIN-GORDON FIELD

From the usual Lagrangian density (see, for example, CFHJ), one obtains, by eq. (1), the Hamiltonian density

$$H_{\mathrm{KG}} = \tfrac{1}{2}m_0c^2\psi^*\psi + 2\kappa(\hbar c)^{-1}\pi^{*\alpha}\pi_\alpha. \tag{13}$$

From the first of eq. (12), applied to ψ and ψ^*, one obtains the usual definition of the momentum densities (see CFHJ), while the second of eq. (12), applied to π^μ and $\pi^{*\mu}$, yields the Klein-Gordon field equations for ψ and ψ^*. (Note that the result is $(\nabla_\alpha\nabla^\alpha + \kappa)\psi = 0$, since we use the signature $(-1, -1, -1, 1)$.)

THE FREE DIRAC FIELD

The Hamiltonian density here cannot be obtained from the Lagrangian density (see CFHJ) by the usual method; but various conjectures suggest

$$H_{\mathrm{D}} = -\tfrac{1}{4}i\kappa\pi^\alpha\gamma_\alpha\psi. \tag{14}$$

That this is, in fact, a suitable Hamiltonian density is seen from the application of (12). Only one non-vanishing momentum density is left, obtained from the Lagrangian formalism (CFHJ). The first of eq. (12) leads to the Dirac equation $(i\gamma^\alpha\nabla_\alpha + \kappa)\psi = 0$, while the second leads to its adjoint $i\nabla_\alpha\psi_{\mathrm{adj}}\gamma^\alpha - \kappa\psi_{\mathrm{adj}} = 0$.

ACKNOWLEDGMENT AND DEDICATION

A grant-in-aid from the Sigma Xi – RESA Research Fund is gratefully acknowledged.

It is a privilege to dedicate this paper to my distinguished teacher, Nathan Rosen, now at Haifa, on the occasion of his fiftieth birthday, March 22, 1959.

REFERENCES

BERGMANN, P. G. and BRUNINGS, J. H. M. 1949. Revs. Modern Phys. **21**, 480.
BORN, M. 1934. Proc. Roy. Soc. (London), A, **143**, 410.
DIRAC, P. A. M. 1947. The principles of quantum mechanics (Oxford at the Clarendon Press).
FREISTADT, H. 1955. Phys. Rev. **97**, 1158.
——— 1956. Phys. Rev. **102**, 274.
——— 1957. Bull. Am. Phys. Soc. Ser. II, **2**, 143.
GOOD, R. H., Jr. 1954. Phys. Rev. **93**, 239.
JAUCH, J. M. and ROHRLICH, F. 1955. The theory of photons and electrons (Addison-Wesley Publishing Co., Inc., Cambridge, Mass.).
SCHWEBER, S. S., BETHE, H. A., and DEHOFFMANN, F. 1955. Mesons and fields, Vol. I (Row, Peterson and Co., Evanston, Ill.).
WENTZEL, G. 1943. Einführung in die Quantentheorie der Wellenfelder (Franz Deuticke, Wien).
WEYL, H. 1934. Phys. Rev. **46**, 505.

CANADIAN STANDARD OF FREQUENCY[1]

S. N. KALRA,[2] C. F. PATTENSON,[3] M. M. THOMSON[4]

ABSTRACT

Over the past 3 years a frequency standard of very high precision has been installed in Canada. It is composed of equipment located in three different laboratories in Ottawa, Ontario, but separated by a few miles. Intercomparison of frequency between these laboratories, which is done by sending signals over telephone lines and related techniques, is briefly described. Results indicate frequency stability of about $2:10^{10}$ over short and long periods. Absolute frequency is determined from astronomical observations. International intercomparison is carried out by phase measurement of standard frequency and by observations of time signals; some of the results are presented.

INTRODUCTION

The interest in accurate measurement of frequency has increased recently because of the advances in atomic and molecular physics, and in radio communication and navigation. In physical measurements the need for accurate frequency determination and the measurement of time intervals is of long standing. Most national laboratories, including our own, have had frequency standards for a long time. However, the increase in accuracy to about $1:10^{10}$ is comparatively recent. In this paper we will attempt a brief description of the steps taken in Canada to achieve a highly precise and stable standard of frequency.

Since the definition of time is so intimately connected with the definition of frequency the definition of one without the other is not practicable. The National Research Council and the Dominion Observatory in Ottawa, therefore, work in close co-operation. All astronomical observations are carried out at the Dominion Observatory. Three laboratories, namely, the Division of Applied Physics and the Radio and Electrical Engineering Division of the National Research Council and the Division of Positional Astronomy of the Dominion Observatory jointly compose and maintain the Canadian Standard of Frequency.

APPARATUS

In this paper features common to the three laboratories will be described. The apparatus may be divided into three parts: (1) crystal oscillators, (2) intercomparison and monitoring equipment, and (3) astronomical observations. The three laboratories are situated in Ottawa at a distance of 4 to 6 miles from one another. Intercomparison among these laboratories is made by transmitting standard frequency signals over telephone wires.

[1]Manuscript received September 9, 1958.
Contribution from the Divisions of Applied Physics and Radio and Electrical Engineering, National Research Council, and the Dominion Observatory, Ottawa, Canada.
Issued as N.R.C. No. 4990.
[2]National Research Council, Division of Applied Physics, Ottawa, Canada.
[3]National Research Council, Division of Radio and Electrical Engineering, Ottawa, Canada.
[4]Dominion Observatory, Division of Positional Astronomy, Ottawa, Canada.

The crystal oscillators used as reference oscillators at 100 kc each consist of an Essen type quartz ring cut in the Z plane and mounted on silk suspensions (Essen 1951), an oven and a resistance bridge type of oven control (Booth and Laver 1942), bridge stabilized oscillator (Booth and Laver 1946), and the required power supplies. These oscillators are protected against electrical mains failure by quick-starting emergency mains power supplies. All the crystal units were made by the British Post Office Radio Research Laboratories and the oscillators obtained earlier were also made by them. In the oscillators obtained at a later date the circuitry was made by Messrs. Airmec Limited under licence. These units are mounted so that they operate free from shock and vibration and are maintained at a constant ambient temperature. Since they are used as reference standards their frequencies are never adjusted and on some of the units the frequency trimmer capacitor has been left out. The physical distribution of these oscillators is as follows: Applied Physics Division has four, Radio and Electrical Engineering Division has three, and the Dominion Observatory has two. In addition to these units each laboratory has a number of other oscillators of various manufacture which are used for other purposes.

Each laboratory has its own monitoring equipment. Usually two types of records are kept. The frequencies of all the oscillators are intercompared

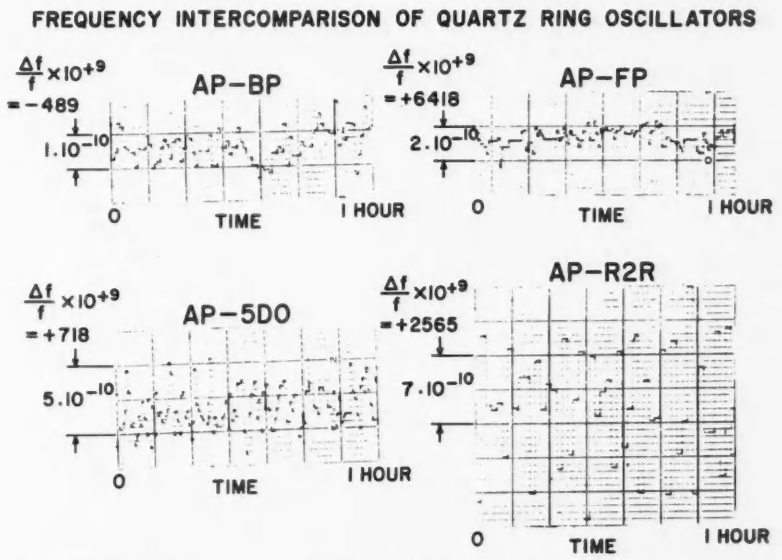

FIG. 1. Spot frequency measurements. Oscillators AP, BP, and FP are located at the Division of Applied Physics, 5DO at the Dominion Observatory, and R2R at the Division of Radio and Electrical Engineering. Measurements are made at the Division of Applied Physics laboratories. The actual fractional difference of frequency expressed in parts per 10^9 $\{(\Delta f/f)\times 10^9 = -\}$ is listed in the top left corner of each graph. The notation on the left gives the scale in each case.

daily using integrating periods of a few seconds each, i.e. spot frequency measurements. The crystal oscillators used as clocks are also monitored for net time gained or lost between different clocks for each successive 24-hour period. From this the 24-hour average frequency is also derived. Beat counters of commercial manufacture are normally used for integrating the number of beats between different sets of crystal oscillators. Accuracy of intercomparison of crystal clocks is about $5:10^{11}$ when using a 24-hour integrating period. This can be increased to about $5:10^{12}$ if the need arises. The accuracy for spot frequency measurements is usually better than $1:10^{10}$ and this can also be increased if the need arises. Figure 1 shows typical results of spot frequency measurements.

The reference frequency signal obtained from the quartz crystal oscillators at 100 kc is divided down to 1 c.p.s. by electronic circuitry. The lower frequencies serve as reference time intervals in addition to being reference frequencies. The signals at 1 c.p.s. serve as clocks and the astronomical observations and other standard time measurements are made with reference to them. Frequency multipliers are used for obtaining higher reference frequencies. Figure 2 shows a photograph of the main part of the installation at the Division of Applied Physics.

In certain types of equipment, e.g. the oven for the crystal, it is essential to maintain continuity of a-c. mains supply. Such units are protected against mains failure by automatic emergency mains supplies with switching and starting times of a fraction of a second. This helps in maintaining stability of operation and continuity of record. The crystal oscillators are protected against variation of loading by means of isolating amplifiers. Other precautions are taken to ensure stability of operation and long operating life of components.

ASTRONOMICAL OBSERVATIONS

The unit of time, the second, formerly was defined as a fraction of the period of rotation of the earth, and as such suffered the same irregularities that were inherent in the rate of rotation of the earth. It is now related to the time, which is the independent variable in the definition of the motion of the earth about the sun, and is designated as Ephemeris Time. The second of time is defined (C.I.P.M. 1957) as the fraction 1/31 556 925.974 7 of the tropical year 1900 January 0 at 1200 hours Ephemeris Time (E.T.). The year referred to is the year for which this date is the middle. For the physical realization of this definition two types of observations are usually made. They are (i) the meridian passage of the stars which yields Universal Time (U.T.2); and (ii) the position of the moon with respect to the stars which yields ΔT (see equation 1). At the Dominion Observatory, stellar transits are observed with a Photographic Zenith Telescope (Thomson 1955) and the lunar observations are made with a Markowitz Moon Camera (Markowitz 1954; Thomson 1958). Figure 3 shows a photograph of this equipment. U.T.2 is a good approximation to a uniform time scale, but is affected by small and unpredictable variations in the period of rotation of the earth which amount to

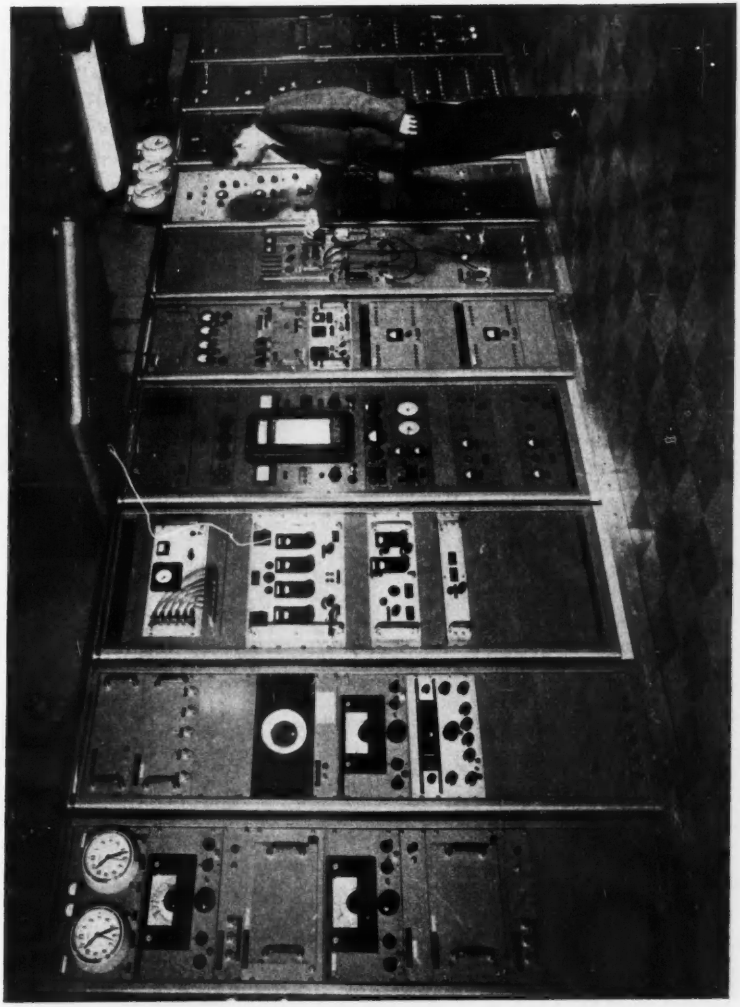

FIG. 2. Main part of the installation at the Division of Applied Physics.

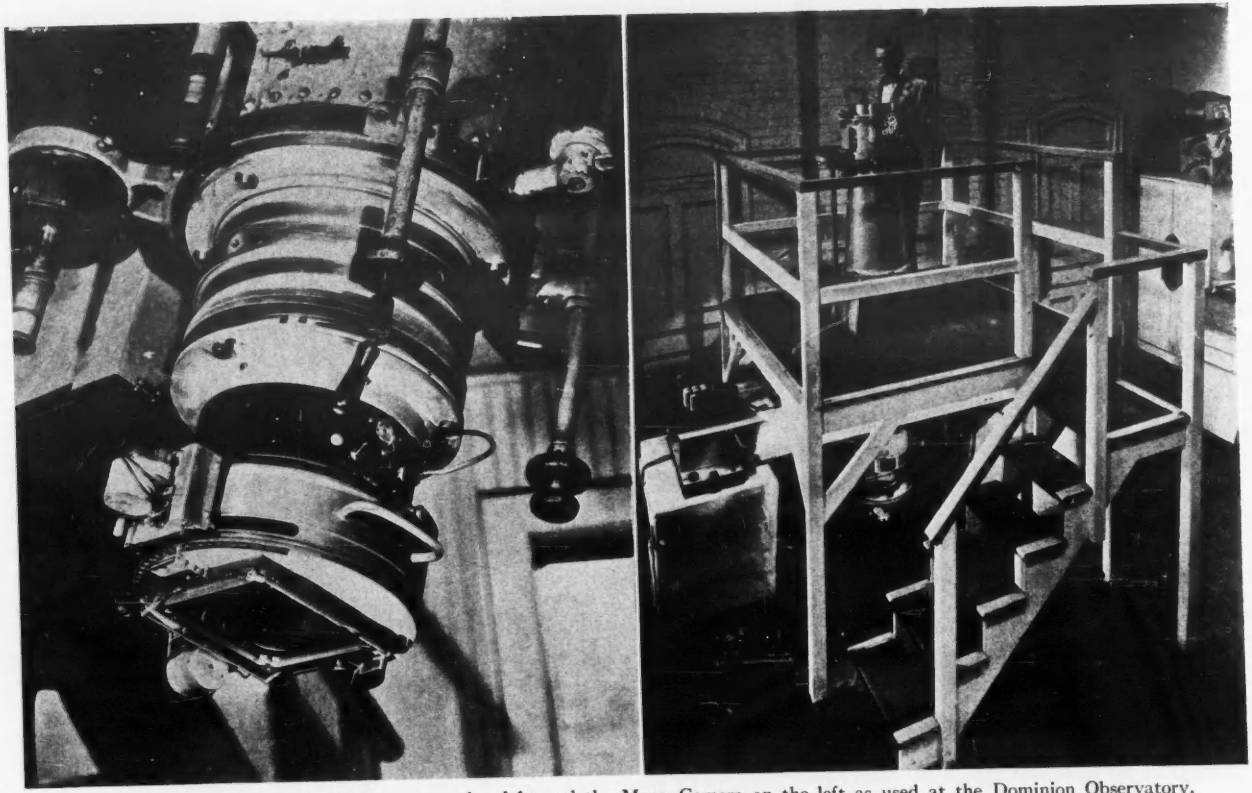

Fig. 3. Photographic Zenith Telescope on the right and the Moon Camera on the left as used at the Dominion Observatory.

a few parts in 10^9 over short periods of time (Essen *et al.* 1958). Observations of the moon are made in U.T.2, and the resulting difference between the observed and predicted positions of the moon is interpreted as the accumulated error in U.T.2 with respect to E.T. Hence the relationship

$$\Delta T = \text{E.T.} - \text{U.T.2.} \tag{1}$$

The quantity ΔT is being determined from star observations made at many observatories combined with the results of about 20 moon cameras built for the International Geophysical Year and dispersed around the world. The result is expected to give a more accurate definition of E.T. than was available with former techniques.

The difference between a second of U.T.2 and the second of E.T. is small and usually the second of U.T.2 is used in the definition of frequency. In the future it will be possible to use the second of E.T. for more precise definition of frequency.

INTERLABORATORY INTERCOMPARISON OF FREQUENCY

As stated earlier the three component parts of the Canadian Frequency Standard are separated by a few miles. A signal at the fundamental frequency of 100 kc from one of the Essen ring quartz crystal oscillators is transmitted to the Applied Physics Division laboratories over standard Bell Telephone lines from each of the other two laboratories. There are no repeater amplifiers on the way and the lines are not disturbed or otherwise used by the Bell Telephone Company. At the Applied Physics Division laboratories these signals are amplified and used in the same manner as the local standard frequency signals. Because of the length of line involved the spot frequency measurements have a slightly higher uncertainty, about $1:10^9$ for the signal from the Dominion Observatory and about $5:10^9$ for the signal from Radio and Electrical Engineering Division laboratory. Using a 24-hour averaging time these uncertainties average to about zero and the accuracy of measurements is better than $1:10^{10}$. Signals at audio frequencies are also transmitted from the Dominion Observatory to the Radio and Electrical Engineering Division and from the Applied Physics Division to the Dominion Observatory, but these are used mainly for confirmation to lesser accuracy of measurements described earlier. Figures 1 and 4 show some of the results of frequency intercomparison.

ABSOLUTE VALUE OF FREQUENCY

All observations are freely exchanged amongst the three laboratories. From analysis of these observations coupled with astronomical observations the absolute frequency of the crystal oscillators is determined by one of the authors (S.N.K.). Figure 5 shows the results of this determination. Similar analysis (by M.M.T.) using shorter observational periods of 1 to 2 months gives the data useful in astronomy. In this work the unit of time used is a second of U.T.2 mentioned above. This can be later converted to a second of E.T. to conform with the definition of time, but in most cases this is not needed.

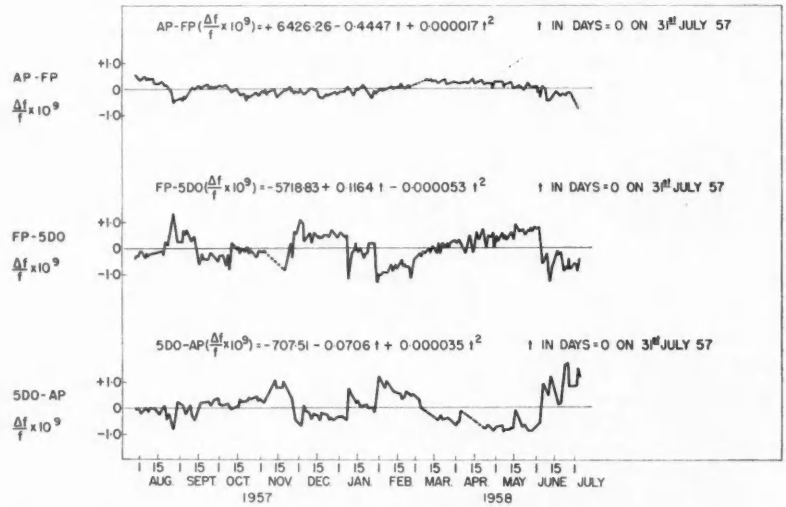

FIG. 4. Long term intercomparison of the frequency of crystal oscillators. In each case the ephemeris calculated from least square analysis of the observational data is listed on the top. The graph shows the difference between the calculated ephemeris and the actual observations.

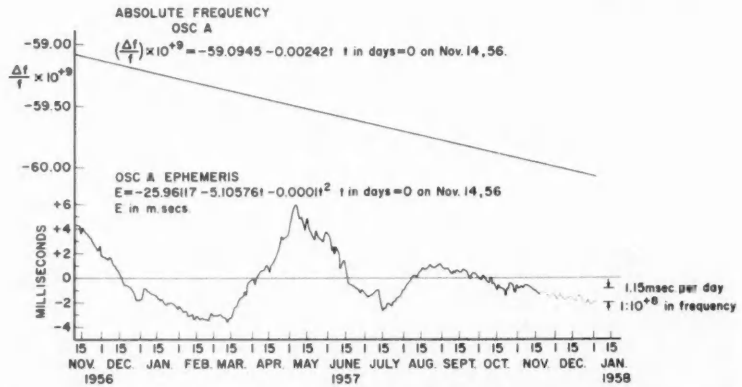

FIG. 5. Absolute frequency determination by oscillator AP. The graph on the top shows the frequency of oscillator AP as given by the ephemeris calculated from analysis of astronomical observations. The equation accompanying the graph is the calculated ephemeris. The graph at the bottom shows the difference between U.T.2 and oscillator AP used as a clock. Only the difference between actual observations and the calculated ephemeris is plotted.

The accuracy of the absolute frequency determination is limited by the errors of astronomical observations and the uncertainty of the corrections to be applied. In most cases it is possible to achieve an accuracy of $5{:}10^9$ if it is assumed that all the corrections needed for the determination of a second of

U.T.2 are known exactly. Recent work of Essen and Markowitz (Essen *et al.* 1958) has shown that there are secular changes in U.T.2. For a further study of these effects and for the investigation of the possibility of redefinition of a time interval in terms of atomic phenomena a cesium beam frequency resonator has been developed by Kalra, Bailey, and Daams (1958).

INTERNATIONAL INTERCOMPARISON OF STANDARDS

Two techniques are used for the purpose of measuring the national standards of the United States of America and Great Britain in terms of the Canadian standard. A number of broadcast stations transmit time signals which are monitored by the national laboratories and observatories and their times of reception are published by the national observatories. The error in measuring the time of reception in terms of the local standard is usually about $\pm 5 \times 10^{-4}$ second. It is therefore seen that if the measurements are averaged over a month the frequency of the oscillator controlling the time signals can be determined to better than $1:10^9$. These measurements are carried out at the Division of Applied Physics and at the Dominion Observatory. Time signals transmitted by stations with the following call signals are used: CHU, WWV, NSS, and GBR. These observations show that the U.S. and British standards agree with the Canadian standard to usually within about $5:10^9$, which is the accuracy of absolute frequency determination quoted above.

A high power broadcast station at Rugby, England, transmits at two frequencies, both controlled in frequency by the same crystal oscillator (Law 1955). The transmitted frequencies are measured at the National Physical Laboratory, Teddington, England, against their cesium beam frequency standard, and the results are published in *Electronic and Radio Engineer*. These signals are compared in phase with the local standard using a technique shown in the block diagram of Fig. 6. The rate of change of phase gives the relative frequency between the two oscillators. Since similar measurements are made at other laboratories, this technique offers a means

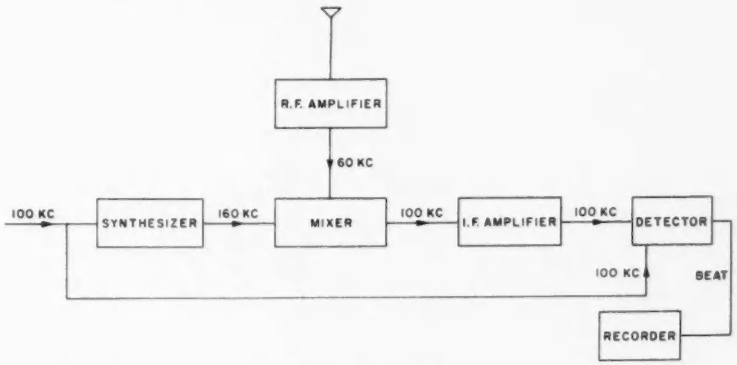

FIG. 6. Block diagram of the MSF 60-kc receiver and frequency comparator.

of intercomparison of standards. This work is done at the Division of Applied Physics and the Division of Radio and Electrical Engineering. The results show good agreement between the national standards of Great Britain and Canada. The relationship between the British cesium beam frequency resonator and U.T.2 has been described by Essen and Markowitz (Essen *et al.* 1958).

CONCLUSIONS AND SUMMARY

Over the past 3 years a frequency standard of very high precision has been installed in Canada. It is composed of equipment located in three different laboratories at Ottawa, which are separated by a few miles. Each laboratory has a set of quartz crystal oscillators of the Essen ring type as reference standards backed by working standards of different types. These oscillators show a stability of about $2:10^{10}$ over both long and short periods of time. Frequency intercomparisons are all made to an accuracy of better than $1:10^{10}$. Intercomparison of frequency between the three laboratories, which is done by sending signals over telephone lines, is made to an accuracy of better than $1:10^{10}$ using 24-hour averaging time and to about $1:10^{9}$ using averaging times of a few seconds.

Absolute frequency is determined from astronomical observations of the Dominion Observatory. A Photographic Zenith Telescope and a Markowitz Moon Camera are used for this purpose.

International intercomparisons of frequency standards are carried out by measurements of time signals and by phase measurement of low frequency carriers. Results show agreement with the United Kingdom and U.S.A. standards to well within $1:10^{8}$ in frequency.

ACKNOWLEDGMENT

The authors wish to express their appreciation for the encouragement and sympathetic interest in this work taken by Dr. B. G. Ballard, Dr. C. S. Beals, and Dr. L. E. Howlett and to Dr. J. T. Henderson and Dr. D. W. R. McKinley, who initiated this project at the National Research Council and have taken an active interest ever since. They are also indebted to their colleagues for their help in various phases of this work and especially to Messrs. B. J. Rafuse, J. C. Swail, and R. W. Tanner.

REFERENCES

BOOTH, C. F. and LAVER, F. J. M. 1942. Post Office Elec. Engrs. J. **35** (I), 8.
——— 1946. J. Inst. Elec. Engrs. **93** (III), 223.
COMITÉ INTERN. POIDS MESURES, Procès-Verbaux des Séances, 2e Sér. 1957. XXV, 77.
ESSEN, L. 1951. Proc. Inst. Elec. Engrs. (London), **98** (II), 154.
ESSEN, L., PARRY, J. V. L., MARKOWITZ, W., and HALL, R. G. 1958. Nature (London), **181**, 1054.
KALRA, S. N., BAILEY, R., and DAAMS, H. 1958. Can. J. Phys. **36**, 1442.
LAW, H. B. 1955. Proc. Inst. Elec. Engrs. (London), **102** (B), 166.
MARKOWITZ, W. 1954. Astron. J. **52**, 69.
THOMSON, M. M. 1955. Publs. Dominion Observatory, Ottawa. XV (4), 319.
——— 1958. J. Roy. Astron. Soc. Can. **52** (3), 112.

A STUDY OF μ-MESONS INCIDENT AT LARGE ZENITH ANGLES[1]

B. G. WILSON[2]

ABSTRACT

A Geiger counter telescope has been employed to study μ-mesons incident at large zenith angles. The counters were hodoscoped in pairs enabling the direction and angle of incidence of the particles to be determined. The intensity has been analyzed as a function of arrival time but no significant variation has been found either in solar time or sidereal time. However, a variation in solar time has been noted on analysis of extensive air showers measured concurrently. The angular variation of intensity has been studied and absolute rates obtained; these rates have been compared with those of an earlier determination showing excellent agreement. Some evidence has been obtained of a directional anisotropy in the μ-meson flux as measured at the apparatus.

INTRODUCTION

Systematic measurements of the intensity of cosmic rays as a function of arrival time have been made for many years. Several variations have been found relating to geomagnetic and meteorological phenomena but there is fairly general agreement that the radiation at some distance from the earth maintains a high degree of isotropy. This symmetry appears to exist even at high particle energies.

To study the radiation at very high energy, experimenters have in general followed one of two courses. Investigation of extensive air showers at sea level throws light on their high energy primaries at the top of the atmosphere while the study of μ-mesons of high energy will also yield information about energetic primaries. Measurements on μ-mesons have generally been performed underground to filter out unwanted low energy mesons.

An alternative method of studying high energy μ-mesons is to observe their incidence at the surface of the earth at large zenith angles, as suggested by Jakeman (1956). Since the atmosphere is not of uniform density the density of the air where the parents of horizontally travelling μ-mesons are created is less than that where the parents of vertically travelling μ-mesons are formed by a factor of about ten. Furthermore the decay interaction competition of the π-mesons increasingly favors decay as the path of the particle varies from the vertical approach to the earth. It would appear therefore that there is considerable advantage in making observations at large zenith angles when studying high energy μ-mesons.

Mesons incident at large zenith angles—'horizontal particles'—have passed through 36,000 g/cm^2 of atmosphere so that the minimum initial energy is about 7×10^{10} ev. The mean arrival energy at sea level for mesons incident at 90° zenith angle has been computed to be 2.5×10^{11} ev, while at 88° it is

[1]Manuscript received October 6, 1958.
Contribution from the Division of Pure Physics, National Research Council, Ottawa, Canada.
Issued as N.R.C. No. 4980.
[2]Postdoctorate Fellow, 1955–57, now at the National Research Council Sulphur Mountain Laboratory, Banff, Alberta.

1.2×10^{11} ev, using the published curves of Jakeman. The horizontal flux is clearly distinguished by its high energy. The present experiment was set up to search for possible time variations in this component.

EXPERIMENTAL ARRANGEMENT

The apparatus consisted of four trays, each containing 16 Geiger counters, 16 in. × 1 in., disposed as in Fig. 1. Counters in trays A and D had their axes horizontal while those in trays B and C were vertical. The telescope

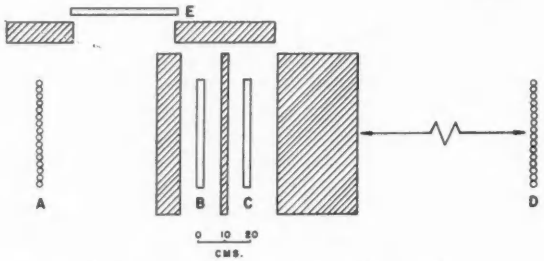

FIG. 1. Experimental arrangement, side elevation.

defined by the extreme trays A and D was 20 ft long with the maximum angle of acceptance 3.8 degrees above the horizontal. The telescope was aligned, at sea level, in the geographic north–south direction at Ottawa (lat. 45.4° N., long. 75.6° W.).

Included in the telescope were 42 cm lead, while trays A, B, and C were shielded by 7.5 cm lead overhead and B and C by 10 cm lead at each side.

Adjacent pairs of counters in all trays had their outputs paralleled and fed to hodoscope circuits and subsequently to neon lamps. The paralleled outputs from each tray also operated separate neons. The selection system utilized a Rossi-type fourfold coincidence circuit operated by the output pulses from the four trays. The resolving time was 4 microseconds. The ABCD master-pulse scanned the hodoscoped circuits operating neon lamps corresponding to discharged counters or trays.

Extensive showers were detected by three unshielded trays of Geiger counters of total area 5200 sq. cm and one tray of area 3600 sq. cm shielded by 10 cm lead. Each extensive tray also operated a neon lamp. Photographs of the neon array together with solar and sidereal clocks were taken with each ABCD coincidence.

The experiment was operated from October 1956 to April 1957 with a total effective operating time of over 2500 hours; 11,000 events were recorded of which about a quarter were 'horizontal particles'.

METHOD OF ANALYSIS

The events were divided into two main categories: extensive, in which any extensive shower tray was struck, and non-extensive. The extensive events

were subdivided by the selection of events in which the shielded extensive tray had been discharged. Extensive events therefore correspond to at least fivefold coincidences, the showers to contain not less than two penetrating particles, while 'shielded extensives' require at least three penetrating particles. The non-extensive category comprises horizontal events whose directions of motion are uniquely determined, single counter pairs only being discharged in the extreme trays; events where the precise direction is not defined owing to multiple discharge of counters; and a small number of events which appear to be incompatible with single particle traversals of the telescope.

Both the horizontal events and the extensive showers have been analyzed as a function of time and the significance of deviations from the mean determined. The hourly rates have been plotted on Figs. 2, 3, and 4.

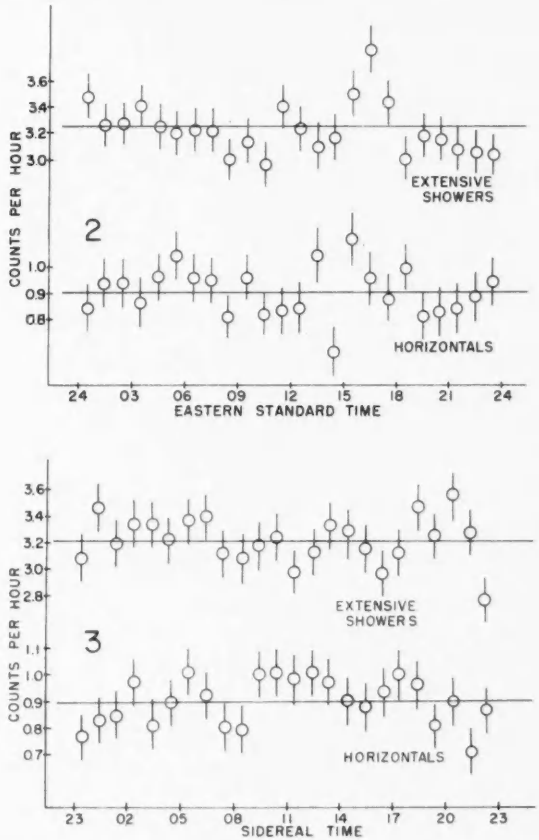

FIGS. 2 and 3. Counting rates per hour for extensive and horizontal events as a function of solar time (Fig. 2) and sidereal time (Fig. 3).

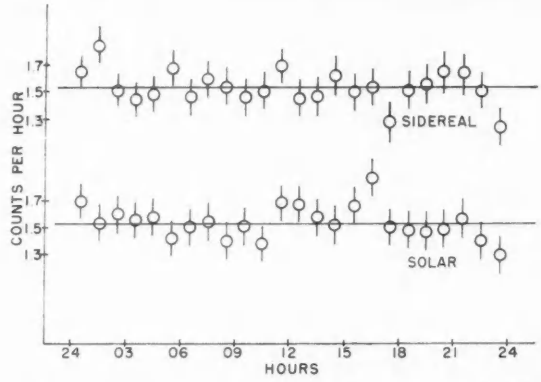

FIG. 4. Counting rates per hour for shielded extensive events in solar and sidereal times.

Horizontal particles formed 95% of the non-extensive events and of these three quarters had a unique direction defined by the single counters struck in trays A and D. These events were analyzed as a function of their angle of incidence and the angular dependence of intensity obtained. After corrections were applied the absolute rates were obtained for each angle measured.

The numbers of horizontal particles from the north and south have been compared. Finally, the production probability of secondaries has been derived.

TIME VARIATIONS

A total of 2296 horizontal events and 8773 extensive showers (including 3881 shielded extensives) have been analyzed in solar and sidereal times and the hourly rates plotted on Figs. 2, 3, and 4. Figure 2 shows the results as a function of solar time for both horizontals and extensives. The statistical errors are also given. To determine whether the distribution of points from the mean is normal, the rates for 3-hour intervals were compiled and a χ^2-test was applied to the eight values to test a null hypothesis. The horizontals are consistent with zero variation but the extensives show a significant divergence with $p = 0.001$ for the null hypothesis. A sine curve was then fitted to the data using the least-squares method for best fit and a curve of 12-hour period and amplitude of 0.17 counts per hour with maxima at 0400 and 1600 E.S.T. was obtained. This corresponds to a variation of 5.4%.

Figure 3 shows the hourly rates plotted as a function of sidereal time. Here the results are not inconsistent with the null hypothesis for both cases.

Figure 4 shows the hourly rates for the shielded extensives in solar and sidereal time. No established variation is apparent in sidereal time; a χ^2-test on the solar rates gives $p = 0.08$ for the null hypothesis, a poor correlation. A sine curve fitted to the data has a 12-hour period and amplitude of 0.085 counts per hour with maxima at 0310 and 1510 E.S.T. This is an excellent fit with the 3-hourly averages ($p = 0.75$) and corresponds to a variation of

5.5%. Even though the shielded results are contained in the extensives, the apparent magnitudes of the variations and their phase angles are remarkably similar.

Apart from the semidiurnal variation the results are in agreement with most previous work on extensive showers and μ-mesons. However, the semidiurnal variation noted is of interest for two reasons. Firstly, the positions of the maxima and minima of the best sine wave fitted to the results correspond with those of the pressure wave for Ottawa. Both waves have a 12-hour period; the two variations, however, are 180° out of phase. If we derive a barometric coefficient by relating the amplitudes of the two variations, the results yield a value of −100% per cm Hg, much greater than the usual value for short-term pressure variations.

Secondly, a variation of 12-hour period in solar time has been detected in high energy nucleon-induced local penetrating showers at sea level by McCusker *et al.* (1955, 1956), in high density extensive showers both in Dublin and Jamaica by McCusker and Reid (1958), and in very large extensive showers by Cranshaw and Galbraith (1957). In each case the times of the maxima and minima of the variations correspond closely with those of the local pressure variations; those of the high density showers are in phase while the other variations are in antiphase with the pressure waves. In these cases, however, barometer coefficients derived by relating amplitudes are very much greater than those usually associated with pressure variations of a short-term nature.

No satisfactory explanation of the correlation and of the high barometric coefficients has been suggested; however, the tie-in with the pressure wave appears well established.

ANGULAR VARIATION OF INTENSITY

The 1778 horizontal particles whose directions have been uniquely determined by comparing the single counter pairs struck in trays A and D have been analyzed as a function of mean zenith angle. For each of these 'single' events the direction of the particle is known within the limits of a single telescope. Table I shows the distribution of events; the number of available telescopes is given for each angle.

Certain corrections must be made to the data in Table I to obtain an accurate

TABLE I

Observed numbers of events for different mean zenith angles

Mean zenith angle (degrees)	No. telescopes	No. events	Av. no. events per telescope
86.5	2	111	55.5
87.0	4	214	53.5
87.5	6	226	37.7
88.0	8	265	33.1
88.5	10	229	22.9
89.0	12	318	26.5
89.5	14	280	20.0
90.0	16	136	8.5

picture of the distribution. These include allowance for obstruction of the earth, scattering of the mesons in the lead absorber within the telescope, normalization for the multiple events and for particles passing outside the telescope but producing secondaries which discharge a tray, simulating normal traversals of the telescope.

Because of the fall off of the terrain to the south of the apparatus, particles from the south moving upward within 0.16° of the horizontal arrive without interruption by the earth. Particles arriving from the north at angles greater than 89.7°, on the other hand, are obstructed by the Gatineau Hills so that the main contribution to the 90° mean zenith angle category comes from the south. This obstruction also affects the contribution to the 89.5° class by particles coming from the north but to a much smaller extent. The fractions of available solid angles for the different telescopes have been calculated.

To determine the possible effects of scattering of the mesons in the lead absorber their arrival energies must be determined. The energy spectrum has been computed from the published curve of Jakeman and the mean energies of particles incident at 90° and 88° obtained. These energies are respectively 2.5×10^{11} ev and 1.2×10^{11} ev.

μ-Mesons of energy about 16 Gev will have a projected angle of scatter of 0.5°, a deflection comparable to the resolution of the telescope. It is clear that the average meson energy is an order of magnitude greater than that required to inhibit measurable effects. It is important, however, to compute the proportion of mesons whose energies are less than 16 Gev and evaluate their contribution to reduction in resolution of the telescope.

The form of the μ-meson spectrum at large zenith angles shows that low energy particles are strongly attenuated as a result of decay processes. At 90° only 10% of the incident mesons have energy less than 16 Gev and only 4% below 10 Gev. The number of particles which might be scattered by as much as the acceptance angle of the telescope is 0.5% of the total flux. At 88° zenith angle about 22% of the mesons have energies below 16 Gev but only 2% may be scattered by as much as 3.8°.

At 86.5° the proportion of low energy mesons will be greater than at the larger angles but particles with energy less than 3 Gev will still be limited. It appears likely that less than 5% of the total incident flux will be of low enough energy to suffer deflections comparable with the acceptance angle of the telescope; it is concluded that no serious error will be introduced into the angular distribution pattern by neglecting the effects of particle scattering.

Multiple discharge of counters in one of the extreme trays makes it impossible to define the angle of trajectory of the particle within 0.5°. Multiples are usually caused by knock-on electrons accompanying the mesons as they traverse a tray and such events must be added to the single events to enable an absolute rate to be determined. The probability of multiple events will not depend strongly on the angle of incidence of the particle; particles which pass through the end counters of a tray will in general contribute less to multiple events than those through the middle counters, but such undetected multiples will have been accepted as singles in any case.

It is not possible to evaluate precisely the contribution of these undetected multiple events to the singles classification; however, an examination of the 136 singles which fall into the 90° category shows that 64 passed through the top two and bottom two counter pairs of each tray while 72 passed through the telescopes defined by the central four counter pairs of the trays. Since the efficiency in recognizing a multiple event is greatest for the central counters, then, if the contribution of undetected multiples is large, the effect should be greatest for the end counters. In the absence of such evidence it is concluded that the contribution of such events is small and no correction has been applied to the results. The multiple events have therefore been divided among the different angles in the same proportions as the single events. This results in a 27% increase in the average numbers.

The same argument applies to corrections for particles which might pass through three trays and miss the fourth but give rise to secondary particles which discharge the fourth tray and therefore simulate single traversals. Events of this type are not expected to be numerous because of the small amount of condensed materials close to the end trays but, if they were frequent, a preponderance of 90° single events through the end counters over events through the central counters would be expected, and this is not so. The absolute rates have been computed and are shown in Table II.

TABLE II

Total number of events, effective number of telescopes, and absolute rates of particles for different zenith angles

Mean zenith angle (degrees)	Total no. events	Effective no. telescopes	Absolute rate: particles/cm²/sec/sterad $\times 10^3$
86.5	141	2	7.00±0.68
87.0	272	4	6.75±0.46
87.5	287	6	4.75±0.31
88.0	337	8	4.11±0.25
88.5	291	10	2.89±0.19
89.0	404	12	3.34±0.19
89.5	356	12.7	2.77±0.17
90.0	173	7.2	2.38±0.21

The intensity of μ-mesons has been plotted as a function of zenith angle in Fig. 5. Also plotted (open squares) are the intensities found by Jakeman. It will be seen that the results of the two experiments are in good agreement and that the values are fairly satisfied by the trend line on the figure representing exponential absorption.

The angular variation of intensity of the hard component for zenith angles up to about 60° is usually written in the form

$$I_\theta = I_0 \cos^n\theta \tag{1}$$

where I_θ is the intensity at zenith angle θ, I_0 is the vertical intensity, and n has a value close to 2.0. A relation of this type, extrapolated to 90°, will

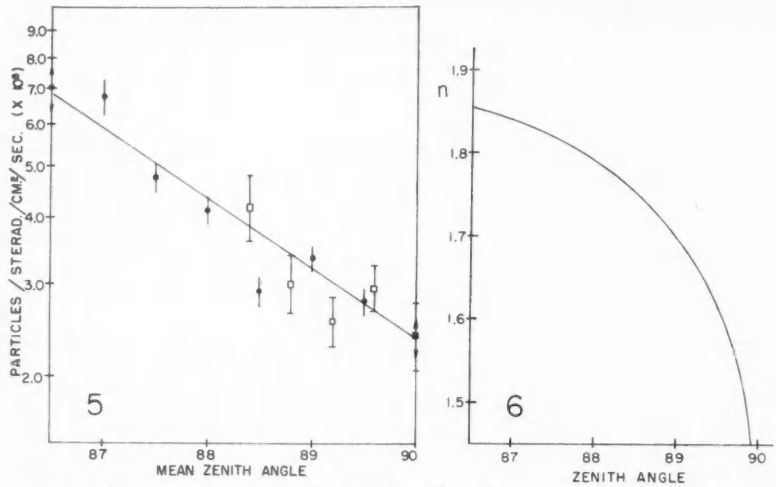

FIG. 5. Mu-meson intensity as a function of zenith angle.
FIG. 6. Variation of cosine exponent 'n' in angular distribution relation as a function of zenith angle.

yield zero intensity. However, a finite intensity at 90° would be expected and has been demonstrated. If equation (1) is altered to

$$I_\theta = I_0 \cos^n\theta + A, \tag{2}$$

where A is the intensity at 90° and is smaller than I_0 by a factor of about three hundred, the variation of intensity over all but the largest zenith angles will approximate closely to that given by (1) while expression will be given to the known finite intensity at 90°. Substituting in (2) values derived from the trend line of Fig. 5 and using Greisen's (1942) value of 0.0082 particles/cm²/sterad/sec for I_0 we obtain a series of values for n, which have been plotted in Fig. 6. This indicates that deviations from the cosine–square dependence of meson intensity become significant only at the largest zenith angles.

DIRECTIONAL ANISOTROPY OF HORIZONTAL PARTICLES

The form of the angular variation of intensity shows little obvious dependence on the arrival direction of the particles. An analysis of single events is presented in Table III. Mesons entering the telescopes at mean zenith angle 90° are omitted from the data since their directions cannot be specified.

TABLE III

Observed number of events at different zenith angles for each direction

Zenith angle	86.5	87.0	87.5	88.0	88.5	89.0	89.5	Total
Particles incident from north	44	72	83	113	97	121	150*	680
Particles incident from south	67	142	143	152	132	197	147	980

*Value normalized to seven effective telescopes.

There appears to be a divergence in intensity between the two directions of incidence. Unfortunately the results are not directly comparable since the mass of lead absorber within the telescope is not symmetrically placed, being in the southernmost quarter of its length. This might be expected to lead to a greater chance of multiple events being detected caused by knock-on processes when the particles are incident from the north, the 16-ft distance from the lead to the north tray biassing detection of events from the south in favor of singles. It is necessary therefore to analyze the multiple events and apportion them to the appropriate primary direction. The 442 multiple events were divided in the following manner.

In 102 cases a single counter pair was discharged in tray A and two or more in tray D, all of which were lower in tray D than the single counter discharged in tray A. These events appeared most likely to have come from the south. Similarly 136 events appeared most likely to have come from the north. The remaining 204 events consisted of cases where more than one counter was discharged in both trays and events where the single counter discharged in one tray was intermediate in vertical position between the several discharged in the other. These events were distributed 76 to the south and 128 to the north on the single assumption that the number of particles associated with a single penetrating meson will generally increase on passage through condensed material.

It is felt that this criterion will hold for the majority of traversals and that the cases in which it does not hold will balance each other to a first approximation. The totals have now become more even:

$$\text{particles incident from the north} \quad 680+136+128 = 944\pm31,$$

$$\text{particles incident from the south} \quad 980+102+76 = 1158\pm34.$$

The difference between south and north intensities of 214 particles amounts to 4.6 standard deviations.

It is important to consider experimental biasses which might be present because of asymmetry of the apparatus. Owing to the position of the lead absorber there appear two possible sources of error. First there is the chance of detection of secondaries produced in the lead where the primary particle discharges only three trays. Owing to the concentration of the lead to the south this would appear to favor particles from the north. There are, however, two balancing effects. There is a larger flux of particles through trays A, B, and C than through D, C, and B owing to the greater acceptance angle; also particles travelling through B, C, and D from the south may produce secondaries in the lead above tray A which could strike that tray, simulating a single traversal. These effects must be small since, as has been noted above, there is no evidence for end effects in the extreme trays when the 136 single events in the 90° category are studied. Further, the number of particles which strike the upper and lower halves of tray D has been determined for a sample 250 events; 50.8% of the particles pass through the lower four counter pairs where 50.0% would be expected if there was no effect due to secondaries.

Secondly, the effect of scattering on the mesons will affect particles from the south to the greater extent as a result of the greater distance from the lead to the extreme tray. As has been seen, however, the number of particles which experience significant scattering is quite small and they are as likely to be scattered upwards as downwards in any case.

Since no evidence of experimental bias has been found it is concluded that there is evidence of a directional anisotropy between north and south in this high energy radiation. It is clear, however, that there are uncertainties inherent in the analysis of the events which may well be as large as the statistical uncertainties quoted.

If the difference in rates between north and south is not experimental in origin there is evidence of a north–south effect of considerable magnitude. A north–south effect in cosmic ray intensity is expected owing to the modification of the primary flux by the earth's magnetic field and subsequently because the solid earth blocks many possible particle trajectories. At the geomagnetic latitude of Ottawa, 56.8° N., the total allowed cone is approximately given by the combined Störmer plus the earth's shadow cone. Alpher (1950) has published curves relating the minimum arrival energy for different azimuths and zenith angles at 10° latitude intervals. For 90° zenith angle the values of $E_{\min}$ for particles arriving from the north and south at Ottawa are 14.0 and 0.5 Gev respectively for protons, i.e. the allowed cones open up away from the pole. However, this considerable bias towards particles from the south will only be apparent at low energies, measured at sea level, and will not affect the primaries of the μ-mesons detected in this experiment. These primaries must have energies in excess of 10^{11} ev and will have a mean energy in excess of 10^{12} ev.

The anisotropy remarked in this paper cannot therefore be related to the influence of the earth's magnetic field and can only be attributed to an asymmetry in the primary radiation at some distance from the earth.

PRODUCTION OF SECONDARIES

In 4588 tray traversals during the experiment, 416 events had multiple discharges in one tray corresponding to a probability of $9.1 \pm 0.45\%$. Assuming that the probability of discharge in any tray is independent of occurrences in another tray, 38 events would be expected to include multiple discharges in both trays. Forty-six such events were obtained.

The average number of secondary electrons leaving a lead plate in association with a μ-meson has been shown to be 0.07, using cloud chambers with horizontal lead plates, by Hazen (1943) and Brown *et al.* (1949). Using an apparatus similar to the present arrangement but arranged vertically, Jakeman found a production probability of 3.5%. Taking, then, an efficiency of 50% for a counter tray in resolving and detecting secondaries, the present experiment shows a probability of $18 \pm 1\%$ for the knock-on phenomenon in lead in association with the horizontal flux of μ-mesons. With the same efficiency factor of 50%, Jakeman's results yield $21 \pm 2\%$ using a narrower telescope and therefore higher mean energy. Underground measurements at

180 meter water equivalent by Naranan *et al.* (1957) show the equilibrium number of electrons to be $17.2\pm1.2\%$ using a cloud chamber technique, in excellent agreement with theoretical prediction. Tiffany and Hazen (1950) at 860 meters obtained a value of 22% also using a cloud chamber. The comparison of these values confirms the high energy character of the horizontally travelling μ-mesons.

ACKNOWLEDGMENTS

The author wishes to thank Dr. D. C. Rose and other members of the Cosmic Ray Group for their assistance in operating the equipment and for many valuable discussions. He is indebted to Professor C. B. A. McCusker for communicating his results before publication. He is particularly grateful to Miss Margaret Stott for her help in analyzing the data throughout the course of the experiment and to Mr. John Legge for assistance in the computational work.

The author also wishes to thank the National Research Council for the award of a Fellowship.

REFERENCES

ALPHER, R. A. 1950. J. Geophys. Research, **55**, 437.
BROWN, W. W., MCKAY, A. S., and PALMATIER, E. D. 1949. Phys. Rev. **76**, 506.
CRANSHAW, T. E. and GALBRAITH, W. 1957. Phil. Mag. Vol. **2**, **18**, 804.
GREISEN, K. 1942. Phys. Rev. **61**, 212.
HAZEN, W. E. 1943. Phys. Rev. **64**, 7.
JAKEMAN, D. 1956. Can. J. Phys. **34**, 432.
MCCUSKER, C. B. A., DARDIS, J. G., and WILSON, B. G. 1955. Proc. Phys. Soc. (London), A, **68**, 585.
MCCUSKER, C. B. A. and REID, R. J. 1958. Private communication.
MCCUSKER, C. B. A. and WILSON, B. G. 1956. Nuovo cimento, Suppl. **2**, Vol. 4, Ser. X, 870.
NARANAN, S., RAMANAMURTY, P. V., SAHIAR, A. B., and SREEKANTAN, B. V. 1957. Nuovo cimento, Vol. 5, Ser. X, 1773.
TIFFANY, O. L. and HAZEN, W. E. 1950. Phys. Rev. **77**, 849.

DIFFUSION IN MULTICOMPONENT METALLIC SYSTEMS

IV. A GENERAL THEOREM FOR CONSTRUCTION OF MULTICOMPONENT SOLUTIONS FROM SOLUTIONS OF THE BINARY DIFFUSION EQUATION[1]

J. S. KIRKALDY

ABSTRACT

If $C = C(x, y, z, Dt)$ is a solution of the binary diffusion equation

$$\frac{\partial C}{\partial t} = D\nabla^2 C$$

for a given boundary condition, then

$$C_i = a_{i0} + \sum_{k=1}^{n-1} a_{ik} C(x,y,z,u_k t),$$

where

$$u_k = \sum_{j=1}^{n-1} D_{ij} a_{jk} / a_{ik}$$

is a solution of

$$\frac{\partial C_i}{\partial t} = \sum_{k=1}^{n-1} D_{ik} \nabla^2 C_k$$

for the i^{th} component of an n-component system subject to the same formal boundary condition. As an example, the ternary diffusion field about an initial point source is calculated. The method of calculation for steady state and transient equilibrium is indicated.

INTRODUCTION

Although a suitable phenomenological description of diffusion in multicomponent systems has been available for some time (Onsager 1945–46; Darken 1951), until recently no attempt has been made to solve the equations and apply the results to the description of diffusing systems. This delay is no doubt a consequence of the natural assumption that the differential equations and solutions are increasingly intractable in proportion to the multiplicity of the system. We intend to demonstrate that this assumption is incorrect and that most solutions now available for binary systems can be extended in a straightforward manner to n-component systems.

In recent publications, Gosting and Fujita (1956) and Kirkaldy (1957; papers I, II, and III 1958) have presented solutions of the multicomponent diffusion equation of the parametric ($x/\sqrt{t}$ dependent) form for specific boundary conditions and for three or more components. Here we present a theorem which applies independently of the geometry and boundary conditions and which leads to a simple rule for finding the n-component solutions from known binary solutions.

[1]Manuscript received June 12, 1958.
Contribution from the Department of Metallurgy and Metallurgical Engineering, McMaster University, Hamilton, Ontario.

METHOD OF SOLUTION

Consider the differential diffusion equation for binary systems

$$\frac{\partial C}{\partial t} = D\nabla^2 C, \tag{1}$$

where D is assumed to be constant. This has a solution of the form

$$C = C(x,y,z,Dt). \tag{2}$$

The generalization of equation (1) to n components is (paper I)

$$\frac{\partial C_i}{\partial t} = \sum_{k=1}^{n-1} D_{ik}\nabla^2 C_k, \tag{3}$$

where again, all D's are assumed to be constant. We now form a trial solution,

$$C_i = a_{i0} + \sum_{k=1}^{n-1} a_{ik} C(x,y,z,u_k t) \tag{4}$$

where C is given by (2) and the u_k remain to be determined. By direct substitution we can show that (4) satisfies (3) provided the indicial equations

$$u_k = \sum_{j=1}^{n-1} D_{ij} a_{jk}/a_{ik} \tag{5}$$

are simultaneously satisfied. If the a_{ik} are independent and the u_k exist, this set uniquely determines the latter in terms of the diffusion coefficients* and provides a further $(n-1)^2-(n-1)$ independent relations between the a_{ik}. When these are combined with $2(n-1)$ boundary values, the $(n-1)^2+(n-1)$ a-coefficients are uniquely determined in terms of the D's and the boundary concentration values. In general, solutions (4) will fit the same formal boundary conditions as (2).

There are some limitations to the application of this procedure. For most physically significant solutions, the u_k (as well as D) must all be real and positive. For $n = 3$ we have previously noted (paper I) that the necessary and sufficient conditions that u_k be real and positive are that

$$D_{ii} > 0 \qquad (i = 1, 2), \tag{6}$$

and

$$-\tfrac{1}{4}(D_{11}-D_{22})^2 < D_{12}D_{21} < D_{11}D_{22}. \tag{7}$$

The only general statement of interest in the mathematical literature concerning equation (5) applies to a symmetric matrix $[D_{ik}]$. In this case the necessary and sufficient conditions that the u_k are all real and positive are that $|D_{ik}|$ and all its principal minors are greater than zero. Comparison of this statement with inequalities (6) and (7) for $n = 3$ suggests that perhaps in general it is necessary that $|D_{ik}|$ and all its principal minors be greater than zero, but this is by no means sufficient. For $n = 3$ at least, the mathematical conditions are consistent with those imposed by the second law of thermodynamics (paper I).

*A special case in which the u_k do not exist has been considered in paper I, p. 904. The u_k are most easily obtained by casting (5) in the matrix form to give the polynomial equation $|\mathbf{D}-u\mathbf{I}| = 0$. The $n-1$ solutions of this are $u_1, u_2, \ldots u_{n-1}$.

A difficulty with solutions of type (4) is that many apparently physically plausible values of the D's and the boundary C's lead to negative C_i's, a result which is quite inadmissible. If the phenomenological scheme is to be preserved, it must be postulated that the D_{ik}, $i \neq k$, vanish with C_i in a suitable fashion. Such a variation can be qualitatively justified on a simple statistical model of solid state diffusion. It has been observed for diffusion in a ternary electrolytic solution by O'Donnell and Gosting (1957). The point requires further theoretical and experimental investigation.

EXAMPLE OF A NON-PARAMETRIC SOLUTION

In previous work, solutions of the multicomponent diffusion equations have been limited to boundary conditions which lead to parametric ($x/\sqrt{t}$ dependent) penetration curves. As an example of the application of our theorem to a more complex problem we consider the diffusion field about a point source consisting of a mixture of two solute atoms deposited at the r origin in a pure semi-infinite matrix. For the binary case, in which the number of atoms deposited is S, the solution of the diffusion equation in units of atoms per unit volume is (Jost 1952)

$$C = \frac{S}{(4\pi Dt)^{3/2}} \exp\left[-\frac{r^2}{4DT}\right]. \tag{8}$$

According to our theorem, for the ternary case

$$C_1 = a_{10} + \frac{a_{11}}{(u_1 t)^{3/2}} \exp\left[-\frac{r^2}{4u_1 t}\right] + \frac{a_{12}}{(u_2 t)^{3/2}} \exp\left[-\frac{r^2}{4u_2 t}\right], \tag{9}$$

and

$$C_2 = a_{20} + \frac{a_{21}}{(u_1 t)^{3/2}} \exp\left[-\frac{r^2}{4u_1 t}\right] + \frac{a_{22}}{(u_2 t)^{3/2}} \exp\left[-\frac{r^2}{4u_2 t}\right]. \tag{10}$$

If the initial point source consists of S_1 and S_2 atoms of components 1 and 2 respectively, then

$$S_1 = 4\pi \int_0^\infty C_1 r^2 dr \tag{11}$$

and

$$S_2 = 4\pi \int_0^\infty C_2 r^2 dr. \tag{12}$$

Combining these relations with the indicial equations (5) we can readily complete the solutions to obtain

$$\begin{aligned}
a_{10} &= a_{20} = 0 \\
a_{11} &= \{S_1[D_{11} - D_{22} + \mathscr{D}]/2 + D_{12}S_2\}/8\pi^{3/2}\mathscr{D} \\
a_{21} &= \{D_{21}S_1 - S_2[D_{11} - D_{22} - \mathscr{D}]/2\}/8\pi^{3/2}\mathscr{D} \\
a_{12} &= S_1/8\pi^{3/2} - a_{11}; \quad a_{22} = S_2/8\pi^{3/2} - a_{21} \\
\mathscr{D} &= \sqrt{\{(D_{11} - D_{22})^2 + 4D_{12}D_{21}\}} \\
u_1 &= (D_{11} + D_{22} + D)/2 \\
u_2 &= (D_{11} + D_{22} - D)/2.
\end{aligned}$$

STEADY STATE SOLUTIONS

Solutions of the equations

$$\sum_{k=1}^{n-1} D_{ik}\nabla^2 C_k = \frac{\partial C_i}{\partial t} = 0 \tag{13}$$

lead from the known solutions of the binary equation

$$\nabla^2 C = 0 \tag{14}$$

in a somewhat trivial manner since, provided $|D_{ik}| \neq 0$, (13) implies

$$\nabla^2 C_k = 0. \tag{15}$$

Accordingly, the diffusion field for a given component depends only on the geometry and the individual boundary conditions and is formally identical with that for a binary system. The multicomponent interactions appear only in the calculation of the diffusion currents,

$$J_i = -\sum_{k=1}^{n-1} D_{ik}\nabla C_k. \tag{16}$$

It is tacitly assumed in the above that all boundary values are fixed. It may, however, be that the first m of a total of $n-1$ components are closed within the system and are therefore free to seek distributions in accord with the constrained distributions. These free distributions finally satisfy the equations $J_i = 0$, $(i = 1, 2, \ldots m)$(de Groot 1952) while the others continue to satisfy (15) $(k = m+1, m+2, \ldots n-1)$.

DIFFUSION THROUGH STATES OF TRANSIENT EQUILIBRIUM

A situation may often arise in solid state multicomponent diffusion where some of the components have such low diffusion rates that their distributions can be assumed to be quasi-stationary. In systems which are finite and closed the diffusion fields of the rapidly diffusing components will tend to come to transient equilibrium with the quasi-stationary fields through the interaction of the cross terms in the diffusion coefficient matrix.

For simplicity, consider a ternary system and let component 1 be rapidly diffusing and component 2 be slowly diffusing. We specify that the initial distribution of component 2 contains no infinite gradients since this would allow it to keep pace with component 1 in spite of its low diffusion coefficient (examples of this type of solution have been considered in papers I, II, and III). In the approach to transient equilibrium C_1 will satisfy the differential equation

$$\frac{\partial C_1}{\partial t} = \nabla \cdot D_{11}\nabla C_1 + \nabla \cdot D_{12}\nabla C_2 \tag{17}$$

where

$$C_2 \cong C_2(\vec{r}) \tag{18}$$

is the quasi-stationary distribution of component 2. When transient equilibrium is attained,

$$-J_1 = D_{11}\nabla C_1 + D_{12}\nabla C_2 \cong 0. \tag{19}$$

For constant coefficients and symmetrical initial conditions this gives on integration,

$$C_1 \cong -\frac{D_{12}}{D_{11}} C_2 + A, \tag{20}$$

where the constant A is determined by the initial condition on component 1. The method can be generalized in a straightforward manner to greater numbers of elements.

CONCLUSIONS

1. With certain qualifications, the work indicates that it is now possible to describe analytically diffusion in multicomponent systems where solutions are available for the corresponding binary problem.

2. The steady state multicomponent diffusion fields are independent and are determined entirely by the geometry and the boundary conditions. The diffusion currents are, however, interdependent.

3. The possibility of solutions in transient equilibrium for $n \geqslant 3$ and the simplicity of their analytical treatment presages an important application of the multicomponent formalism to segregation problems in alloys.

ACKNOWLEDGMENTS

The author is indebted to Dr. P. R. Beesack of the McMaster University Mathematics Department for reviewing the manuscript and to Drs. N. D. Lane and J. H. H. Chalk of the same department for their advice on the behavior of systems of equations.

REFERENCES

DARKEN, L. S. 1951. Atom movements (American Society for Metals).
DE GROOT, S. R. 1952. Thermodynamics of irreversible processes (North-Holland Pub. Co., Amsterdam), p. 196.
GOSTING, L. J. and FUJITA, H. 1956. J. Am. Chem. Soc. **78**, 1099.
JOST, W. 1952. Diffusion in solids, liquids, gases (Academic Press Inc., New York), p. 19.
KIRKALDY, J. S. 1957. Can. J. Phys. **35**, 435.
——— 1958. Can. J. Phys. **36**, 899; 907; 917.
O'DONNELL, I. J. and GOSTING, L. J. 1957. Symposium on electrolytes (John Wiley and Sons, Inc., New York).
ONSAGER, L. 1945–46. Ann. N.Y. Acad. Sci. **46**, 241.

DETERMINATION OF THE UNIT OF CAPACITANCE[1]

A. F. DUNN

ABSTRACT

As part of the program to establish a wholly self-consistent group of basic electrical units for the country, the unit of capacitance maintained in the National Research Council has been determined in an absolute sense in terms of the frequency and resistance units maintained in the laboratories, with an accuracy comparable to that of the primary standards. The determination was made by connecting additional components to an existing capacitance and conductance measuring bridge to form a modified Wien bridge network. The results obtained indicate an accuracy of $\pm 0.0025\%$.

INTRODUCTION

The unit of capacitance may be derived from those of resistance and frequency, but of the methods which have been proposed, few yield the accuracy with which the standards of resistance and frequency are known and reproducible. The present paper describes the adaptation of a bridge circuit due to Wien (1891), successfully used by Ferguson and Bartlett (1928) of the Bell Telephone Laboratories, which permits a determination of capacitance with high accuracy. Although it is not essential for the measurement, the use of the Type 12 Capacitance and Conductance Bridge developed at the Bell Telephone Laboratories by Shackelton and Ferguson (1928) eases the problems of carrying out the measurement.

In its simplest form, the bridge shown in Fig. 1 consists of two equal resistance ratio arms, a third arm containing a capacitance and resistance in series,

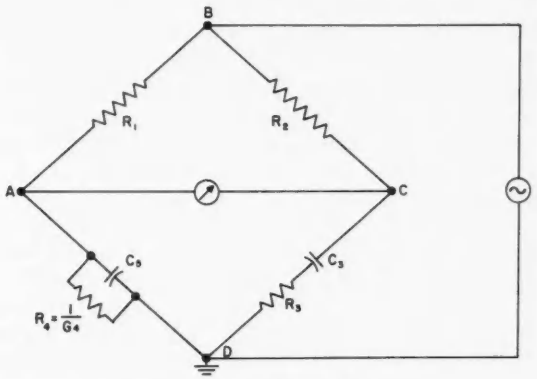

FIG. 1. Basic Wien network.

[1]Manuscript received September 22, 1958.
Contribution from the Division of Applied Physics, National Research Council, Ottawa, Canada.
Issued as N.R.C. No. 4993.

and a fourth arm containing a capacitance and resistance in parallel. A balance is easily obtained by varying any two of the five variables, i.e. the two capacitances, the two resistances associated with them, and the frequency.

The equations for balance given below are such that if the ratio of the capacitances and the value of the frequency are known, the magnitudes of the capacitances may be determined from the knowledge of only one of the resistances, say that in the series arm. Since the ratio of two capacitances may be obtained with a high degree of precision by supplementary measurements, it therefore becomes possible to use this network without a knowledge of the parallel resistance, the measurement of which presents certain difficulties.

THEORY OF THE CIRCUIT

If in Fig. 1 the ratio arms are equal in resistance and time constant (or phase angle), then the equation of balance may be written

$$\frac{Z_3}{Z_4} = Z_3 Y_4 = \frac{Z_2}{Z_1} = \frac{R_2}{R_1} = 1 \tag{1}$$

so

$$\left(R_3 + \frac{1}{j\omega C_3}\right)(G_4 + j\omega C_5) = 1, \tag{2}$$

and by separating the real and imaginary components

$$G_4 = \omega^2 C_3 C_5 R_3, \tag{3}$$

$$C_5 - C_3 + C_3 R_3 G_4 = 0, \tag{4}$$

from which

$$\omega^2 C_3^2 R_3^2 = C_3/C_5 - 1. \tag{5}$$

If the capacitances C_3 and C_5 are measured on the same capacitance bridge which has a wholly self-consistent calibration, then the measured values C_3' and C_5' will differ from the absolute values C_3 and C_5 by a constant ratio $K = 1+\alpha$, or

$$\begin{aligned} C_3 &= KC_3' = (1+\alpha)C_3' \\ C_5 &= KC_5' = (1+\alpha)C_5'. \end{aligned} \tag{6}$$

The balance equation of the network may now be written

$$C_3 = \frac{1}{\omega R_3}\left[\frac{C_3'(1+\alpha)}{C_5'(1+\alpha)} - 1\right]^{\frac{1}{2}} = \frac{1}{\omega R_3}\left[\frac{C_3'}{C_5'} - 1\right]^{\frac{1}{2}} \tag{7}$$

or

$$1+\alpha = \frac{1}{\omega C_3' R_3}\left[\frac{C_3'}{C_5'} - 1\right]^{\frac{1}{2}}. \tag{8}$$

Thus, the absolute value of C_3, or the value of the ratio factor $K = 1+\alpha$, may be determined from measured values of capacitance, resistance, and

frequency. Because many values of C_3 were used, the end result of these measurements is a knowledge of the ratio factor K, or briefly the correction factor α. With this information, any subsequent measurements may be referred to an absolute scale of capacitance directly.

In the foregoing, C_3 and C_5 were assumed to be pure capacitances and R_3 and R_4 pure resistances. Of course neither are obtainable in practice; the former will always have some slight conductance and the latter some slight reactance. If capacitors having small losses are used, the conductance of C_5 may be considered as a resistance R_{P4} in parallel with R_4 and that of C_3 as a resistance R_{S3} in series with R_3. The reactances of the resistors R_1, R_2, R_3, R_4 may be included as lumped constants associated with the resistors and considered as a part of the over-all bridge network.

One feature of the measurements made here is the fact that the primary bridge balance and all secondary balances are made with the Type 12 Capacitance and Conductance Bridge as originally designed and built. Because of this, it is necessary to consider the entire bridge network when analyzing any balance. The schematic arrangement of the whole bridge when connected for either of the possible Wien network measurements is shown in Fig. 2. Both of the possible network arrangements shown in Fig. 2 were used, and a final measurement of K or α comes from the mean of the results for the NORMAL and the REVERSED bridges, which results in reducing the corrections due to the inequality of time constant of the ratio resistors from a first-order correction to a negligible second-order term.

The networks shown in Fig. 2 were analyzed, and detailed balance equations obtained.* This leads to a value of K, or $1+\alpha$, corresponding to equation (8) given by

$$(9)\quad (1+\alpha)^2 = K^2 = \frac{\{(D_4-D_{40})_3/(D_4-D_{40})_5\}-1}{\omega_0^2(D_4-D_{40})_3^2(R_3^*)^2}\left[1+\Sigma_N+\frac{\tau_2-\tau_1}{(D_4-D_{40})_5R_3}\right]^{-1}$$

for the NORMAL bridge. For the REVERSED bridge the factor in the square bracket becomes

$$\left[1+\Sigma_R-\frac{\tau_2-\tau_1}{(D_4-D_{40})_5R_3}\right]^{-1}.$$

In each of these equations, $(D_4-D_{40})_3$ and $(D_4-D_{40})_5$ are the settings of the mica capacitor dials on the Type 12 bridge when capacitors C_3 and C_5 are measured, ω_0 is the nominal frequency of operation, R_3^* is the nominal value of resistor R_3, $(\tau_2-\tau_1)$ is the difference in time constant of the ratio resistors, and Σ_N and Σ_R refer to the summation of the correction terms for the NORMAL or REVERSED bridges. It will be seen that the algebraic sign applying to $\tau_2-\tau_1$ is reversed for the two bridges, and hence the term is eliminated by taking the mean of the results.

APPARATUS

The basic bridge used in this determination is a completely shielded

*Division of Applied Physics Report APEM-386.

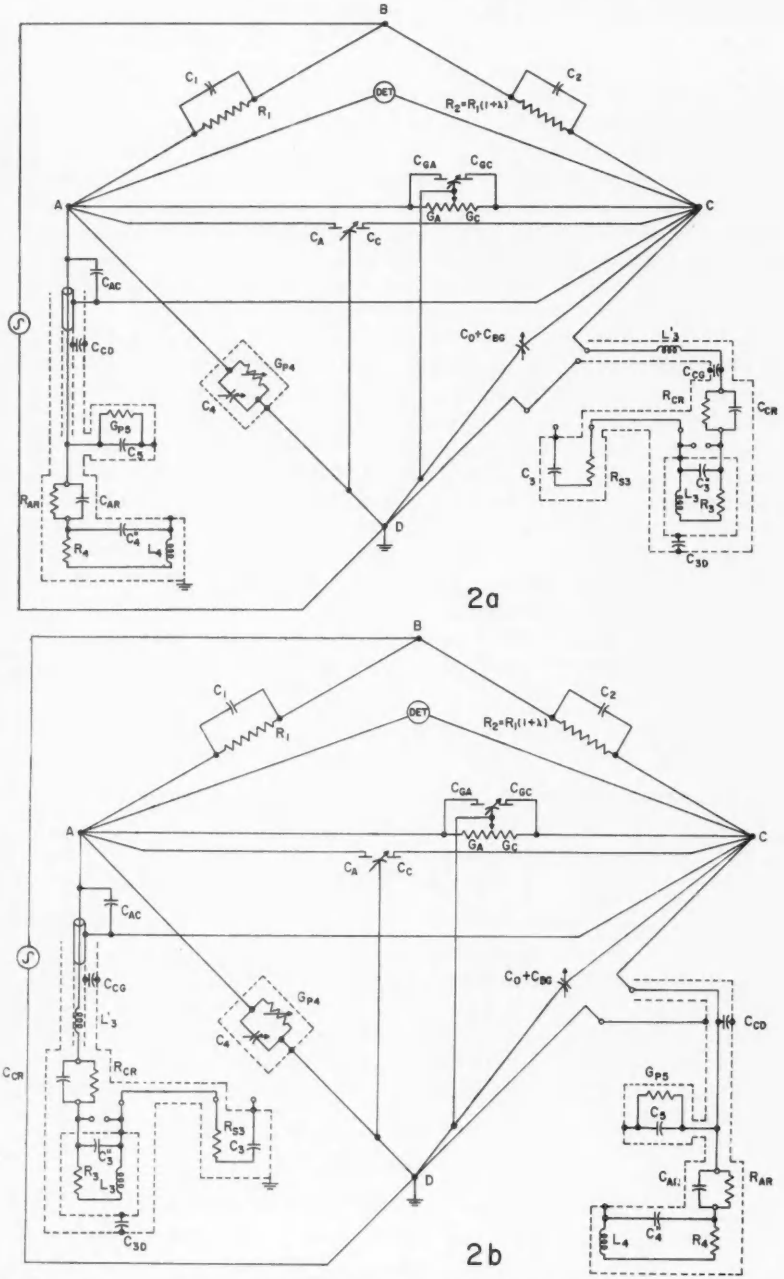

FIG. 2. Schematic diagram of Wien network on Type 12 bridge. 2*a*. Normal. 2*b*. Reversed.

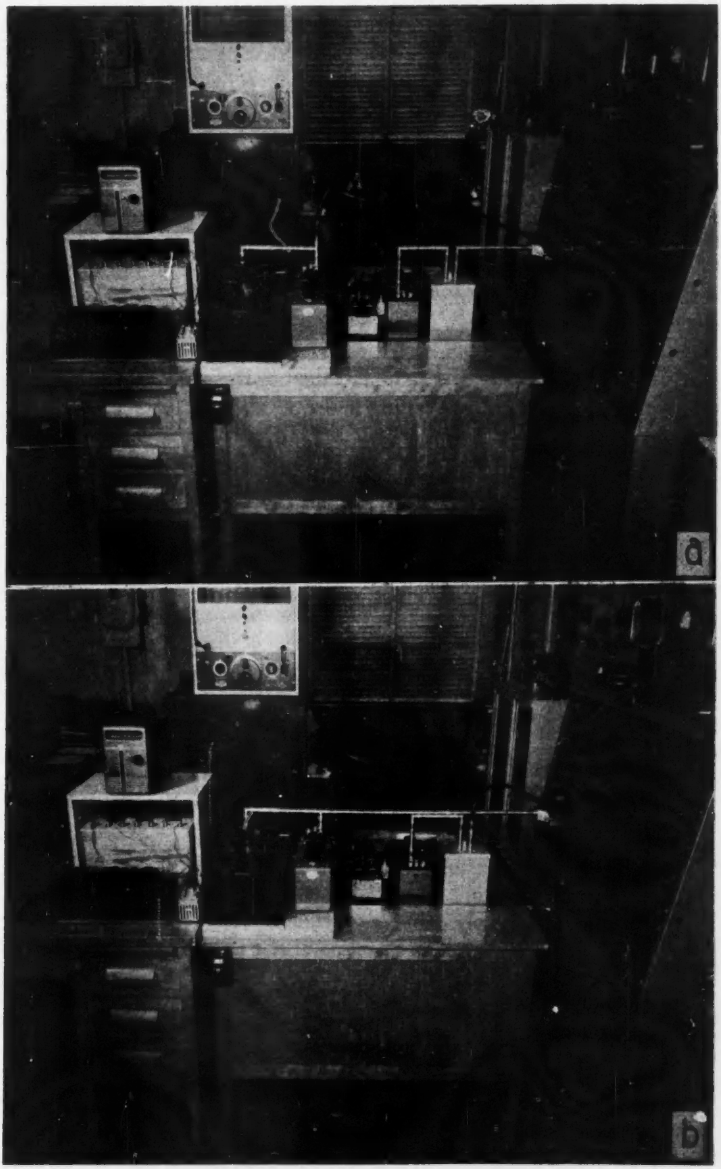

FIG. 3. Wien network components connected to Type 12 bridge. 3*a*. Normal. 3*b*. Reversed.

equal-ratio bridge designed by the Bell Telephone Laboratories and known as the Type 12 Capacitance and Conductance Bridge, Style W-10105. A similar type of differential element bridge may be found in Harris (1952). The additional components needed to complete the Wien network were connected to the bridge through the normal terminals. The schematic diagram is shown in Fig. 2, and photos of the complete bridge connected for either the NORMAL or REVERSED Wien network are shown in Fig. 3.

In order to ensure that the additional capacitances C_{CD}, C_{CG}, and C_{3D} remain constant during the measurements, special care must be taken with the shielding of the external components. Commercially available rigid coaxial line elements were used wherever possible, as seen in Fig. 3, and the double shielded lines connecting to R_3 were made from special coaxial cable with good insulation between the shields. The resistors used for R_3 were oil immersed in a metal case with a separate screen terminal, and were mounted on insulating pillars in a relatively large metal box which may be seen closest to the main bridge in Fig. 3. The inner shield of the resistor was connected to the junction between R_3 and C_3, as indicated in Fig. 2, in order to specify capacitance C_{3D} and keep it constant.

The effect of this shielding has been to eliminate any detectable effect due to the proximity of other bodies. The stability of the shielding arrangement was such that the whole of the exterior network could be removed and then reassembled without changing any of the balances by more than one or two micromicrofarads; the effect on the determination of K was not more than one or two parts in a million. In this way it was possible to make the required balances with assurance.

With any one of four resistors available for R_3, there was a wide range of values of C_3, C_5, and R_4 which would satisfy the main balance equation. Commercially available three-dial decade capacitance boxes and a six-dial decade resistance box were used for these components. The capacitance or time constant of each of these units with their connecting lines was measured at the time of the determination and thus the units need to remain stable for a period of 30 minutes only.

In order to establish the unit of capacitance in terms of resistance it was necessary to measure resistor R_3 in terms of known standards of resistance, which was done at the time of each measurement by means of an auxiliary Wheatstone Bridge network. The d-c. value of R_3 was obtained with a precision of 4 or 5 parts in a million in terms of the basic 1-ohm standards maintained in the laboratory. It was obtained within 20 minutes of the main bridge balances and hence the temperature stability obtained from the system of double shielding and oil-immersion in a temperature-controlled room is sufficient to warrant this accuracy.

The power to the bridge network was derived from a crystal-controlled oscillator supplying a frequency of 1000 c.p.s., or from a tuning fork oscillator supplying 1591.55 c.p.s. ($\omega = 10^4$). In either case the frequency was monitored by the Standard Frequency Laboratory, and the frequency values used were accurate to within $\pm 1 \times 10^{-6}$ for 1000 c.p.s. and $\pm 10 \times 10^{-6}$ for 1591.55 c.p.s.

The detection system used for the measurements had a sensitivity of better

than 0.5 microvolts at either frequency, which corresponds to detectable changes in balance of a few parts in 10 million for most measurements. The input bridge voltage was 10 volts r.m.s., at which level there were no detectable changes in balance due to self-heating of the components.

PROCEDURE

It is seen that a determination of the unit of capacitance, or of the constant $K = 1+\alpha$, consists of the primary Wien network balance and a number of secondary balances. Each measurement made with the bridge consists of a zero balance and a measure balance with the measured value being defined by the difference between the two. In each of the programmed measurements, the zero balance was made first, followed by the measure balance, then by zero, by measure, by zero, and so on. Thus, if four zero balances are made, interspersed with three measure balances, a total of six differences are obtained, which may be averaged to give a mean measurement. In this way, accidental readings or fluctuations may be eliminated, or a drift due to temperature or some other cause will be seen. In the program, the measurements were made in the following sequence: C_3, C_5, Wien, C_5, C_3, τ_4/R_4, R_3. If there is a drift in value between the sets of measurements, say for C_3, a mean of all the measurements for C_3 will give a result which represents the value of C_3 at the time the Wien balance was made. As C_5 is always smaller than C_3, and the reading sensitivity of the bridge dials approaches the limit of error desired for the measurement of C_5, this measurement was made as close to the Wien balance as possible. Altogether, for either the NORMAL or REVERSED bridge, there were 12 measurements of C_3, 12 of C_5, and 10 of the Wien balance, as well as 6 of τ_4/R_4 for each individual determination of α. By taking the average of each group, a representative mean value is obtained, and a suggestion of a standard deviation or a probable error appears.

In this determination, all the measurements are made by means of the Type 12 Capacitance and Conductance Bridge, using the various capacitors built into the bridge as standards of reference. As with all measuring bridges, the indications of the dials are not wholly correct and the bridge must be calibrated. This may be done in the present bridge by a step-down method of autocalibration, i.e. by comparing a step on one dial with 10 steps on the next lower dial. Since the capacitors in each decade are completely shielded from those in the other decades this procedure gives an accurate comparison between nominally equal dial settings. When extended over the five decades of capacity, this furnishes a precise comparison of any bridge setting with any other, although it gives no information as to the absolute values of any of the settings. The absolute value may be determined by measuring the value of a known standard and adjusting the whole calibration to fit. Alternatively, it may be assumed that the dial settings, when corrected for their relative values, differ from the absolute value by some constant ratio $K = 1+\alpha$, which is what is done in this case. It will be seen that the whole of this determination depends on the precision of the relative values obtained from the autocalibration, as well as the stability of the bridge units.

It is believed that the autocalibrations performed on this bridge are of

adequate precision. In addition, comparison of results for about four years shows no appreciable relative shift of the values obtained. As this includes both air decades and mica decades of capacitance, the assumption of constancy or stability is more reasonable than postulating that two such widely different types of capacitor should change by the same relative amounts.

The measurements which make up this determination of the unit of capacitance divide themselves into three distinct sets, as follows:

Set No. 1 (December, 1956)—frequency 1000 c.p.s.; total number of determinations, 21.

Set No. 2 (May, 1957)—frequency 1000 c.p.s.; total number of determinations, 20.

Set No. 3 (June, 1957)—frequency 1591.55 c.p.s.; total number of determinations, 20.

Set No. 1 was the first group of measurements which could be considered to be other than exploratory, and is given equal weight with the later measurements. As a result of the experience gained from this set, the whole circuit was rebuilt in a more stable form. Set No. 2 was then obtained under these improved conditions, but is nominally identical with set No. 1, except for the 6-month difference in time. Set No. 3 is a repeat of set No. 2 at a different frequency, but at essentially the same time. In all cases, the results were corrected for variation of temperature, relative humidity, and barometric pressure. Thus, the final results represent a value of α for atmospheric conditions of 22° C, 50% relative humidity, and barometric pressure of 29.9 in. of mercury.

DISCUSSION OF RESULTS

The values obtained from the three sets of measurements are shown in Tables I, II, and III. Each value of $2\alpha \mp (\tau_2 - \tau_1)/C_5R_3$ (coming from eq. 9) is derived from eight terms which are experimentally obtained from the main and auxiliary bridge balances, two terms which come from the autocalibration of the bridge, and one term from the temperature at which the experiment was made and the temperature coefficient of the capacitors in the bridge. Of these 11 terms which make up the value of Σ in equation 9, some are more precise than others, and an estimate of the standard deviation of each has been made. The total effect on the value of $2\alpha \mp (\tau_2 - \tau_1)/C_5R_3$ is given by

$$\sigma_{2\alpha}{}^2 = \sigma_1{}^2 + \sigma_2{}^2 \ldots + \sigma_{11}{}^2. \tag{10}$$

The value of α itself is obtained as a mean of the NORMAL and REVERSED measurements, and the standard deviation of the resulting value is given by

$$\sigma_{2\alpha}{}^2 = 4\sigma_\alpha{}^2 = \frac{\sigma_N{}^2 + \sigma_R{}^2}{2} + \frac{(2\alpha_N - 2\alpha_R)^2}{4}. \tag{11}$$

The values of σ obtained by this method are shown as indeterminacies in the values of 2α and α in the tables.

Examination of the data in Tables I, II, and III shows what appears to be a correlation between the values of α and the value of resistor R_3 used

TABLE I

Value of α at 1000 c.p.s., December 1956

R_3 (Ω)	C_3 (μf)	C_5 (μf)	N $2\alpha-(\tau_2-\tau_1)/C_5R_3$ ($\times10^{-6}$)	R $2\alpha+(\tau_2-\tau_1)/C_5R_3$ ($\times10^{-6}$)	α ($\times10^{-6}$)	$\alpha-\alpha_{EQ}$ ($\times10^{-6}$)
500	1.030	.090	−223±57	−170±60	−98±32	+0.1
	.790	.110	−177±98	−217±95	−98±49	+0.1
	.610	.130	−165±94	−240±94	−101±50	−2.9
	.450	.150	−179±98	−213±95	−98±49	+0.1
1000	.810	.030	−131±72	−189±73	−80±39	−12.4
	.590	.040	−139±59	−233±60	−93±38	−25.4
	.450	.050	−102±54	−191±53	−73±35	−5.4
	.350	.060	−111±52	−189±51	−75±32	−7.4
	.270	.070	−109±56	−197±52	−76±35	−8.4
	.160	.080	−37±76	−198±74	−59±53	+8.6
2000	.620	.010	−129±115	−166±109	−74±56	−21.6
	.300	.020	−127±83	−162±81	−72±42	−19.6
	.170	.030	−161±83	−151±82	−78±42	−25.6
	.080	.040	−130±81	−251±82	−95±51	−42.6
5000	.140	.007	−30±151	+19±152	−3±77	+40.2
	.120	.008	+37±143	+12±141	+12±71	+55.2
	.100	.009	−95±133	−87±127	−45±65	−1.8
	.090	.010	−111±102	−59±102	−42±53	+1.2
	.080	.011	−66±101	−75±101	−35±51	+8.2
	.070	.012	−84±95	−228±96	−78±60	−34.8
	.060	.013	−56±90	−302±91	−89±77	−45.8

TABLE II

Values of α at 1000 c.p.s., May 1957

R_3 (Ω)	C_3 (μf)	C_5 (μf)	N $2\alpha-(\tau_2-\tau_1)/C_5R_3$ ($\times10^{-6}$)	R $2\alpha+(\tau_2-\tau_1)/C_5R_3$ ($\times10^{-6}$)	α ($\times10^{-6}$)	$\alpha-\alpha_{EQ}$ ($\times10^{-6}$)
500	.900	.100	−183±96	−359±92	−135±65	−36.9
	.700	.120	−277±95	−357±96	−158±54	−59.9
	.550	.138	−244±92	−299±101	−136±51	−37.9
	.450	.150	−184±95	−384±95	−142±69	−43.9
	.360	.158	−202±102	−275±105	−119±55	−20.9
1000	.760	.032	−93±71	−220±75	−78±48	−10.4
	.590	.040	−95±62	−184±62	−70±38	−2.4
	.450	.050	−100±58	−167±57	−68±34	−0.4
	.350	.060	−95±60	−267±52	−90±52	−22.4
	.180	.079	−66±70	−261±58	−82±59	−14.4
2000	.295	.020	−89±87	−148±80	−59±45	−6.6
	.225	.025	−90±85	−151±80	−60±44	−7.6
	.175	.030	−158±80	−144±80	−75±40	−22.6
	.117	.037	−186±75	−158±78	−86±39	−33.6
	.097	.039	−105±80	−150±77	−64±41	−11.6
5000	.118	.008	−33±150	−142±136	−44±77	−0.8
	.103	.009	−145±127	−2±143	−38±77	+5.2
	.090	.010	−135±102	−104±103	−60±52	−16.8
	.079	.011	−118±105	−110±109	−57±54	−13.8
	.070	.012	−116±104	−152±102	−67±53	−23.8

TABLE III

Values of α at 1591.55 c.p.s., June 1957

R_3 (Ω)	C_3 (μf)	C_5 (μf)	N $2\alpha-(\tau_2-\tau_1)/C_5R_3$ (×10⁻⁶)	R $2\alpha+(\tau_2-\tau_1)/C_5R_3$ (×10⁻⁶)	α (×10⁻⁶)	$\alpha-\alpha_{EQ}$ (×10⁻⁶)
500	.958	.040	−93±85	−249±96	−85±60	+13.1
	.747	.050	−33±87	−232±92	−66±67	+32.1
	.600	.060	−70±87	−278±96	−87±69	+11.1
	.400	.080	−101±87	−224±102	−81±57	+17.1
	.200	.100	−40±121	−103±134	−36±66	+62.1
1000	.990	.010	+116±108	−184±117	−17±94	+50.6
	.479	.020	−72±74	−73±100	−36±44	+31.6
	.300	.030	−72±69	−38±88	−27±40	+40.6
	.200	.040	+27±82	−52±85	−6±46	+61.6
	.100	.050	−4±104	−49±101	−13±53	+54.6
2000	.304	.008	+140±91	−146±92	−2±85	+50.4
	.240	.010	+62±90	−135±76	−18±65	+34.4
	.150	.015	−30±87	−128±69	−39±46	+13.4
	.100	.020	−44±76	−165±61	−52±46	+0.4
	.050	.025	−17±79	−226±50	−61±62	−8.6
5000	.060	.006	−60±88	+90±95	+7±59	+50.2
	.049	.007	−70±79	+52±87	−4±52	+39.2
	.040	.008	−56±79	−103±57	−40±36	+3.2
	.032	.009	−96±71	−135±57	−58±34	−14.8
	.020	.010	−251±75	−250±69	−125±36	−81.8

in the determination. Following a general statistical method, a correlation coefficient between α and $G_3 = 1/R_3$ was determined, indicating strong correlation for the 1000 c.p.s. results and a questionable correlation for the 1591.6 c.p.s. results. In a general way, this effect is to be expected from a discussion of the effects of intermodulation distortion in the detector.*

The data in Tables I, II, and III show no significant differences when treated individually, which is to be expected if α is to be independent of time and frequency over the narrow ranges considered. In the final treatment of the data, the three sets of values were considered as one, leading to an equation of correlation given by

$$\alpha_{EQ} = [-37-.030G_3]10^{-6} \qquad (G_3 \text{ expressed in } \mu\text{mho}) \tag{12}$$

with a correlation coefficient of −0.96. It is now possible to obtain a standard deviation for the results by comparing the individual values of α with the mean values predicted by equation (12). The deviations are listed in Tables I, II, and III in the columns headed $(\alpha-\alpha_{EQ})$. A value of σ, the standard deviation, suggests a precision for the individual values of a group making up a mean value, but in itself does not suggest anything about the reliability of the mean value although a figure that is often quoted as representing the accuracy of a mean value is $3\sigma_M = 3\sigma/\sqrt{n}$. The standard deviation and accuracy of the mean for this data amount to $\pm 31\times10^{-6}$ and $\pm 12\times10^{-6}$ respectively. Application of the criterion that half of the residuals will be

*Division of Applied Physics Report APEM-386.

less in absolute magnitude than the probable error indicates a value of $\pm 20 \times 10^{-6}$ for the probable error of a single observation, compared with $\pm 21 \times 10^{-6}$ derived from the standard deviation. This agreement indicates an approximate Gaussian distribution of the data obtained here. From these considerations, a final value of α for operating frequencies in the neighborhood of 1000 c.p.s. may be given as

$$\alpha = [-37 \pm 15 - .030 G_3] 10^{-6}. \tag{13}$$

The normal use of the Type 12 Capacitance Bridge is not frequency sensitive, and the effects of intermodulation distortion are eliminated. Thus the appropriate value of α to be used in normal measurements is that obtained for small or zero G_3, i.e.

$$\alpha = (-37 \pm 15) 10^{-6} \tag{14}$$

for our laboratory atmospheric conditions, i.e. 22° C, 50% R.H., and 29.9 in. barometric pressure.

The figure of $\pm 15 \times 10^{-6}$ is an estimate of the magnitude of the random errors of the experiment. To this must be added the estimates of the various systematic errors which are also present, such as

$\pm 5 \times 10^{-6}$ due to scaling the unit of resistance from 1 ohm to 10,000 ohms.

$\pm 5 \times 10^{-6}$ representing the indeterminacy in the ratio of a-c. resistance to d-c. resistance.

$\pm 1 \times 10^{-6}$ due to source frequency of 1000 c.p.s.

or

$\pm 10 \times 10^{-6}$ due to source frequency of 1591.6 c.p.s.

Because the 1591.6 c.p.s. results make up only one-third of the total data, a figure of $\pm 25 \times 10^{-6}$ has been taken as a measure of the total error involved in the experiment.

In this way, any normal capacitance measurement made with the Type 12 Capacitance and Conductance Bridge used here may be referred to an absolute scale of capacitance by the relation

$$\begin{aligned} C_{\text{abs}} &= \Delta C_{\text{dials}}(1+\alpha), \\ &= \Delta C_{\text{dials}}[1-(37 \pm 25) 10^{-6}]. \end{aligned}$$

An indication of the validity of these capacitance measurements may be obtained by comparing results on two high quality quartz air capacitors of value 5000 $\mu\mu$f and 10,000 $\mu\mu$f which had been measured at the National Physical Laboratory, Teddington, before delivery to Canada. The comparative measurements are shown in Table IV.

It is to be noted that the unit of capacitance determined here is based on the absolute unit of resistance maintained in this laboratory by a group of 1-ohm standard resistors, which in turn are periodically compared with representative units of other national standardizing laboratories through the services of the International Bureau of Weights and Measures in Sèvres,

TABLE IV

Absolute values of quartz air capacitors

Date	5000 $\mu\mu$f	10,000 $\mu\mu$f
1/57	$4999.8_7 \pm .02$	$9998._{78} \pm .25$
4/57	$4999.8_1 \pm .02$	Not measured
7/57	$4999.9_7 \pm .02$	$9998._{33} \pm .25$
12/57	$5000.0_4 \pm .02$	$9998.8_1 \pm .05$

NOTE: All values reduced to atmospheric conditions of 22° C, 50% R.H., 29.9 in. pressure. The indeterminacies listed above are the precision of measurement and computation. The accuracy of the measurements is ±0.0025%, or ±0.13 $\mu\mu$f for the 5000 $\mu\mu$f unit and ±0.25 $\mu\mu$f for the 10,000 $\mu\mu$f unit.

In September, 1956, the same capacitors were measured at the National Physical Laboratories, Teddington, England, before delivery to Canada. The values obtained at that time were 5000.0_6 and 9999.3_9 $\mu\mu$f.

France. In addition, a direct comparison between our laboratory standards and an absolute ohm derived from our primary inductor by Romanowski and Olson (1957) substantiates the validity of this basis for resistance measurements.

CONCLUSION

An absolute unit of capacitance has been derived from the units of resistance and frequency maintained in the laboratory, by means of a modified Wien bridge circuit and the use of a Type 12 Capacitance and Conductance Bridge. It has been found that the unit of capacitance maintained by the standard capacitors forming part of the bridge differs from the absolute unit by 37 parts in a million. The accuracy assigned to this determination is ±0.0025%. This means that the measuring bridge has been constructed and adjusted with high precision, and for most work of a routine nature it is not necessary to make any correction. The unit of capacitance derived here will subsequently be maintained in this laboratory by a group of high quality capacitance standards as well as the standards in the bridge, and the bridge unit may be checked at any time. Periodic redeterminations of the unit of capacitance in an absolute sense by the method reported here will ensure that the unit remains consistent.

REFERENCES

FERGUSON, J. G. and BARTLETT, B. W. 1928. Bell System Tech. J. **7**, 420.
HARRIS, F. K. 1952. Electrical measurements, John Wiley & Sons, Inc. p. 727.
ROMANOWSKI, M. and OLSON, N. 1957. Can. J. Phys. **35**, 1312.
SHACKELTON, W. F. and FERGUSON, J. G. 1928. Bell System Tech. J. **7**, 70.
WIEN, M. 1891. Ann. Physik u. Chem. **44**, 689.

NOTE ON THE MOTION OF ELECTRONS AND HOLES IN PERTURBED LATTICES[1]

R. R. HAERING

ABSTRACT

A new set of orthogonal, localized functions is discussed. The functions bear the same relation to the functions of Luttinger and Kohn as the Wannier functions bear to the Bloch functions. The new functions are used to give an alternative derivation of the effective mass equation.

1. INTRODUCTION

The problem of the motion of charge carriers in a perturbed periodic field has received a good deal of attention in recent years. For slowly varying potentials, Slater (1949) derived the so-called effective mass equation by expanding the eigenfunctions of the perturbed Hamiltonian in terms of a set of localized, orthogonal functions first introduced by Wannier (1937). An equivalent derivation can be given by using an expansion in terms of Bloch functions (Kohn 1958). Both of these treatments suffer the disadvantage that they apply only to simple band structures (i.e. nondegenerate bands with extremum at $\mathbf{k} = 0$), and that they are not readily generalized to more complicated cases. This difficulty was overcome by Luttinger and Kohn (1955) through the introduction of a new set of functions. Their derivation for the simple band case is somewhat more involved than previous treatments; however, it has the great advantage of being readily generalized to more complicated band structures.

In the following sections, we shall define a new set of localized, orthogonal functions, and use these to give an alternative derivation of the effective mass equation. The new functions may be defined in terms of those of Luttinger and Kohn and bear the same relation to the latter as the Wannier functions bear to the Bloch functions. However, contrary to the derivation in terms of Wannier functions, the present treatment is readily generalized to more complicated band structures.

2. LOCALIZED ORTHOGONAL FUNCTIONS

We begin by defining the functions of Luttinger and Kohn (1955) for box normalization.[2] Let

$$\varphi_{n\mathbf{k}}^{\mathbf{k}_0} = e^{i(\mathbf{k}-\mathbf{k}_0)\cdot\mathbf{r}}\psi_{n\mathbf{k}_0}. \tag{1}$$

According to Bloch's theorem we may write

$$\psi_{n\mathbf{k}_0} = e^{i\mathbf{k}_0\cdot\mathbf{r}}u_{n\mathbf{k}_0}$$

[1]Manuscript received September 29, 1958.
Contribution from the Department of Physics, McMaster University, Hamilton, Ontario.

[2]Our definition of the functions $\varphi_{n\mathbf{k}}^{\mathbf{k}_0}$ differs from the definition of Luttinger and Kohn by a factor $e^{-i\mathbf{k}_0\cdot\mathbf{r}}$. This change is desirable so that $\varphi_{n\mathbf{k}_0}^{\mathbf{k}_0} = \psi_{n\mathbf{k}_0}$.

where $u_{n\mathbf{k}_0}$ is a function with the lattice periodicity. Hence we may also write equation (1) in the form

$$\varphi_{n\mathbf{k}}^{\mathbf{k}_0} = e^{i\mathbf{k}\cdot\mathbf{r}} u_{n\mathbf{k}_0}. \tag{1a}$$

It is readily checked that the functions $\varphi_{n\mathbf{k}}^{\mathbf{k}_0}$ defined by (1) and (1*a*) form a complete orthonormal set if the Bloch functions form such a set. Hence if

$$(\psi_{n\mathbf{k}}, \psi_{n'\mathbf{k}'}) = \delta_{nn'}\delta_{\mathbf{k}\mathbf{k}'} \tag{2}$$

then

$$(\varphi_{n\mathbf{k}}^{\mathbf{k}_0}, \varphi_{n'\mathbf{k}'}^{\mathbf{k}_0}) = \delta_{nn'}\delta_{\mathbf{k}\mathbf{k}'}. \tag{3}$$

Consider now the functions defined by

$$\begin{aligned} b_n^{\mathbf{k}_0}(\mathbf{r}, \mathbf{R}_j) &= \frac{1}{\sqrt{N}} \sum_{\mathbf{k}} e^{-i\mathbf{k}\cdot\mathbf{R}_j} \varphi_{n\mathbf{k}}^{\mathbf{k}_0}, \\ &= \frac{1}{\sqrt{N}} u_{n\mathbf{k}_0} \sum_{\mathbf{k}} e^{i\mathbf{k}\cdot(\mathbf{r}-\mathbf{R}_j)}. \end{aligned} \tag{4}$$

In equation (4), N denotes the number of cells in the crystal, $\mathbf{R}_j$ denotes a lattice vector, and the sum over $\mathbf{k}$ extends over the first Brillouin zone. (In what follows, all $\mathbf{k}$-sums will extend over this region.)

Let us compare (4) with the Wannier functions, $a_n(\mathbf{r}-\mathbf{R}_j)$, whose definition is

$$a_n(\mathbf{r}-\mathbf{R}_j) = \frac{1}{\sqrt{N}} \sum_{\mathbf{k}} e^{-i\mathbf{k}\cdot\mathbf{R}_j} \psi_{n\mathbf{k}}. \tag{5}$$

A comparison of (4) and (5) shows that our b_n's bear the same relation to the $\varphi_{n\mathbf{k}}^{\mathbf{k}_0}$ as the a_n's bear to the $\psi_{n\mathbf{k}}$. From the second line in equation (4), it is also clear that the b_n's like the a_n's are functions only of $\mathbf{r}-\mathbf{R}_j$.

The localization of $b_n(\mathbf{r}-\mathbf{R}_j)$ is apparent from (4). We write

$$b_n(\mathbf{r}-\mathbf{R}_j) = \frac{1}{\sqrt{N}} u_{n\mathbf{k}_0} \Delta(\mathbf{r}-\mathbf{R}_j)$$

where

$$\Delta(\mathbf{r}-\mathbf{R}_j) = \sum_{\mathbf{k}} e^{i\mathbf{k}\cdot(\mathbf{r}-\mathbf{R}_j)}.$$

$\Delta(\mathbf{r}-\mathbf{R}_j)$ is a δ-like function with a spread of about one lattice spacing, peaked at $\mathbf{r} = \mathbf{R}_j$. Apart from a factor of $(NV)^{-\frac{1}{2}}$, $\Delta(\mathbf{r}-\mathbf{R}_j)$ is in fact the Wannier function for free electrons.

Our claim is now that the b_n's form a complete orthonormal set of localized functions. We thus have

$$(b_n^{\mathbf{k}_0}(\mathbf{r}-\mathbf{R}_j), b_{n'}^{\mathbf{k}_0}(\mathbf{r}-\mathbf{R}_{j'})) = \delta_{nn'}\delta_{jj'}. \tag{6}$$

Let us first test the completeness. If we expand an arbitrary function $f(\mathbf{r})$ in terms of the b_n's, we write

$$f(\mathbf{r}) = \sum_{n,j} \xi_n(\mathbf{R}_j) b_n^{\mathbf{k}_0}(\mathbf{r}-\mathbf{R}_j). \tag{7}$$

Because of (4), this is equivalent to

$$f(\mathbf{r}) = \sum_{n,\mathbf{k}} \rho_n(\mathbf{k}) \varphi_{n\mathbf{k}}^{\mathbf{k}_0} \tag{7a}$$

where

$$\rho_n(\mathbf{k}) = \frac{1}{\sqrt{N}} \sum_j \xi_n(\mathbf{R}_j) e^{-i\mathbf{k}\cdot\mathbf{R}_j}.$$

Hence the b_n's form a complete set if the $\varphi_{n\mathbf{k}}^{\mathbf{k}_0}$ do.

The orthonormality is also readily established. From (4) we have

$$\begin{aligned} (b_n^{\mathbf{k}_0}(\mathbf{r}-\mathbf{R}_j), b_{n'}^{\mathbf{k}_0}(\mathbf{r}-\mathbf{R}_{j'})), & \\ &= \frac{1}{N} \sum_{\mathbf{k},\mathbf{k}'} e^{i\mathbf{k}\cdot\mathbf{R}_j} e^{-i\mathbf{k}'\cdot\mathbf{R}_{j'}} \int d\tau \varphi_{n\mathbf{k}}^{\mathbf{k}_0 *} \varphi_{n'\mathbf{k}'}^{\mathbf{k}_0}, \\ &= \frac{1}{N} \sum_{\mathbf{k},\mathbf{k}'} e^{i\mathbf{k}\cdot\mathbf{R}_j} e^{-i\mathbf{k}'\cdot\mathbf{R}_{j'}} \delta_{nn'}\delta_{\mathbf{k}\mathbf{k}'}, \\ &= \delta_{nn'}\delta_{jj'}, \end{aligned} \tag{8}$$

which establishes equation (6). Finally, we point out that (4) is readily inverted to give

$$\varphi_{n\mathbf{k}}^{\mathbf{k}_0} = \frac{1}{\sqrt{N}} \sum_j e^{i\mathbf{k}\cdot\mathbf{R}_j} b_n^{\mathbf{k}_0}(\mathbf{r}-\mathbf{R}_j). \tag{9}$$

The close analogy between equations (4), (8), (9) and the corresponding relations for Wannier functions need hardly be stressed.

3. DERIVATION OF THE EFFECTIVE MASS EQUATION

As an application of our localized functions we shall derive the effective mass equation for a simple band with extremum at $\mathbf{k} = 0$. The generalization of this result to more complex band structures will become obvious.

For the case of a simple band we choose the set of localized functions

$$\begin{aligned} b_n^0(\mathbf{r}-\mathbf{R}_j) &= \frac{1}{\sqrt{N}} u_{n0} \sum_{\mathbf{k}} e^{i\mathbf{k}\cdot(\mathbf{r}-\mathbf{R}_j)}, \\ &= \frac{1}{\sqrt{N}} \sum_{\mathbf{k}} e^{-i\mathbf{k}\cdot\mathbf{R}_j} \varphi_{n\mathbf{k}}^{0}. \end{aligned} \tag{10}$$

In order not to complicate the notation, we omit the superscript zero in what follows.

Consider now the Schrödinger equation in the presence of a perturbation $U(\mathbf{r})$.

$$H\Psi = E\Psi \tag{11}$$

where

$$H = H_0 + U(\mathbf{r}).$$

The eigenfunctions of H_0 are the Bloch functions

$$H_0\psi_{n\mathbf{k}} = \epsilon_n(\mathbf{k})\psi_{n\mathbf{k}}. \tag{12}$$

To solve (11), we expand Ψ in terms of the b_n's

$$\Psi = \sum_{n',j'} c_{n'}(\mathbf{R}_{j'}) b_{n'}(\mathbf{r}-\mathbf{R}_{j'}). \tag{13}$$

Substituting (13) in (11), multiplying by $b_n^*(\mathbf{r}-\mathbf{R}_j)$ on the left and integrating over the crystal volume, one obtains a set of equations for the coefficients $c_n(\mathbf{R}_j)$.

$$\sum_{n',j'} (nj|H_0|n'j')c_{n'}(\mathbf{R}_{j'}) + \sum_{n',j'} (nj|U|n'j')c_{n'}(\mathbf{R}_{j'}) = Ec_n(\mathbf{R}_j) \tag{14}$$

where

$$(nj|H_0|n'j') = \int d\tau b_n^*(\mathbf{r}-\mathbf{R}_j) H_0 b_{n'}(\mathbf{r}-\mathbf{R}_{j'}) \tag{14a}$$

and

$$(nj|U|n'j') = \int d\tau b_n^*(\mathbf{r}-\mathbf{R}_j)\, U(\mathbf{r}) b_{n'}(\mathbf{r}-\mathbf{R}_{j'}). \tag{14b}$$

Let us look at the matrix elements (14a) and (14b) more closely. Consider first the matrix elements of the perturbation $U(\mathbf{r})$. We assume at this stage that $U(\mathbf{r})$ is a slowly varying function of $\mathbf{r}$.[3] Since $b_n(\mathbf{r}-\mathbf{R}_j)$ is strongly peaked at $\mathbf{r} = \mathbf{R}_j$, we may then replace $U(\mathbf{r})$ by $U(\mathbf{R}_j)$ in (14b), and use equation (6) to obtain

$$(nj|U|n'j') = U(\mathbf{R}_j)\delta_{nn'}\delta_{jj'}. \tag{15}$$

For later convenience it is desirable to rewrite (15) somewhat.

$$\begin{aligned}(nj|U|n'j') &= U(\mathbf{R}_j)\delta_{nn'}\delta_{jj'}, \\ &= \frac{1}{N}\sum_{\mathbf{k},\mathbf{k}'} e^{i\mathbf{k}\cdot\mathbf{R}_j} e^{-i\mathbf{k}'\cdot\mathbf{R}_{j'}} (n\mathbf{k}|U|n'\mathbf{k}'),\end{aligned} \tag{15a}$$

where

$$(n\mathbf{k}|U|n'\mathbf{k}') = \frac{1}{N}\delta_{nn'}\sum_l e^{i(\mathbf{k}'-\mathbf{k})\cdot\mathbf{R}_l} U(\mathbf{R}_l).$$

Next consider the matrix element (14a).

$$(nj|H_0|n'j') = \frac{1}{N}\sum_{\mathbf{k},\mathbf{k}'} e^{i\mathbf{k}\cdot\mathbf{R}_j} e^{-i\mathbf{k}'\cdot\mathbf{R}_{j'}} (n\mathbf{k}|H_0|n'\mathbf{k}') \tag{16}$$

where

$$(n\mathbf{k}|H_0|n'\mathbf{k}') = \int d\tau \varphi_{n\mathbf{k}}^* H_0 \varphi_{n'\mathbf{k}'}.$$

The matrix element $(n\mathbf{k}|H_0|n'\mathbf{k}')$ has been evaluated by Luttinger and Kohn (1955). One readily finds that:

$$(n\mathbf{k}|H_0|n'\mathbf{k}') = \left[\left\{\epsilon_n(0) + \frac{\hbar^2 k^2}{2m}\right\}\delta_{nn'} + \frac{\hbar\mathbf{k}\cdot\mathbf{p}_{nn'}}{m}\right]\delta_{\mathbf{k}\mathbf{k}'}, \tag{17}$$

where

$$\mathbf{p}_{nn'} = \int d\tau u_{n0}^*(-i\hbar\nabla)u_{n'0}. \qquad (\mathbf{p}_{nn} = 0)$$

[3]Not all perturbations realized in practice satisfy this condition. For a further discussion, see Feuer (1952).

It is desirable to split $(nj|H_0|n'j')$ into a part diagonal in the n indices and an off-diagonal part. We write $H_0 = H_0^0 + H_0^1$ where

$$(nj|H_0^0|n'j') = \frac{1}{N}\sum_{\mathbf{k},\mathbf{k}'} e^{i\mathbf{k}\cdot\mathbf{R}_j} e^{-i\mathbf{k}'\cdot\mathbf{R}_{j'}} (n\mathbf{k}|H_0^0|n'\mathbf{k}'), \tag{18a}$$

$$(nj|H_0^1|n'j') = \frac{1}{N}\sum_{\mathbf{k},\mathbf{k}'} e^{i\mathbf{k}\cdot\mathbf{R}_j} e^{-i\mathbf{k}'\cdot\mathbf{R}_{j'}} (n\mathbf{k}|H_0^1|n'\mathbf{k}'), \tag{18b}$$

and

$$(n\mathbf{k}|H_0^0|n'\mathbf{k}') = \left[\epsilon_n(0) + \frac{\hbar^2 k^2}{2m}\right]\delta_{nn'}\delta_{\mathbf{k}\mathbf{k}'},$$

$$(n\mathbf{k}|H_0^1|n'\mathbf{k}') = \left[\frac{\hbar\mathbf{k}\cdot\mathbf{p}_{nn'}}{m}\right]\delta_{\mathbf{k}\mathbf{k}'}.$$

A comparison of equations (14), (15a), (18a), and (18b) then shows that the equations for the various $c_n(\mathbf{R}_j)$ are still coupled via the terms $(nj|H_0^1|n'j')$. We now proceed to eliminate this coupling by a canonical transformation. Define new coefficients $d_n(\mathbf{R}_j)$ by

$$c_n(\mathbf{R}_j) = \sum_{n',j'} (nj|e^S|n'j') d_{n'}(\mathbf{R}_{j'}). \tag{19}$$

The equations satisfied by the $d_n(\mathbf{R}_j)$ are then

$$\sum_{n',j'} (nj|e^{-S}(H_0^0 + H_0^1 + U)e^S|n'j') d_{n'}(\mathbf{R}_{j'}) = E d_n(\mathbf{R}_j). \tag{20}$$

Here, S is to be chosen so that the equations for the $d_n(\mathbf{R}_j)$ are decoupled to first order. We shall not give the details of this transformation here, since it is closely related to that of Luttinger and Kohn (1955). If we choose S to have the following matrix elements in the b_n representation

$$(nj|S|n'j') = \frac{1}{N}\sum_{\mathbf{k},\mathbf{k}'} e^{i\mathbf{k}\cdot\mathbf{R}_j} e^{-i\mathbf{k}'\cdot\mathbf{R}_{j'}} (n\mathbf{k}|S|n'\mathbf{k}'), \tag{21}$$

where

$$(n\mathbf{k}|S|n'\mathbf{k}') = -(n\mathbf{k}|H_0^1|n'\mathbf{k}'), \qquad (n' \neq n)$$

$$= 0, \qquad (n' = n)$$

then the equation for $d_n(\mathbf{R}_j)$ becomes

$$\frac{1}{N}\sum_{\mathbf{k},j'} e^{i\mathbf{k}\cdot(\mathbf{R}_j - \mathbf{R}_{j'})} \epsilon_n(\mathbf{k}) d_n(\mathbf{R}_{j'}) + U(\mathbf{R}_j) d_n(\mathbf{R}_j) = E d_n(\mathbf{R}_j). \tag{22}$$

Here

$$\epsilon_n(\mathbf{k}) = \epsilon_n(0) + \frac{1}{2}\frac{\partial^2 \epsilon_n(0)}{\partial k^2} k^2$$

is the expansion of the Bloch energy $\epsilon_n(k)$ about $\mathbf{k} = 0$. Equation (22) ignores the (reduced) coupling with equations for $d_m(\mathbf{R}_j)$, $(m \neq n)$. This coupling can be shown to be negligible if the potential is slowly varying.

Putting $\mathbf{R}_S = \mathbf{R}_j - \mathbf{R}_{j'}$ in (22) and using the displacement operator equation

$$f(\mathbf{R}_j - \mathbf{R}_S) = e^{-\mathbf{R}_S \cdot \nabla_j} f(\mathbf{R}_j)$$

we readily find

$$\frac{1}{N}\sum_{\mathbf{k},S} e^{i(\mathbf{k}+i\nabla_j)\cdot\mathbf{R}_S}\epsilon_n(\mathbf{k})d_n(\mathbf{R}_j) + U(\mathbf{R}_j)d_n(\mathbf{R}_j) = Ed_n(\mathbf{R}_j), \tag{23}$$

which becomes, on performing the sum over $\mathbf{R}_S$

$$[\epsilon_n(-i\nabla) + U(\mathbf{R}_j)]d_n(\mathbf{R}_j) = Ed_n(\mathbf{R}_j). \tag{24}$$

If $\mathbf{R}_j$ is treated as a continuous variable, equation (24) is the equation which determines the eigenvalues E of the perturbed problem.

4. DISCUSSION

Equation (24) is identical with the equation derived on the basis of Wannier functions (Slater 1949). It would however be a trivial matter to generalize (24) to more complex band structures using our b_n's, while a similar generalization is not possible in a Wannier function treatment. For instance, in the case of multiple minima we would simply replace the b_n's defined by (10) by

$$b_n^{\mathbf{k}_0}(\mathbf{r}-\mathbf{R}_j) = \frac{1}{\sqrt{N}} u_{n\mathbf{k}_0} \sum_{\mathbf{k}} e^{i\mathbf{k}\cdot(\mathbf{r}-\mathbf{R}_j)}.$$

A completely analogous derivation then leads to equation III.6 of Luttinger and Kohn (1955). A similar generalization is possible when the bands are degenerate.

ACKNOWLEDGMENTS

The author would like to thank Professor R. E. Peierls for a stimulating discussion. The financial support of the National Research Council in the form of an N.R.C. postdoctoral fellowship is gratefully acknowledged.

REFERENCES

FEUER, P. 1952. Phys. Rev. **88**, 92.
KOHN, W. 1958. Solid state physics, Vol. 5 (Academic Press Inc., New York), p. 257.
LUTTINGER, J. M. and KOHN, W. 1955. Phys. Rev. **97**, 869.
SLATER, J. C. 1949. Phys. Rev. **76**, 1592.
WANNIER, G. H. 1937. Phys. Rev. **52**, 191.

SOME PROPERTIES OF THE 2.23-MEV EXCITED STATE OF P^{31} [1]

A. E. Litherland, E. B. Paul,[2] G. A. Bartholomew, and H. E. Gove

ABSTRACT

The 2.23-Mev excited state of P^{31} has been studied by means of the capture gamma rays from the 1.70-Mev resonance in the reaction $Si^{30}(p\gamma)P^{31}$. The angular correlation of the ground state gamma ray established that the resonance had total angular momentum 3/2, and triple correlation measurements of the cascading gamma rays from the compound state showed that the angular momentum of the 2.23-Mev state was 5/2. Coincidence measurements showed that the cascade gamma rays from the 2.23-Mev state to the first excited state at 1.27-Mev were $< 3\%$ of the transitions to the ground state.

INTRODUCTION

The excited states of P^{31} have been studied recently and the work has been summarized in a review article by Endt and Braams (1957). Some information, regarding the spins and parities of the low-lying states, has been obtained from the study of the correlations of the gamma rays from the reaction $Si^{30}(p\gamma)P^{31}$. The zero spin of the nucleus Si^{30} provides an important simplification in the interpretation of these correlations because the only unknown properties of the compound state are the spin and parity. A nonzero spin of the bombarded nucleus introduces other parameters such as the channel spin mixture and the orbital angular momentum mixture which increase the ambiguity of a single correlation measurement (Paul *et al.* 1955).

This paper is a more detailed account of the work on $Si^{30}(p\gamma)P^{31}$, reported briefly by Paul *et al.* (1956), and also includes the results of some later measurements taken with improved apparatus. The work produced the first evidence that the second excited state of P^{31} has a spin 5/2. This conclusion has been recently confirmed by Broude (1958).

APPARATUS

The experimental equipment used for the first set of measurements, reported briefly by Paul *et al.* (1956), has been described in detail by Litherland *et al.* (1956). For the second set of measurements a conventional fast–slow coincidence arrangement (Bell *et al.* 1952) permitted resolving times of approximately 50 millimicroseconds to be used. A 100-channel pulse height analyzer of the Hutchinson–Scarrott (1952) type* was also used in addition to the 30-channel analyzer.

The proton beam from the Chalk River electrostatic generator was used to bombard a thin enriched target of Si^{30}* (approximately 10 kev thick at 1.70 Mev) deposited onto a 0.02-in. tantalum backing.

[1]Manuscript received October 14, 1958.
Contribution from the Physics Division, Atomic Energy of Canada Limited, Chalk River, Ontario.
Issued as A.E.C.L. No. 725.
[2]Now at Physics Division, Atomic Energy Research Establishment, Harwell, England.
*Obtained from Atomic Energy Research Establishment, Harwell, England.

EXPERIMENTAL PROCEDURE

The yield of gamma rays, of energies between 3.5 Mev and 10.5 Mev, from the reaction $Si^{30}(p\gamma)P^{31}$ was measured with a 5-in. diameter by 4-in. long NaI(Tl) crystal placed 2 inches from the target at 90° to the beam. The yield curve, shown in Fig. 1, was studied for proton energies lying between 1.64 Mev and 2.34 Mev. At each resonance a capture gamma ray spectrum

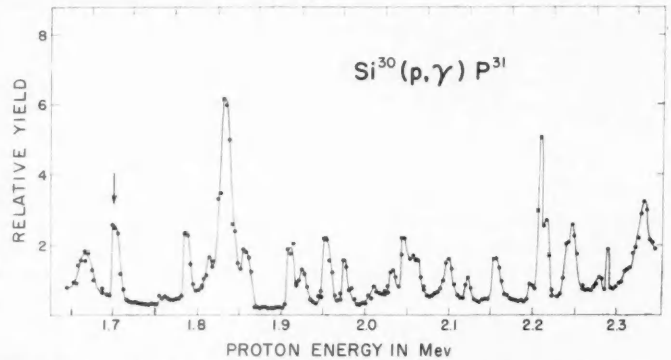

FIG. 1. The yield of gamma rays from the reaction $Si^{30}(p\gamma)P^{31}$, with energies between 3.5 Mev and 10.5 Mev, is shown as a function of proton bombarding energy. The arrow indicates the resonance studied in detail.

was obtained. The 1.70-Mev resonance was chosen for further study because of the prominent ground state and second excited state gamma ray transitions. The proton energy of the resonance was determined to be $1.697 \pm .005$ Mev by comparison with the $Li^7(p, n)$ threshold. The gamma ray pulse spectrum obtained at the 1.70-Mev resonance is shown in Fig. 2(*a*). The yield curve was then studied in more detail to check that only one resonance

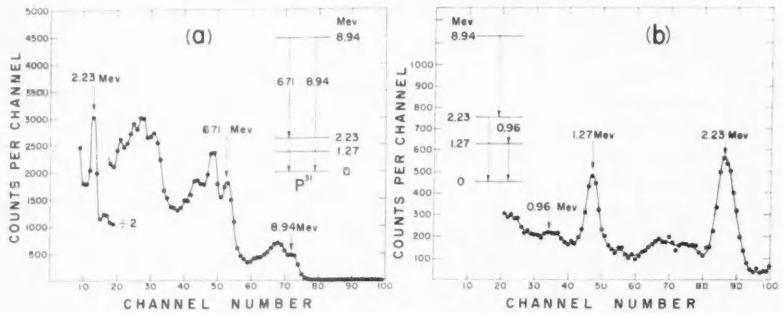

FIG. 2. (*a*) A portion of the gamma ray pulse spectrum, taken at 90° to the beam, from the $Si^{30}(p\gamma)P^{31}$ reaction at the 1.70-Mev resonance.
(*b*) The low energy region of the gamma ray pulse spectrum taken in coincidence with a gate including the 6.71-Mev gamma rays. This figure illustrates that the predominant mode of decay of the 2.23-Mev state of P^{31} is by a gamma ray transition to the ground state.

was involved. Yield curve measurements at 90° to the beam of the ground state gamma ray showed that the background contribution at the 1.70-Mev resonance from other resonances was $<5\%$. Prior to the study of the coincidence or triple correlation of the 2.23-Mev* and 6.71-Mev gamma rays, a coincidence yield curve of these gamma rays was taken. This showed that, with both 5-in. by 4-in. NaI(Tl) crystals at 90° to the beam, there was $<1\%$ contribution to the resonance at 1.70 Mev from other resonances. It should be emphasized that only one target was available for the $Si^{30}(p\gamma)P^{31}$ measurements so that it was not possible to determine whether the resonance was a close doublet nor was it possible to determine the natural width of the resonance.

The decay scheme of the 2.23-Mev state in P^{31} was determined by observing the gamma rays in coincidence with the high energy capture gamma rays. The spectrum in Fig. 2(*b*) shows a typical pulse spectrum obtained. It is clear that there is no evidence for the existence of a 0.96-Mev cascade gamma ray transition to the 1.27-Mev excited state of P^{31}. An upper limit of 3% was placed on the branching ratio. The 1.27-Mev gamma ray observed in the coincidence spectrum is due partly to the presence of a weak primary to the first excited state of P^{31} and to the complex cascading of higher states in P^{31}.

The angular correlation of the ground state gamma ray was measured using a 5-in. by 4-in. NaI(Tl) crystal situated with its front face 8.2 inches from the target spot. Care was taken to prevent the weak primary transition to the 1.27-Mev state from influencing the measured correlation. Figure 3(*a*) shows the experimental angular correlation together with the theoretical correlations (Sharp *et al.* 1953) for various spin assignments of the 1.70-Mev resonance. The least squares analysis of the angular correlation is given in Table I. The spin and parity of the ground state of P^{31} were assumed to be 1/2 and even

TABLE I

Angular distribution analysis

a_1	S.D.	a_2	S.D.	a_3	S.D.	a_4	S.D.
+0.05	0.04	−0.830	0.05	−0.03	0.06	0.003	0.05

NOTE: The angular distribution of the ground state gamma ray at the 1.70-Mev resonance in $Si^{30}(p\gamma)P^{31}$ is given in the table. The angular distribution was analyzed by the method of least squares into Legendre polynomials. The coefficients are given together with their standard deviations (S.D.). The coefficient a_0 is arbitrarily made equal to unity.

To correct for the finite solid angle of the NaI crystal the absolute value of the a_1 coefficient should be increased by approximately five per cent (Gove and Rutledge 1958). This corrected value is shown in Fig. 3(*b*).

for these comparisons (Endt and Braams 1957). If the assumption is made that magnetic quadrupole radiation cannot compete to any appreciable extent with that of the electric dipole,† then it follows that the spin and

*The measured energy of the gamma ray from the second excited state was 2.23±.03 Mev. All energy values quoted subsequently are from Endt and Braams (1957).

†The ratios Γ_{E2}/Γ_{M1} and Γ_{M2}/Γ_{E1} for the ground state transition can be evaluated on the extreme single particle model (Wilkinson 1958). They are approximately 10^{-2} and 10^{-5} respectively, which give some weight to the assumption made above.

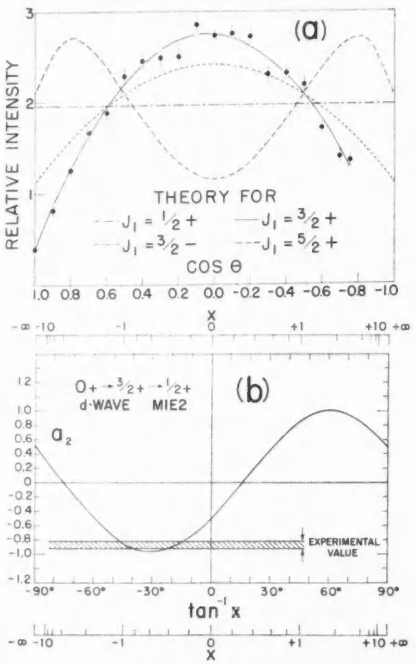

FIG. 3. (*a*) The angular correlation of the ground state gamma ray from the 1.70-Mev resonance is shown together with the theoretical curves (not corrected for geometrical effects) for various assignments of spin and parity to the resonance. The experimental curve requires a dipole–quadrupole mixture in the radiation favoring 3/2+ for the resonance. This point is discussed in the text.

(*b*) The theoretical value of the $P_2(\cos\theta)$ coefficient of the angular correlation is shown as a function of the magnetic dipole – electric quadrupole amplitude mixture of the ground state transition. The experimental value of the coefficient has been corrected for the effects of finite geometry.

parity of the 1.70-Mev resonance are 3/2 and even, since the theoretical curve for a pure dipole transition does not fit the experimental correlation. The measured value of the amplitude of the quadrupole radiation divided by the amplitude of the dipole radiation, x, can be deduced from Fig. 3(*b*). The mixing ratio x lies between -1.0 and -0.3. The large uncertainty of the determination arises from the insensitivity of the correlation coefficient to the mixing ratio in the region of $x = -0.6$ and the uncertainty of the geometrical correction to the correlation coefficient. There is also uncertainty of the ground state angular correlation coefficient due to the $\lesssim 5\%$ contributions from other resonances at the 1.70-Mev resonance.

The uncertainty of the geometrical correction is due to the inclusion of only the high-energy portion of the pulse spectrum in the measured correlation. The calculated correction is valid only if all pulses corresponding to the gamma ray under study are measured as a function of angle. The correction

factor of approximately 0.945 (Gove and Rutledge 1958) is consequently an overestimate. In spite of these uncertainties the correlation demonstrates that dipole–quadrupole mixing occurs in the ground state gamma ray transition. A rough measurement of 0.1 electron volts was made of the quantity $\Gamma_{\gamma_0}\Gamma_p/\Gamma$ at the 1.70-Mev resonance. If the assumption is made that Γ_p is approximately equal to Γ, then the experimental value of Γ_{γ_0} is small compared with the extreme single particle estimate of 20 electron volts for magnetic dipole radiation (Wilkinson) 1958. It is, however, roughly comparable with the extreme single particle estimate, for electric quadrupole radiation, of 0.3 electron volts. This implies that the large quadrupole admixture in the ground state radiation from the 1.70-Mev resonance in the reaction $Si^{30}(p\gamma)P^{31}$ is due probably to the inhibition of the dipole radiation and not the enhancement of the quadrupole radiation.

Having established the properties of the 1.70-Mev resonance by studying the ground state transition, it is possible to study the properties of the 2.23-Mev state by studying the angular correlation of the primary gamma ray transition to that state. Experience has shown, however, that the angular correlations of capture radiation are ambiguous even in the favorable case of protons bombarding a zero-spin nucleus, provided dipole–quadrupole mixtures are taken into account. The case of the triple or coincidence correlation is quite different. In the case to be discussed, of the coincidence correlation of the 2.23-Mev and 6.71-Mev gamma rays from the 1.70-Mev resonance, there are four unknown nuclear quantities. These are the spin and parity of the 2.23-Mev excited state of P^{31} and the dipole–quadrupole mixtures of the cascading gamma rays. The assumption can be made that octopole radiation does not play a significant role.* The theoretical triple correlation coefficients depend upon the geometrical arrangement of the detectors employed for the coincidence measurements (Ferguson and Rutledge 1957). Consequently, by employing several different geometrical arrangements, it is possible to obtain information about the gamma ray cascade. In the case to be discussed two geometrical arrangements sufficed to determine the spin of the 2.23-Mev state and the dipole–quadrupole mixtures of the cascading radiations. The parity of the 2.23-Mev state was also assigned upon the basis of reasonable assumptions which are discussed below.

Two very convenient spatial arrangements of the gamma ray counters are shown in Fig. 4, together with the experimental correlations of the gamma rays. These spatial arrangements can be called, for convenience, geometry A and geometry B. For the correlations shown in Fig. 4, the coincidence counting rate as a function of angle was measured by observing (*a*) the 2.23-Mev gamma ray in the fixed, $\theta = 90°$, counter (geometry A) and (*b*) the 6.71-Mev gamma ray in the fixed counter (geometry B). In each case the coincidence counts at each angle were related to each other by counting the number of ground state gamma rays in the fixed counter. This procedure corrected for

*The ratio Γ_{M3}/Γ_{E2} can be evaluated on the extreme single particle model (Wilkinson 1958). The ratio for the 6.71-Mev gamma ray is approximately 10^{-5} and for the 2.23-gamma ray is approximately 10^{-6}.

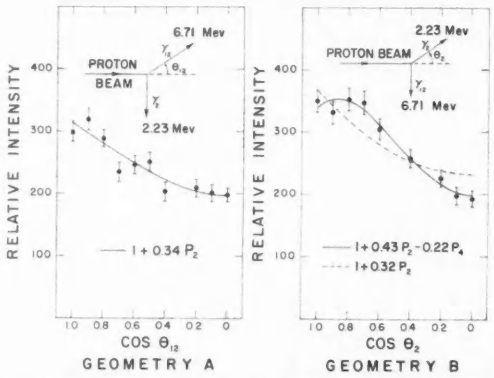

FIG. 4. The experimental results of two triple correlation measurements at the 1.70-Mev resonance are shown. The geometrical arrangements employed together with the gamma rays studied in coincidence are also shown. Curves fitted by the method of least squares are shown as solid or dotted lines.

possible variations of target thickness during bombardment. Proton currents between 5 and 10 microamperes were used during the measurements. The results of a least squares analysis of the data are presented in Table II(*b*) and

TABLE II

Triple correlation analysis

	Geometry	a_2	S.D.	a_4	S.D.
(*a*)	A	+0.21	0.08	+0.03	0.09
	B	+0.61	0.08	−0.39	0.09
(*b*)	A	+0.34	0.05	−0.04	0.06
	B	+0.43	0.03	−0.22	0.04

NOTE: Table II gives the results of the analysis of the triple correlations of the 2.23- and 6.71-Mev gamma rays and the proton beam. The two different geometrical arrangements A and B are illustrated in Fig. 4. The correlations were analyzed into even order Legendre polynomials by the method of least squares. The coefficients are given together with their standard deviations (S.D.).

The coefficients given in 2(*a*) were obtained from data taken at six angles with the NaI crystals at 8.5 inches from the target. In 2(*b*) the coefficients were obtained from data taken at nine angles with the NaI crystals at 6.2 inches from the target.

To correct the coefficients in 2(*a*) for the effects of finite geometry the a_2 and a_4 coefficients should be divided by 0.90 and 0.71 respectively. In the case of 2(*b*) the corresponding numbers are 0.83 and 0.56 (Gove and Rutledge 1958).

are also shown as solid or dotted lines in Fig. 4. The observation of a significant $P_4(\cos\theta)$ coefficient in geometry B implies that the angular momentum of the 2.23-Mev state is $\geqslant 5/2$. The dotted curve shows the data for geometry B fitted by $1 + a_2P_2(\cos\theta)$. The fit is a poor one and it can be estimated that if $1 + a_2P_2(\cos\theta)$ were in fact the actual correlation then the experimental correlation would be obtained in only one in a hundred tries. Since the first measurement of these triple correlations briefly reported by Paul *et al.* (1956) and given in Table II(*a*) also gave a significant $P_4(\cos\theta)$ coefficient in the geometry B correlation, the assignment of an angular momentum of $\geqslant 5/2$ to the 2.23-Mev state can be considered to be a strong one.

Figure 5 shows the theoretical values of the triple correlation coefficients on the assumption that the 3/2+ resonance decays by a 6.71-Mev gamma ray to a 5/2+ state in P^{31} at 2.23 Mev which in turn decays to the 1/2+

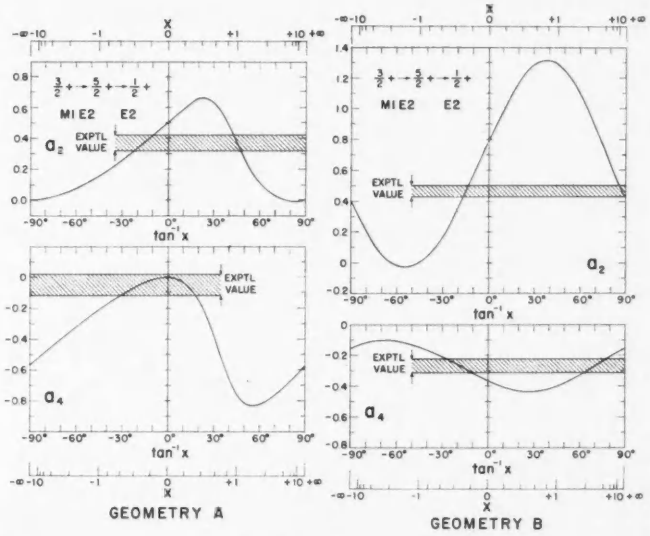

FIG. 5. The theoretical values of the triple correlation coefficients are shown as a function of x, the magnetic dipole – electric quadrupole amplitude mixture of the 6.71-Mev radiation. The spin and parity of the 2.23-Mev excited state are assumed to be 5/2 and even. The experimental values of the a_2 and a_4 coefficients have been increased by 10% and 25% respectively to correct for the effect of finite geometry. After this figure had been prepared more accurate estimates of the corrections (Gove and Rutledge 1958) indicated that they are probably underestimates. The conclusions in the text are not altered by the change required in the figure.

ground state. These theoretical coefficients were obtained from Ferguson and Rutledge (1957). Good agreement between theory and the experimental coefficients taken from Table II(b) for this sequence is obtained for values of the mixing parameter x lying between -0.3 and -0.15.* The agreement between theory and experiment for the less accurate coefficients taken from Table II(a) is less satisfactory because the values of the mixing parameter x needed to fit the correlations in the two geometries are different. This discrepancy provided one of the reasons for repeating the measurements. The measurements, however, support the assignment of 5/2+ to the 2.23-Mev state in P^{31}.

An angular momentum assignment of 7/2 is completely eliminated by the data. This elimination can be illustrated most clearly by considering the ratios of the a_2 coefficients obtained from the two geometrical arrangements

*This conclusion is not sensitive to the uncertainties in the correction to be applied to the correlation coefficient due to the finite angular spread of the counter. The maximum values of this correction are given in Table II.

employed in the measurements. Since the same distances of the counters from the target were used for the geometry A correlation and for the geometry B correlation the ratio of the a_2 coefficients for the two geometries is independent of the distance of the counters from the target. The values of this ratio obtained from Table II(a) and II(b) are 0.34 ± 0.10 and 0.79 ± 0.13 respectively. The value calculated for an intermediate state spin of 7/2 is -0.26.

A useful feature of the triple correlation method can be illustrated by considering as an alternative to the above assignment the following possibility. The 2.23-Mev gamma ray need not be a secondary transition since the time sequence of the 6.71-Mev and 2.23-Mev gamma rays is not determined by the apparatus. Let us suppose, then, that the 2.23-Mev gamma ray is a primary to a state of spin and parity 3/2+ at 6.71 Mev in P^{31}. For this cascade the geometrical arrangements A and B, Fig. 4, are interchanged. The original geometry A becomes the new geometry B′ and the original

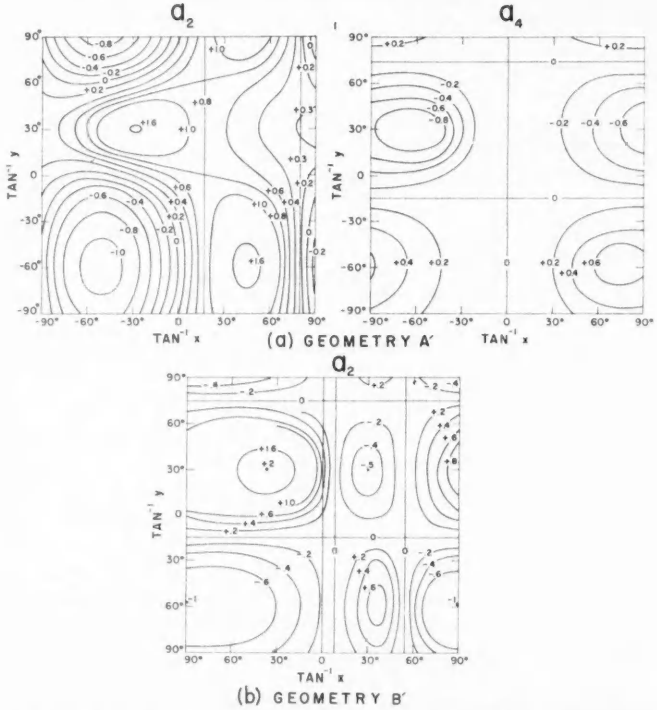

FIG. 6. The theoretical values of the triple correlation coefficients, for the geometries A′ and B′, are shown as a function of x, the dipole–quadrupole amplitude mixture of the 6.71-Mev radiation, and y, the dipole–quadrupole amplitude mixture of the 2.23-Mev radiation. The spin and parity of the resonance and the 2.23-Mev state are assumed to be 3/2 and even. The results of the calculations are shown as contour plots of the correlation coefficients a_2 and a_4.
(a) The a_2 and a_4 coefficients for geometry A′. (b) The a_2 coefficient for geometry B′.

geometry B becomes the new geometry A′. It is possible in this case to have a nonzero a_4 coefficient for the geometry A′ correlation even though all spins involved in the gamma ray cascade are $\leqslant 3/2$. The theoretical correlation coefficients are shown in Fig. 6. It is possible to obtain values of the mixing parameters x and y from the experimental geometry A′ correlation coefficients. However, the theoretical geometry B′ correlation deduced from the knowledge of x and y is then very badly in disagreement with experiment ($a_2 \sim 1$) so that the experimental correlations do not agree with the above assumptions. By similar arguments it can be shown that the experimental correlations also do not support the possibility that the 2.23-Mev and the 6.71-Mev cascade proceeds through a $5/2+$ state at 6.71 Mev.

CONCLUSIONS

The 2.23-Mev state in P^{31} has been shown to have an angular momentum of $5/2$ by exploiting the technique of triple correlations. The parity of this state is undetermined unless the assumption is made that magnetic quadrupole radiation cannot compete significantly with electric dipole radiation. If this assumption is made, then the parity of the 2.23-Mev state is even since the transition from the $3/2+$ capturing state is experimentally a mixed dipole–quadrupole transition.

In conclusion it is interesting to point out the similarities between the first three states of Si^{29} and P^{31}. The available information (Bromley *et al.* 1957), and the work reported in this paper, are shown in Fig. 7. The strong $E2$ crossover in each case has stimulated the application of the collective model to Si^{29} (Bromley *et al.* 1957) and P^{31} (Broude, private communication).

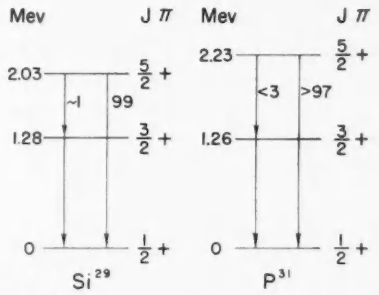

FIG. 7. A comparison of the experimental properties of the low states of the nuclei Si^{29} and P^{31}.

ACKNOWLEDGMENTS

The authors are indebted to Mr. W. T. Sharp and Dr. A. J. Ferguson for many discussions on triple correlation theory, to Dr. A. J. Ferguson and Miss A. E. Rutledge for their valuable compilation of triple correlation coefficients, to Dr. J. M. Kennedy for the least squares analysis of the correlation data on the Chalk River Datatron Computer, to Mr. J. Bollier for

his drafting work, and finally to Mr. P. G. Ashbaugh and the operating staff for their efficient operation of the accelerator.

REFERENCES

BELL, R. E., GRAHAM, R., and PETCH, H. E. 1952. Can. J. Phys. **30**, 35.
BROMLEY, D. A., GOVE, H. E., and LITHERLAND, A. E. 1957. Can. J. Phys. **35**, 1057.
BROUDE, C. Private communication.
ENDT, P. M. and BRAAMS, C. M. 1957. Revs. Modern Phys. **29**, 683.
FERGUSON, A. J. and RUTLEDGE, A. R. 1957. Coefficients for triple correlation analysis in nuclear bombardment experiments. Chalk River Project CRP-615, Chalk River, Ontario (unpublished).
GOVE, H. E. and RUTLEDGE, A. R. 1958. Finite geometry corrections to gamma-ray angular correlations measured with 5 in. diameter by 4 in. long NaI(Tl) crystals. Chalk River Project Report CRP-755, Chalk River, Ontario (unpublished).
HUTCHINSON, G. W. and SCARROTT, G. G. 1951. Phil. Mag. **42**, 792.
LITHERLAND, A. E., PAUL, E. B., BARTHOLOMEW, G. A., and GOVE, H. E. 1956. Phys. Rev. **102**, 208.
PAUL, E. B., GOVE, H. E., LITHERLAND, A. E., and BARTHOLOMEW, G. A. 1955. Phys. Rev. **99**, 1339.
PAUL, E. B., BARTHOLOMEW, G. A., GOVE, H. E., and LITHERLAND, A. E. 1956. Bull. Am. Phys. Soc. Ser. II, **1**, 39.
ROSE, M. E. 1953. Phys. Rev. **91**, 610.
SHARP, W. T., KENNEDY, J. M., SEARS, B. J., and HOYLE, M. G. 1953. Tables of coefficients for angular distribution analysis. Chalk River Project CRT-556, Chalk River, Ontario (unpublished).
WILKINSON, D. H. 1958. Atomic Energy Research Establishment, Harwell. A.E.R.E. T/R 2492.

ON THE GENERAL PLANE PROBLEM OF PLASTICITY AND ITS GEOPHYSICAL SIGNIFICANCE[1]

SISIR CHANDRA DAS[2]

ABSTRACT

The results obtained from the fault plane studies made in the Dominion Observatory show strong horizontal displacements in the focus of earthquakes. This indicates a marked deviation from the existing theories of geotectonics. To account mathematically for them, the study of the plane problem of plasticity is proposed using as yield condition a general functional relation between the stresses.

The differential equations involved in the problem are of *non-linear* type. For solutions these are replaced by a different set of completely equivalent equations expressing variations along families of curves, known as *characteristics*, across which certain derivatives may be discontinuous under suitable boundary conditions.

Physically, the elastic-plastic (or rigid-plastic) interface is taken as a characteristic curve which is a fundamentally unknown thing, and which must be ascertained from symmetry of the problem or by proper experimentation. Investigations in this direction are now being done in connection with the International Geophysical Year. Meanwhile here we discuss the various relatively modern methods of linearization of the stress equations. Each of them essentially deals with transformations of co-ordinates, depending upon the form of the yield condition, though in every case the generalized nature is maintained.

INTRODUCTION

One of the important problems facing geologists is to explain the orogenic belt which surrounds the Pacific basin. This belt is made up of a number of mountain ranges, island arcs, and ocean deeps, arranged parallel to the boundary of the basin, usually with associated volcanoes. That the zone is active is proved by the great number of large earthquakes associated with it. These earthquakes have foci at depths ranging from the surface to more than 600 km, and appear to define zones, approximately planar, striking parallel to the basin and dipping beneath the continents at angles of 45° to 60°.

Most explanations of this orogenic belt have suggested that it is the result of forces acting normal to the Pacific boundary; this would explain the folding up of mountains and the downthrusting of deeps parallel to the boundary. Because the earthquake foci appear to define a plane, it was assumed that this was the fault plane of the earthquakes and that motion was either up or down this plane. Such faulting would have a strong vertical component which is consistent with the vertical displacement in mountains and deeps. In recent years seismologists (Hodgson 1957; Keylis-Borok 1956) have been investigating the nature of this displacement and find that the usual assumptions are not valid. Most of the faults are nearly vertical, the planes do not,

[1]Manuscript received May 12, 1958.
Published by permission of the Deputy Minister, Department of Mines and Technical Surveys, Ottawa. Contributions from the Dominion Observatory, Ottawa, Vol. 3, No. 21.
[2]On study leave of absence from the Department of Mathematics, Chandernagore College, Chandernagore, West Bengal, India.

in general, coincide with the plane of the foci, and the displacement is almost purely horizontal with only a minor vertical component.

How is this apparent discrepancy to be reconciled? It may be that the forces do not act normal to the ocean boundary, or it may be that the properties of the material are different from those usually assumed. Because there are so many reasons for supposing that the forces are normal to the Pacific boundary, the second possibility appears to offer the more fruitful field for investigation.

Most geological studies regard the earth as perfectly elastic but, since we are dealing with conditions at depths as great as 600 km, where the temperatures and pressures are very high, this is not satisfactory in the present problem. Nor can we regard the material as viscous; viscous material cannot fail by fracture, and earthquakes are certainly the result of fracture. We conclude that the material must be regarded as plastic, and the problem becomes one of defining the yield conditions of this plastic material.

Much of the literature on plasticity, particularly that relating to the plastic failure of metals, has made use of particular yield conditions, either those defined by von Mises, or those defined by Tresca. These two conditions become the same in two-dimensional problems, and they have the advantage of much physical confirmation in the field of metals. However, it seems doubtful if they can properly be applied to the present problem, considering the very high temperatures and pressures involved, and the fact that these are active for a very long time. One might search for other specific yield conditions but it is difficult to justify any particular set of conditions in the absence of physical evidence. Moreover there is no reason to suppose that the same yield conditions operate at all times or at all places. It will therefore be informative to discuss the problem in full generality, taking the yield conditions in the form of a general functional relationship. That is the purpose of the present paper.

It should be mentioned that a considerable literature exists in a field intermediate between that of the failure of metals and that of the failure of the earth. This is the discipline of soil mechanics in which the soil is usually replaced by an idealized material which behaves elastically up to some state of stress at which slip or yielding occurs. A certain amount of similarity between Prandtl's theory of plasticity (1920) and the theory of earthy media has been shown by Sokolovsky (1939). In more complete plane investigations an extended Coulomb's rule is used (Terzaghi 1943). Implications of assuming the soil to be a perfectly plastic body have been shown to be far reaching by Drucker and Prager (1952). The former author (Drucker 1953) has further extended the idea of limit analysis towards an interesting development of complete solutions. Thus it is necessary in such a situation to study general yield conditions; this supports the conclusion that general yield conditions are necessary in the larger problem of the failure of the earth.

It must be understood that the investigation of the properties of the materials of the earth's interior is much more complicated than the equivalent problem in soil mechanics because data on the properties of the materials are seldom known conclusively and laboratory experiments are not possible.

Further, the usual assumptions of incompressibility and isotropy of elasticity, and the usual plasticity theories, most likely cannot be taken for granted in our case. For example, the stress–strain relations in horizontal directions and in vertical directions should not be taken to be the same, and change in volume is naturally expected under high pressures and temperatures.

The present analysis is limited to the plane problem. This simplifies the mathematics, and, as in other branches of applied mathematics, we may expect it to produce useful results through the proper orientation of coordinates. Indeed it has already done so; the two-dimensional study of approaching parallel rigid plates has shown that, for viscous fluids or for plastic or Bingham substances, flow can take place along directions perpendicular to the applied forces (Das 1958). This helps to explain the observations mentioned earlier that the motions in large earthquakes may be transverse to the forces causing them.

The practical limitations of these studies must be emphasized. We have no knowledge of the yield point or the stress–strain relationship appropriate to any point or zone, although observations are being made in this direction in both the U.S.A. and the U.S.S.R. in connection with the I.G.Y. (Gzovskii 1957; Risznichenko 1957). Moreover, there are not very many problems for which the boundary values can be stated in such a way as to ensure the existence and uniqueness of solutions. Nevertheless, the knowledge obtained of the pattern of stress state and of the process by which fracture develops will allow a better understanding of the physical situation. This in turn will allow a more precise evaluation of the problem.

The development of the solutions of the general plane problem is comparatively modern and has not yet been included in any monogram of plasticity. The problem is rather difficult. It is non-linear and, moreover, the solutions are not usually orthogonal nor everywhere hyperbolic. The determination of the regions in which the solutions are not hyperbolic must be made at the same time that the solutions are obtained.

Three methods of solution will be discussed in this paper, those of Neuber (1948), Sauer (1949), and Sokolovsky (1955). Geiringer (1953) has already reviewed the work of Neuber and Sauer on the linearization of the stress equations, but apparently was unaware of an earlier paper of Neuber (1947) in which he gives a somewhat fuller treatment of the anisotropic case.

In Neuber's method for linearization of the stress equations, $(\sigma_x - \sigma_y)$ and τ_{xy} have been used as stress variables. Sauer takes σ_x and τ_{xy} instead, and derives a nonlinear differential equation of second order, which he then transforms into a linear equation by means of Legendre transformation. Both methods are capable of applications in anisotropic medium as well, and equally simple construction of the characteristics have been obtained in both cases.

Sokolovsky extends the usual method of solution for von Mises (and Tresca's) condition of yield to cover the general condition of yield expressed as a function of mean normal stress and shear stress intensities, without assuming the incompressibility of the material. Different methods of transformations have been indicated to deal with both hyperbolic and elliptic

nature of the equations of characteristics and solutions have been obtained in the form of trigonometric series.

METHODS OF LINEARIZATION

1. $(\sigma_x-\sigma_y)$ and τ_{xy} as Stress Variables

The usual equations of equilibrium in plane problem in cartesian co-ordinates are

$$\begin{aligned}\frac{\partial\sigma_x}{\partial x}+\frac{\partial\tau_{xy}}{\partial y}&=0,\\ \frac{\partial\tau_{xy}}{\partial x}+\frac{\partial\sigma_y}{\partial y}&=0,\end{aligned}\tag{1.1}$$

where σ_x, σ_y are the normal components of the stress and τ_{xy} is the shearing stress.

The compatibility conditions of elasticity are replaced by the condition of plasticity or the law of plastic flow. This is a functional relationship between the stress components and is written in its most general form as

$$f(\sigma_x, \sigma_y, \tau_{xy}) = 0.\tag{1.2}$$

It is to be noted that this relationship is applicable to both isotropic and anisotropic cases, i.e. it is not necessarily composed from the invariants.

All attempts to solve these equations consist of different ways of transformation to different systems of variables.

The basic equation is obtained by Neuber in two stress variables $\sigma_x-\sigma_y$ and $2\tau_{xy}$ in a system of oblique co-ordinates u, v. Denoting the inclination of u and v directions with the x-axis by α_u and α_v respectively (Fig. 1), equations (1.1) take the form

$$\begin{aligned}\frac{1}{h_u}\left[\sin\alpha_v\frac{\partial\sigma_x}{\partial u}-\cos\alpha_v\frac{\partial\tau_{xy}}{\partial u}\right]-\frac{1}{h_v}\left[\sin\alpha_u\frac{\partial\sigma_x}{\partial v}-\cos\alpha_u\frac{\partial\tau_{xy}}{\partial v}\right]&=0,\\ \frac{1}{h_u}\left[\sin\alpha_v\frac{\partial\tau_{xy}}{\partial u}-\cos\alpha_v\frac{\partial\sigma_y}{\partial u}\right]-\frac{1}{h_v}\left[\sin\alpha_u\frac{\partial\tau_{xy}}{\partial v}-\cos\alpha_u\frac{\partial\sigma_y}{\partial v}\right]&=0,\end{aligned}\tag{1.3}$$

where $h_u du$ and $h_v dv$ are the line elements.

Restrictions are now imposed upon α_u and α_v in such a way that the equations (1.3) are obtained in terms of derivatives with respect to u only in the first equation and v only in the second by taking

$$\begin{aligned}\sin\alpha_u\frac{\partial\sigma_x}{\partial v}-\cos\alpha_u\frac{\partial\tau_{xy}}{\partial v}&=0,\\ \sin\alpha_v\frac{\partial\tau_{xy}}{\partial u}-\cos\alpha_v\frac{\partial\sigma_y}{\partial u}&=0.\end{aligned}\tag{1.4}$$

Then equations (1.3) become

$$\begin{aligned}\sin\alpha_v\frac{\partial\sigma_x}{\partial u}-\cos\alpha_v\frac{\partial\tau_{xy}}{\partial u}&=0,\\ \sin\alpha_u\frac{\partial\tau_{xy}}{\partial v}-\cos\alpha_u\frac{\partial\sigma_y}{\partial v}&=0.\end{aligned}\tag{1.5}$$

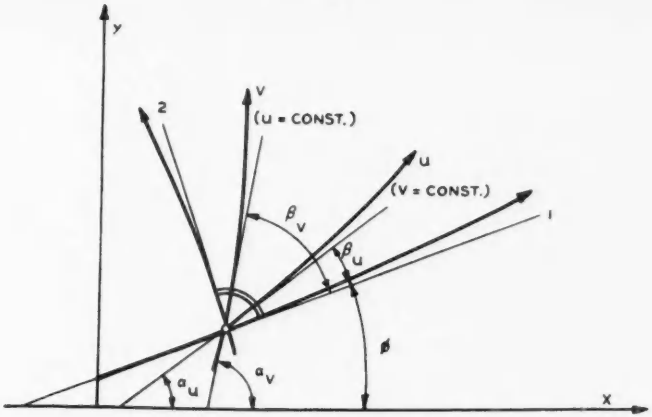

FIG. 1. Transformation of characteristics.

From these two sets of equations we get

$$\begin{aligned} &\frac{\partial \sigma_x}{\partial u} \cdot \frac{\partial \sigma_y}{\partial u} - \left(\frac{\partial \tau_{xy}}{\partial u}\right)^2 = 0 \qquad \text{along } v = \text{const.} \\ &\frac{\partial \sigma_x}{\partial v} \cdot \frac{\partial \sigma_y}{\partial v} - \left(\frac{\partial \tau_{xy}}{\partial v}\right)^2 = 0 \qquad \text{along } u = \text{const.} \end{aligned} \tag{1.6}$$

Therefore for both these families of curves in general we have

$$(d\sigma_x)(d\sigma_y) - (d\tau_{xy})^2 = 0, \tag{1.7}$$

which can be written in the form

$$[d(\sigma_x+\sigma_y)]^2 = [d(\sigma_x-\sigma_y)]^2 + [d(2\tau_{xy})]^2. \tag{1.8}$$

The yield condition expressed in terms of $\sigma_x+\sigma_y$, $\sigma_x-\sigma_y$, $2\tau_{xy}$ can now be interpreted as a surface called a "plasticity surface" (Fig. 2).

Equation (1.8) clearly indicates that the characteristics of the differential equations of the general two-dimensional plasticity problem correspond to the 45° slopes of the plasticity surface. On the plasticity surface the lines u = constant or v = constant constitute 45° slope lines for the angle α (i.e. α_u or α_v).

From equations (1.4) and (1.5) it clearly follows that

$$\tan \alpha = d\sigma_y/d\tau_{xy}$$

and

$$\cot \alpha = d\sigma_x/d\tau_{xy}. \tag{1.9}$$

Hence

$$\cot 2\alpha = d(\sigma_x-\sigma_y)/d(2\tau_{xy}), \tag{1.10}$$

i.e. 2α is the angle between the tangent to the projection of the line v = constant (or u = constant) on the $(\sigma_x-\sigma_y)$, $(2\tau_{xy})$-plane, and the $(\sigma_x-\sigma_y)$-axis.

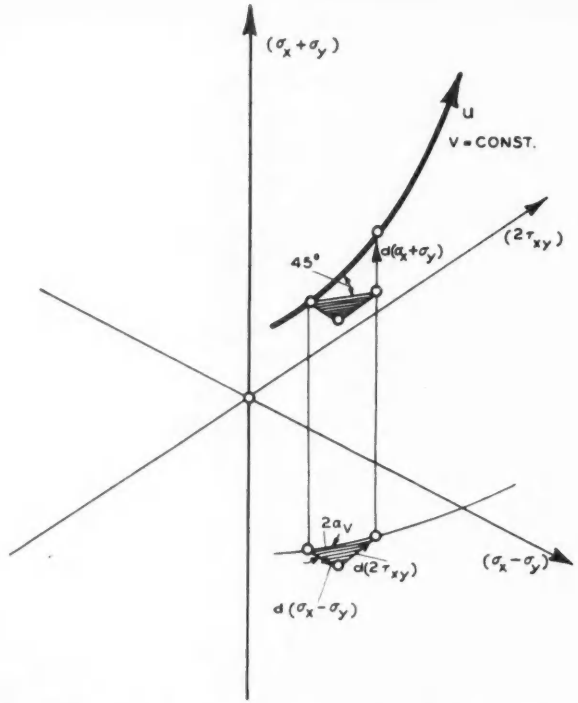

FIG. 2. The line v = const. on the plasticity surface and in the drawing plane (after Neuber).

The integration now can be done by the method of projection. Substituting ξ, η for $\sigma_x-\sigma_y$ and $2\tau_{xy}$ it is observed that x, y-plane is projected to ξ, η-plane by transforming the u, v-lines of the x, y-plane into the 45° slope line of the plasticity surface projected on to ξ, η-plane. The 45° slope lines give a unique picture of the x, y-plane and its state of stress.

It should be noticed that the inclination of the tangent to a line u = const. or v = const. is equal to half of the inclination of a tangent to a line v = const. or u = const. respectively, in the corresponding point of x, y-plane.

The use of the stress variables $\sigma_x-\sigma_y$ and $2\tau_{xy}$ (i.e. ξ, η-plane to be the basic plane of the plasticity surface) has the advantage that slope lines can be very easily constructed from the contour line $(\sigma_x+\sigma_y) = p$ = const.

2. σ_x and τ_{xy} as Stress Variables

Sauer uses σ_x, τ_{xy} as stress variables. His method also covers the anisotropic case. He deduces a second order nonlinear differential equation and then transforms it into a linear equation by means of Legendre's transformation.

The flow condition is written in the form

$$\sigma_y = f(\sigma_x, \tau_{xy}). \tag{2.1}$$

The potential function $\phi(x, y)$ defined by

$$\sigma_x = \frac{\partial \phi}{\partial y}, \qquad \tau_{xy} = -\frac{\partial \phi}{\partial x} \tag{2.2}$$

is now introduced and the quasi-linear equation of second order,

$$\frac{\partial^2 \phi}{\partial x^2} - \frac{\partial f}{\partial x}\frac{\partial^2 \phi}{\partial y^2} + \frac{\partial f}{\partial \tau_{xy}}\frac{\partial^2 \phi}{\partial x \partial y} = 0 \tag{2.3}$$

is obtained. Applying Legendre's transformation

$$\begin{aligned} u &= \frac{\partial \phi}{\partial x} = -\tau_{xy}, \\ v &= \frac{\partial \phi}{\partial y} = \sigma_x, \\ \Phi &= ux + vy - \phi = \sigma_x y - \tau_{xy} x - \phi, \\ x &= \frac{\partial \Phi}{\partial u} = -\frac{\partial \Phi}{\partial \tau_{xy}}, \\ y &= \frac{\partial \Phi}{\partial v} = \frac{\partial \Phi}{\partial \sigma_x}, \end{aligned} \tag{2.4}$$

in (2.4) we get the homogeneous linear equation,

$$\frac{\partial^2 \Phi}{\partial \sigma_x^2} - \frac{\partial f}{\partial \sigma_x} \cdot \frac{\partial^2 \Phi}{\partial \tau_{xy}^2} + \frac{\partial f}{\partial \tau_{xy}} \cdot \frac{\partial^2 \Phi}{\partial \sigma_x \partial \tau_{xy}} = 0, \tag{2.5}$$

where

$$\frac{\partial u}{\partial x} \cdot \frac{\partial v}{\partial y} \neq \frac{\partial v}{\partial x} \cdot \frac{\partial v}{\partial y},$$

which we assume to be the case.

The function $f(\sigma_x, \tau_{xy})$ as well as its derivatives $\partial f/\partial \sigma_x$ and $\partial f/\partial \tau_{xy}$ may be quite complicated when the yield condition is symmetric. For the characteristics in the physical plane from (2.4) we find

$$dy^2 - \frac{\partial f}{\partial \sigma_x} dx^2 - \frac{\partial f}{\partial \tau_{xy}} dy\, dx = 0 \tag{2.6}$$

and in view of $u = -\tau_{xy}$ and $v = \sigma_x$ the compatibility conditions

$$\begin{aligned} \left(\frac{d\sigma_x}{d\tau_{xy}}\right)_1 &= \left(\frac{dx}{dy}\right)_2, \\ \left(\frac{d\sigma_x}{d\tau_{xy}}\right)_2 &= \left(\frac{dx}{dy}\right)_1 \end{aligned} \tag{2.7}$$

are obtained where 1, 2 denote two characteristics.

From this, both corresponding families of characteristics of equations (2.6) are obtained as

$$d\tau_{xy}^2 - \frac{\partial f}{\partial \sigma_x} d\sigma_x^2 - \frac{\partial f}{\partial \tau_{xy}} d\sigma_x d\tau_{xy} = d\tau_{xy}^2 - d\sigma_x \cdot d\sigma_y = 0, \tag{2.8}$$

which coincides with (1.7).

The characteristics are the slip lines of the present plastic stress field and from their properties methods have been developed by Sauer to construct them.

The slip line nets like the σ_x,τ-characteristic nets corresponding to them consist of two orthogonal families of curves when $\partial f/\partial\sigma_x \equiv 1$. They are thus characterized by the form

$$\sigma_x - \sigma_y = g(\tau_{xy}) \tag{2.9}$$

where $g(\tau_{xy})$ is an arbitrary function of τ_{xy}.

If this is the case we get from (2.9)

$$\left(\frac{d\tau_{xy}}{d\sigma_x}\right)_{1,2} = \frac{1}{2}\left[\frac{dg}{d\tau_{xy}} \pm \sqrt{4+\left(\frac{dg}{d\tau_{xy}}\right)^2}\right]. \tag{2.10}$$

The σ_x, τ characteristics intersect the lines τ_{xy} = const. at a fixed angle and are therefore parallel and congruent.

It may be remarked in this connection that the orthogonal family of nets will be particularly useful in explaining the probable fault planes obtained by geometrical methods from the recordings of a single earthquake made from different places. Taking for granted that fault movements occur along slip lines, which most likely is the case, they are obtained as along either of two perpendicular planes. Because of the uniqueness of null vectors (Hodgson 1957) each of them denotes some point, in the plane case, where the two slip lines, each of different families, meet.

3. Extension of the Classical Method

The general condition of plasticity has been written by Sokolovsky in the form

$$\Phi(\sigma, \tau) = 0,$$

or

$$\tau = \tau(\sigma), \tag{3.1}$$

where σ and τ are the mean normal stress and the intensity of stress respectively.

Introducing s and t defined by

$$s = \tfrac{1}{2}(\sigma_x+\sigma_y)$$

and

$$t = \sqrt{\{\tfrac{1}{4}(\sigma_x-\sigma_y)^2+\tau_{xy}^2\}},$$

the conditions of plasticity for both plane strain and plane stress can be written in the form

$$F(s, t) = 0,$$

or

$$t = t(s). \tag{3.2}$$

Taking F as a plastic potential and following Drucker and Prager (1952) we can have

$$\frac{\epsilon_x}{\frac{\partial F}{\partial \sigma_x}} = \frac{\epsilon_y}{\frac{\partial F}{\partial \sigma_y}} = \frac{\epsilon_z}{\frac{\partial F}{\partial \sigma_z}} = \frac{2\gamma_{xy}}{\frac{\partial F}{\partial \tau_{xy}}} \tag{3.3}$$

$\epsilon_x, \ldots, \gamma_{xy}, \ldots$ being the components of strain. Introducing e and g, defined by

$$e = \tfrac{1}{2}(e_1+e_2) = \tfrac{1}{2}(\epsilon_x+\epsilon_y),$$
$$g = \tfrac{1}{2}(e_1-e_2) = \sqrt{\{\tfrac{1}{4}(\epsilon_x-\epsilon_y)^2+\gamma_{xy}^2\}},$$

e_1 and e_2 being the principal strain ($e_1 > e_2$), we get

$$\begin{aligned} \epsilon_x-\epsilon &= g/t(\sigma_x-s), \\ \epsilon_y-\epsilon &= g/t(\sigma_y-s), \\ \epsilon_z-\epsilon &= g/t(\sigma_z-s), \\ \gamma_{xy} &= g/t\tau_{xy} \end{aligned} \tag{3.4}$$

and

$$e = g\{(\partial F/\partial s)/(\partial F/\partial t)\} = gh \tag{3.5}$$

where h is a known function of s and t.
The stress components can also be written in the form

$$\begin{aligned} \sigma_x &= s+k\cos 2\phi, \\ \sigma_y &= s-t\cos 2\phi, \\ \tau_{xy} &= t\sin 2\phi, \end{aligned} \tag{3.6}$$

where ϕ is the angle between the x-axis and the direction of principal stress. And similarly for strain components we get

$$\begin{aligned} \epsilon_x &= e+g\cos 2\phi, \\ \epsilon_y &= e-g\cos 2\phi, \\ \gamma_{xy} &= g\sin 2\phi. \end{aligned} \tag{3.7}$$

Substituting the values of σ_x, σ_y, τ_{xy} from (3.6) in equations of equilibrium (1.1) we get

$$\begin{aligned} &\frac{\partial s}{\partial x}+\cos 2\phi\,\frac{\partial t}{\partial x}+\sin 2\phi\,\frac{\partial k}{\partial y}-2t\left(\sin 2\phi\,\frac{\partial \phi}{\partial x}-\cos 2\phi\,\frac{\partial \phi}{\partial y}\right) = 0, \\ &\frac{\partial s}{\partial y}+\sin 2\phi\,\frac{\partial t}{\partial x}-\cos 2\phi\,\frac{\partial k}{\partial y}+2t\left(\cos 2\phi\,\frac{\partial \phi}{\partial x}+\sin 2\phi\,\frac{\partial \phi}{\partial y}\right) = 0. \end{aligned} \tag{3.8}$$

The procedure is exactly the same as that followed in the case of classical plane problems with Tresca's (and that of Mises) yield condition. The only change in equation (3.8) is due to the fact that t is not a constant in this case.

Further from (3.7) we can have

$$\begin{aligned} &2\sin 2\phi\,\frac{\partial u}{\partial x}-(h+\cos 2\phi)\left(\frac{\partial v}{\partial x}+\frac{\partial u}{\partial y}\right) = 0, \\ &2\sin 2\phi\,\frac{\partial v}{\partial y}-(h-\cos 2\phi)\left(\frac{\partial v}{\partial x}+\frac{\partial u}{\partial y}\right) = 0. \end{aligned} \tag{3.9}$$

The characteristics of equations (3.8) and (3.9) are of the form

$$d\phi \pm \frac{\sqrt{(1-h^2)}}{2h}\, d \ln t = 0,$$

$$\frac{dy}{dx} = \frac{\sin 2\phi \mp \sqrt{(1-h^2)}}{\cos 2\phi - h}, \tag{3.10}$$

$$\frac{dv}{du} = \frac{\sin 2\phi \pm \sqrt{(1-h^2)}}{\cos 2\phi + h}.$$

It is clearly seen that these equations are not confined to the hyperbolic case alone but may well be elliptic in type depending on whether $|h| < 1$ or $|h| > 1$.

In the hyperbolic case ($|h| < 1$) introducing ψ and λ defined by

$$dt/ds = -h = \cos 2\psi$$

and

$$\begin{aligned} 2d\lambda &= \sqrt{(1-h^2)}(ds/t), \\ &= \sin 2\psi\, ds/t, \\ &= \tan 2\psi\, d \ln t, \end{aligned} \tag{3.11}$$

the characteristics of the system of equations (3.8) and (3.9) are determined by the equations

$$\begin{aligned} \eta &= \lambda(\psi) - \phi = \text{const.}, \\ dy/dx &= \tan(\phi - \psi), \\ du/dv &= -\tan(\phi - \psi); \end{aligned} \tag{3.12}$$

$$\begin{aligned} \xi &= \lambda(\psi) + \phi = \text{const.}, \\ dy/dx &= \tan(\phi + \psi), \\ du/dv &= -\tan(\phi + \psi). \end{aligned} \tag{3.13}$$

It should be noted that characteristics in the x, y plane are always orthogonal to the corresponding characteristics in the u, v plane as from (3.12) and (3.13) it is seen that for both families

$$(dy/dx)(dv/du) = -1.$$

By further substitutions given by

$$\bar{x} = \frac{1}{\sin 2\psi}[x \sin(\phi + \psi) - y \cos(\phi + \psi)]$$

$$\bar{y} = \frac{1}{\sin 2\psi}[y \cos(\phi - \psi) - x \sin(\phi - \psi)]$$

$$\bar{u} = \frac{1}{\sin 2\psi}[u \cos(\phi - \psi) + v \sin(\phi - \psi)]$$

$$\bar{v} = \frac{1}{\sin 2\psi}[u \cos(\phi + \psi) + v \sin(\phi + \psi)]$$

and then introducing new variables, X, Y, U, V, defined by

$$\frac{X}{\bar{x}} = \frac{Y}{\bar{y}} = \sqrt{\left(\frac{t}{k}\right)\sin 2\psi},$$

$$\frac{U}{\bar{u}} = \frac{V}{\bar{v}} = \sqrt{\left(\frac{t}{k}\right)\sin 2\psi},$$

and finally putting

$$P(\lambda) = \frac{1-\frac{d\psi}{d\lambda}}{\sin 2\psi},$$

equations (3.12) and (3.13) become

$$\eta = \lambda(\psi) - \phi = \text{const.}, \quad dy + XPd\lambda = 0, \quad dU = VPd\lambda, \tag{3.14}$$

$$\xi = \lambda(\psi) + \phi = \text{const.}, \quad dX + YPd\lambda = 0, \quad dV = VPd\lambda, \tag{3.15}$$

from which the canonical forms for co-ordinates and the velocities can be obtained as

$$\frac{\partial Y}{\partial \xi} + \frac{P}{2}X = 0, \qquad \frac{\partial X}{\partial \eta} = \frac{P}{2}Y \tag{3.16}$$

and

$$\frac{\partial U}{\partial \xi} = \frac{P}{2}V, \qquad \frac{\partial V}{\partial \eta} = \frac{P}{2}U \tag{3.17}$$

respectively.

Several particular solutions, namely, for the cases when (i) the family of characteristics (3.15) consists of straight lines ξ = const., and when (ii) the family of characteristics (3.14), in the (x, y) plane, consists of straight lines η = const., and finally when (iii) both the families of characteristics (3.15) and (3.14) represent systems of parallel straight lines, have been discussed by Sokolovsky.

Sokolovsky has also dealt with another method of transformation where he has extended his method (Sokolovsky 1950) for $\tau = k$ (const.) to suit the general form of plasticity condition. Following the practice in plane gas flow he has obtained the results in the form of trigonometric series. The method is applicable for both hyperbolic and elliptic cases.

SUMMARY

The different solutions of the problems discussed in the paper cannot be compared with observation because of the generality of the assumptions, but they are believed to be of geophysical significance, particularly for explaining deep focus earthquake mechanism and the probable fault movements there. The geometry of the methods discussed here can be used to determine the flow (or fracture) pattern, if the boundary stresses as well as the particular yield condition are known. Conversely it will also help to understand the

nature of stresses and the yield condition provided the displacements are ascertained. It is both interesting and useful to proceed with various yield conditions and to find their influences on the solutions. The conclusions can only be decisive when comparisons with actual observations and experiences will be possible.

ACKNOWLEDGMENTS

The work comes under the fault plane research project undertaken in the Seismology Division of the Dominion Observatory at Ottawa and was made possible through a postdoctorate fellowship awarded by the National Research Council of Canada.

The author is greatly indebted to Dr. J. H. Hodgson, Chief of the Division, for many useful discussions and advice during the course of the work. The author sincerely thanks Dr. C. S. Beals for his encouragement and interest.

REFERENCES

DAS, S. C. 1958. International Congress of Mathematicians, Edinburgh. To be published.
DRUCKER, D. C. 1953. J. Mech. and Phys. Solids. **1**, 217.
DRUCKER, D. C. and PRAGER, W. 1952. Quart. Appl. Math. **X**(2), 157.
GEIRINGER, H. 1953. Advances in applied mechanics III (Academic Press, Inc.) 197.
GZOVSKII, M. V. 1957. Bull. Acad. Sci. U.S.S.R. (Geophys. Ser.), No. 2, p. 15.
HODGSON, J. H. 1957. Bull. Geol. Soc. Amer. **68**, 611.
KEYLIS-BOROK, V. I. 1956. Publ. Bur. Centr. Seismol. Intern. Ser. A, **19**, 383.
NEUBER, H. 1948. Ministry of Supply (Air). Volkemrode Reports of Transactions 610. 1947. National Research Council Can. Tech. Trans. No. 86. Also see Z. angew. Math. Mech. **28**, 253.
PRANDTL, L. 1920. Ges. Wiss. Gottingen, Math.–Phys. Kl., Nachr. p. 74.
RISZNICHENKO, I. V. 1957. Bull. Acad. Sci. U.S.S.R. (Geophys. Ser.), No. 2, p. 1.
SAUER, R. 1949. Z. angew Math. Mech. **29**, 274.
SOKOLOVSKY, V. V. 1939. Izvest. Akad. Nauk S.S.S.R., Otdel. Teckh. Nauk **2**, 107.
——— 1950. Theory of plasticity (in Russian) 2nd ed. (Gostechirdat). German translation, 1955 (Verlag Technik, Berlin).
——— 1955. Priklanaya Mat. i Mech. **19** (1) 41.
TERZAGHI, K. 1943. Theoretical soil mechanics (John Wiley and Sons, Inc.) pp. **22**, **59**.

NOTES

AN ISOTOPE EFFECT IN ANTIFERROMAGNETISM AT LOW TEMPERATURES

J. M. DANIELS

It is known, as a consequence of Nernst's heat theorem, that all paramagnetic substances must become either ferromagnetic or antiferromagnetic at low enough temperatures. In most of the substances so far investigated experimentally, the low temperature state appears to be antiferromagnetic. The Néel temperatures of many hydrated salts containing paramagnetic ions are well below 1° K, for example $KCr(SO_4)_2.12H_2O$ has a Néel temperature of about 0.01° K. The purpose of this note is to point out that the macroscopic properties of the antiferromagnetic state can be greatly influenced by the isotopic composition of the paramagnetic ions, because the hyperfine coupling between the unpaired electrons and the nuclear spins of the paramagnetic ions can be much larger than the coupling between individual ions. As examples, let us consider Mo^{5+} as an impurity in $K_3InCl_6.2H_2O$, and also $Sm(C_2H_5SO_4)_3.9H_2O$. These examples are chosen because these ions have an isotropic g-factor but an anisotropic hyperfine coupling.

The Mo^{5+} ions can be represented approximately by a spin-Hamiltonian

$$\mathscr{H} = g\beta\mathbf{H}.\mathbf{S}+AS_zI_z+B(S_xI_x+S_yI_y) \tag{1}$$

where $g \simeq 1.95$, $A \simeq 0.008\ \text{cm}^{-1}$, $B \simeq 0.004\ \text{cm}^{-1}$,

β is the Bohr magneton, and I is the nuclear spin; in this case $I = 5/2$ for the odd isotopes Mo^{95} and Mo^{97}. (For a definition and explanation of the spin-Hamiltonian, see Bowers and Owen (1955), where the figures quoted are tabulated.) It is clear that for the even molybdenum isotopes the hyperfine interaction is absent ($I = 0$) and the antiferromagnetism is that of free isotropic spins; hence the anisotropy energy is expected to be small. For the odd isotopes, the anisotropic hyperfine coupling introduces an anisotropy energy, and we now derive an expression for this.

Let us consider just one sublattice of spins all with the same crystalline field (z) axis. Assume that we can replace the interaction between spins by an effective field H whose magnitude is independent of direction. In a typical paramagnetic substance (though perhaps not for this, for which few data exist), H would be about 250 gauss. The total splitting in this field is $g\beta H \simeq 0.063\ \text{cm}^{-1}$, while the hyperfine splitting amounts to $5A/2$ or about $0.02\ \text{cm}^{-1}$. Under these circumstances, one can find the energy levels of (1), treating the hyperfine interaction as a perturbation (see, for example, Bleaney (1951)). It is then a straightforward though tedious matter to write down the free energy $F = kT \ln \sum e^{-E_r/kT}$. At the absolute zero, however, F is equal to the lowest eigenvalue of $\mathscr{H}$; this is to second order

$$-g\beta H-\frac{5K}{4}-\frac{25}{16}\cos^2\theta\sin^2\theta\left(\frac{B^2-A^2}{K}\right)^2\frac{1}{2g\beta H+(5K/2)}$$
$$-\frac{5}{16}B^2\left(\frac{A-K}{K}\right)^2\frac{1}{2g\beta H+(3K/2)}$$

where $K^2 = A^2\cos^2\theta+B^2\sin^2\theta$, and θ is the angle between **H** and the z-axis. Expanding this, we have

$$F_0+\cos^2\theta\left[\frac{5}{8}\frac{A^2-B^2}{B}+O\left(\frac{A}{g\beta H}\right)\right]+O(\cos^4\theta) \tag{2}$$

where F_0 is that part of the free energy which does not contain θ. Now θ is the angle between z and **H** while the anisotropy energy is usually determined in terms of an angle φ between z and **S**. The components of the magnetic moment vector μ, which is parallel to **S**, can be found from (2) using $\mu_x = \partial F/\partial H_x$; $\mu_z = \partial F/\partial H_z$, from which it follows that the difference between θ and φ is negligible if $A, B \ll g\beta H$ and θ and φ are small. According to one convention for defining H_a the anisotropy field (Nagamiya, Yosida, and Kubo 1955), we have from (2)

$$H_a = \left\{\frac{5}{8}\frac{A^2-B^2}{B}\Big/\frac{1}{2}g\beta\right\} \simeq 160 \text{ gauss.}$$

Thus, in the case of Mo^{5+} the anisotropy field at the absolute zero for the odd isotopes is about 160 gauss larger than it is for the even isotopes. This will be noticed macroscopically by a change in the antiferromagnetic resonance frequency, in the field at which spin flipping takes place, in the Néel temperature, and in other macroscopic phenomena into which H_a enters.

The case of Sm^{3+} is much more extreme. Here the spin-Hamiltonian is as for Mo^{5+}, but with $g \simeq 0.6$, $A \simeq 0.006\ \text{cm}^{-1}$, $B \simeq 0.025\ \text{cm}^{-1}$, $I = 7/2$, or 0. The even isotopes should behave rather like an ordinary isotropic antiferromagnetic as before. The interaction field can be estimated to be about 30 gauss (using $H \simeq \mu/d^3$); this produces a splitting of about $8\times10^{-4}\ \text{cm}^{-1}$, which is much less than the hyperfine splitting. Thus for the odd isotopes of samarium the hyperfine interaction is the most important feature of the antiferromagnetic state. It is not very convenient here to talk about an anisotropy field (which in this case would be very much larger than the interaction field). Since the splitting in the interaction field is only about $8\times10^{-4}\ \text{cm}^{-1}$, a Néel temperature of not more than 1 or 2×10^{-3} °K is to be expected. At such temperatures, only the lowest pair of hyperfine levels is appreciably populated, and other hyperfine levels should be ignored in treating the antiferromagnetic state, in a manner analogous to the treatment of crystalline field splittings in more familiar substances. If A were greater than B, it would be appropriate to use an "Ising model" to treat this problem.

These two examples, Mo^{5+} and Sm^{3+}, are not really representative of magnetic substances, since it is not usual to find an isotropic g-factor combined with an anisotropic hyperfine coupling. Usually both the g-factor and the hyperfine coupling are anisotropic. In this case, too, there is a significant

difference between the antiferromagnetic properties of various isotopes; the hyperfine coupling is large enough to produce such an effect in the rare earths and in the actinides.

BLEANEY, B. 1951. Phil. Mag. **42**, 441.
BOWERS, K. D. and OWEN, J. 1955. Repts. Progr. Phys. **18**, 304.
NAGAMIYA, T., YOSIDA, K., and KUBO, R. 1955. Advances in Phys. **4**, 1.

RECEIVED SEPTEMBER 30, 1958.
DEPARTMENT OF PHYSICS,
UNIVERSITY OF BRITISH COLUMBIA,
VANCOUVER, BRITISH COLUMBIA.

A NOTE ON THE SCATTERING OF A PLANE ELECTROMAGNETIC WAVE BY A SMALL, THIN-WALLED, CYLINDRICAL DIELECTRIC TUBE*

J. Y. WONG

The problem of scattering of a plane electromagnetic wave by a hollow cylindrical dielectric tube, as described in this note, was undertaken as a result of model UHF shipborne antenna studies carried out at the Radio and Electrical Engineering Division laboratories of the National Research Council for the Royal Canadian Navy. In such applications, the antenna is usually a vertical dipole located near the top of the ship's pole mast in order to obtain an omnidirectional pattern in the azimuthal plane. From our studies it was found that in addition to the adjacent superstructure, the pole mast itself contributed significantly to the pattern deterioration. Measurements showed that a more uniform pattern could be achieved by replacing the hollow metal pole with one of dielectric.

In this note, the amplitude coefficient of the scattered field is derived for the case of a plane electromagnetic wave normally incident on a small thin-walled cylindrical dielectric tube. The results are a special case of the general problem of scattering by a coaxial cylinder of arbitrary constants which has been treated by Tang (1956). Figure 1 illustrates the geometrical arrangement used in the analysis. Following Tang's notation, the scattered field in region (1) is of the form:

$$E_1^s = \sum_{-\infty}^{\infty} i^n A_n H_n^{(1)}(k_1\rho) \exp(in\theta) \tag{1}$$

where $k^2 = \omega^2\mu\epsilon + i\omega\sigma\mu$ and A_n is the scattering coefficient.

Let $k_1 = k_3 = k$, and in region (2), $\sigma_2 = 0$. The resulting configuration becomes a lossless dielectric tube having inner and outer radii of a and b respectively. Furthermore, it is assumed that a and b are small in terms of wavelength and that $a/b > 0.9$. Introducing these restrictions in the general expression for the scattering coefficient (Eq. 22, Tang), and employing the

*Issued as N.R.C. No. 4981.

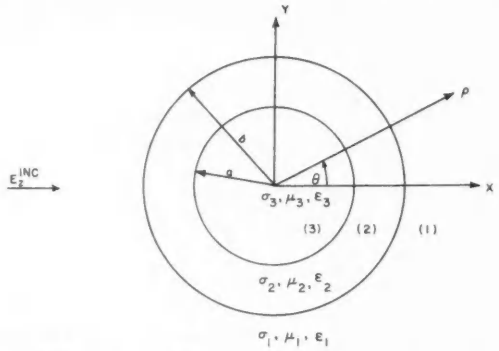

FIG. 1. Coaxial cylinder with arbitrary media constants.

small argument approximation for the cylindrical functions, the following result is obtained for the zero-order term of the scattering coefficient,

$$A_0 \approx -\frac{i\pi}{4} k^2 ab \left\{\left(\epsilon_2^2-1\right)\left(\frac{b}{a}-\frac{a}{b}\right)\right\}, \tag{2}$$

$$\approx -\frac{i\pi}{4} k^2 (b^2-a^2)(\epsilon_2^2-1).$$

The other coefficients are of higher powers in kb and hence for this case are vanishingly small. As to be expected, the result given in Eq. (2) implies that the small dielectric tube acts as a line source, i.e., a uniform scatterer.

It is interesting to compare our result with that obtained by Wait (1955) for a small solid dielectric cylinder. The zero-order term of the scattering coefficient for a solid cylinder is given by

$$a_0^s \approx \frac{i\pi}{4} k^2 a^2 (\epsilon^2-1) \tag{3}$$

where ϵ is the dielectric constant of the cylinder material. By equating eqs. (2) and (3) one obtains an expression for the "equivalent radius" of the tube in terms of a solid dielectric cylinder. Note that the difference in signs for the two coefficients occurs because of the difference in the positive direction of the azimuthal angle of incidence. There results an expression for the equivalent radius,

$$a_{equi} = \sqrt{(b^2-a^2)}. \tag{4}$$

TANG, C. C. H. 1956. Cruft Laboratory Scientific Report No. 6.
WAIT, J. R. 1955. Can. J. Phys. **33**, 189.

RECEIVED IN ORIGINAL FORM AUGUST 19, 1958,
AND, AS REVISED, OCTOBER 2, 1958.
RADIO AND ELECTRICAL ENGINEERING DIVISION,
NATIONAL RESEARCH COUNCIL,
OTTAWA, CANADA.

LOW ENERGY PROTON FLUX AT SEA LEVEL*

I. B. McDiarmid

In the course of an experiment carried out to search for a 500 m_e particle, the vertical proton flux in the momentum interval 716–828 Mev/c, at latitude 57° N. and average atmospheric pressure 1002 mb has been measured. Such a measurement was thought worthwhile since considerable spread exists in previous measurements of the flux around 700 Mev/c. (For a summary of the work up to 1955 see Ogilvie 1955.) The present experiment was relatively free from uncertainties in the identification of protons, and had the advantage of a relatively small acceptance angle (half angle in one plane of 9.8° and 5.8° in a perpendicular plane).

The experimental arrangement shown in Fig. 1 is similar to one described previously (McDiarmid 1958). The cloud chamber contained two plastic

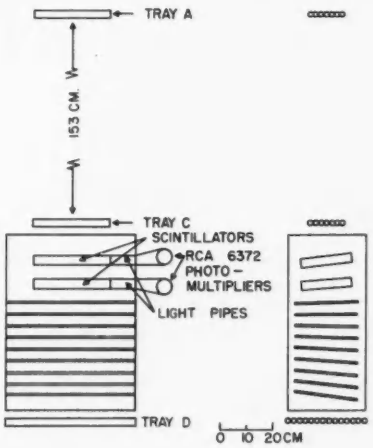

FIG. 1. Experimental arrangement.

scintillators and nine Al plates each 2.16 g/cm² thick. The chamber was expanded and the scintillator pulse heights recorded when the following selection criterion was satisfied:

$$A+C+(T > 12 \text{ v})+(B > 14 \text{ v})-D$$

where T and B refer to the pulse heights from top and bottom scintillators respectively. (The most probable pulse size due to a relativistic μ-meson travelling vertically was 8 v, and that due to a proton stopping in plate 3 was 23 v and 28 v in top and bottom scintillators respectively.) This selects

*Issued as N.R.C. No. 4989.

protons stopping in one of the plates in the chamber with an efficiency of very nearly 100%, but μ-mesons stopping are detected with an efficiency of only 6%. The apparatus operated 1500 hours from March to June 1958 during which time 270 particles were observed to stop in the bottom scintillator and 504 in the Al plates. The tracks of stopping particles were reprojected and the pulse heights corrected for variation of scintillator response with position as described previously (McDiarmid 1958). The corrected pulse heights and the residual ranges were used to identify protons as shown in Fig. 2 in which the top scintillator pulse height is plotted against the bottom scintillator pulse

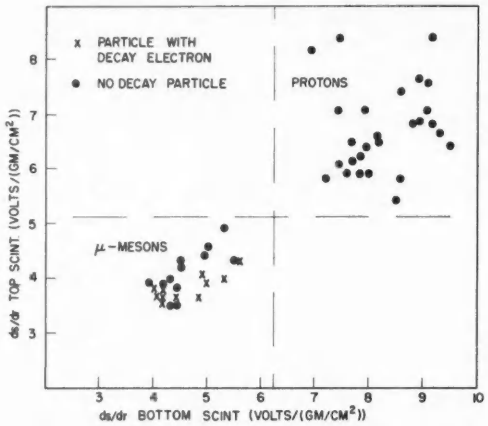

FIG. 2. Pulse height divided by path length in top scintillator vs. corresponding quantity in bottom scintillator for particles stopping in plate 3.

height for particles stopping in plate 3. In this way 100 particles stopping in the bottom scintillator and 206 particles stopping in the nine Al plates were identified as protons. A less satisfactory separation of protons and μ-mesons was also made from a visual estimate of the ionization of the stopping particle in the last few compartments.

For protons stopping in the lower scintillator the selection system required that on entering this scintillator the particles had, on the average, an energy >20.5 Mev to be detected. This energy corresponds to a residual range in the scintillator of 0.44 g/cm^2 and this thickness had to be added to the total amount of absorber above the bottom scintillator (this included the top scintillator, the chamber walls, counter trays, supports, and roof) to obtain the minimum range of the protons detected. The range limits in g/cm^2 Al equivalent* are given in Table I for protons stopping in the bottom scintillator and in the Al plates. Also given in Table I are the corresponding momentum limits and the absolute proton intensities obtained using a solid angle $\times$ area $\times$ time factor, $\Omega At = 2.55 \times 10^7$ cm^2 sec, which was corrected for counter wall

*The range energy tables in U.C.R.L. Report 2301 were used to convert thicknesses of the various materials to equivalent thicknesses of Al.

thickness and chamber dead time. A mean absorption length of 170 g/cm² was used to correct for proton absorption in the material above positions in the chamber where particles were observed. No scattering corrections have been applied since these were estimated to be less than 7%.

TABLE I

Number of protons observed	Range interval, g/cm² Al equiv.	Momentum interval, Mev/c	Intensity particles/ cm²/sec/sterad/(Mev/c)
100	45.5–50	716–739	$2.4\pm.3\times10^{-7}$
206	50 –69.4	739–828	$1.3\pm.1\times10^{-7}$

The intensities obtained here are plotted in Fig. 3 along with those given by other authors in the same momentum region. The point at 783 Mev/c is in

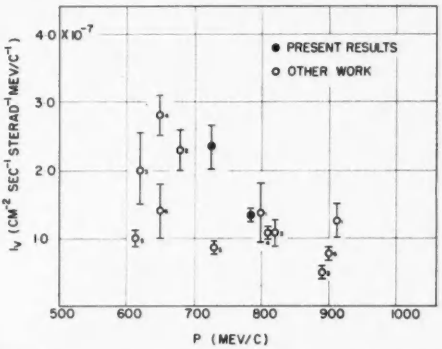

FIG. 3. Proton intensity vs. momentum. 1, Ballam and Lichtenstein (1954); 2, Merkle, Goldwasser, and Brode (1950); 3, Mylroi and Wilson (1951); 4, York (1952); 5, Filthüth (1955); 6, Ogilvie (1955).

agreement with values reported by Mylroi and Wilson (1951), York (1952), and Ballam and Lichtenstein (1954) while the point at 727 Mev/c supports the higher intensity values, being at least a factor of two higher than the measurements of Filthüth (1955).

The author wishes to thank Dr. D. C. Rose for the interest he has taken in this work.

BALLAM, J. and LICHTENSTEIN, P. G. 1954. Phys. Rev. **93**. 851.
FILTHÜTH, H. 1955. Z. Naturforsch. Pt. *a*, **10**, 219.
MCDIARMID, I. B. 1958. Phys. Rev. **109**, 1792.
MERKLE, T. C., GOLDWASSER, E. L., and BRODE, R. B. 1950. Phys. Rev. **79**, 926.
MYLROI, M. G. and WILSON, J. G. 1951. Proc. Phys. Soc. (London), A, **64**, 404.
OGILVIE, K. W. 1955. Can. J. Phys. **33**, 746.
YORK, C. M. 1952. Proc. Phys. Soc. (London), A, **65**, 559.

RECEIVED OCTOBER 9, 1958.
DIVISION OF PURE PHYSICS,
NATIONAL RESEARCH COUNCIL,
OTTAWA, CANADA.

Under this heading brief reports of important discoveries in physics may be published. These reports should not exceed 600 words and, for any issue, should be submitted not later than six weeks previous to the first day of the month of issue. No proof will be sent to the authors.

Nuclear Orientation of Cobalt-60 in Antiferromagnetic $Co(NH_4)_2(SO_4)_2.6H_2O$

We have prepared a single crystal of cobalt ammonium sulphate, containing about 5μc of Co-60, and weighing about 0.25 g. This crystal was cooled to approximately 0.05° K, in contact with potassium chromium alum, by adiabatic demagnetization. γ-Ray counters were placed along the K_1 and K_2 axes of the crystal to count the γ-rays emitted by the Co-60, and to determine the anisotropy of emission of the γ-rays. (For a detailed description of the crystallography of this salt, and of the techniques involved in nuclear orientation experiments, see Bleaney *et al.* (1954).) Anisotropies of up to 5½% were measured. A very similar experiment to this, using the antiferromagnetism of cobalt ammonium sulphate to produce nuclear alignment, was tried by a group at Leiden, Holland, in 1951, during the time when workers in this field were searching for a method of achieving nuclear alignment. This group reported a negative result (Poppema 1954); however, Poppema does not give enough detail for us to try to explain why a negative result should have been obtained. In view of this, we believe it is of value to describe our experimental arrangement and results.

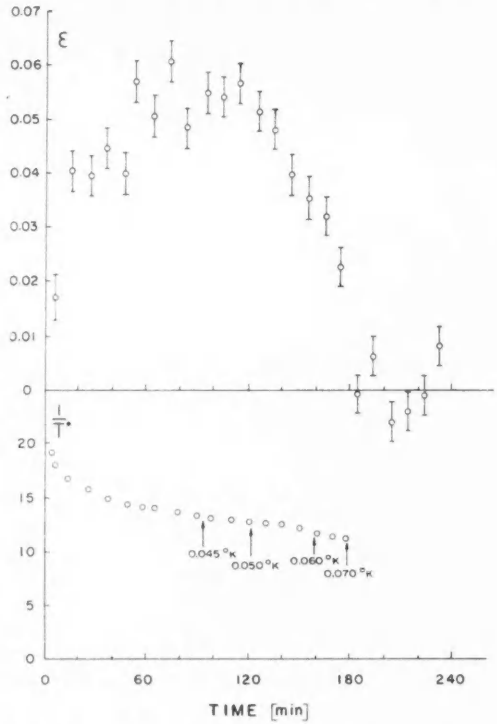

FIG. 1. After 180 minutes, the sample was warmed up to 1.3° K to obtain a normalizing count, which is shown.

To one side of a copper disk, 1 cm diameter, were soft-soldered 100 No. 36 B&S copper wires; surface area about 70 cm². This disk was placed in a pill press, potassium chromium alum powder was poured on to the wires, and the whole was compressed. This formed a cylinder of chrome alum, 1 cm diameter × 4 cm long, with a copper disk on one end. The wires, which stretched the whole length of the cylinder, served to conduct heat between the copper disk and the remote corners of the chrome alum. The crystal of cobalt ammonium sulphate was sandwiched between the copper disks of two such chrome alum cylinders, and thermal contact was provided between the disks and the crystal by means of Apiezon grease N. The whole sample was cooled by adiabatic demagnetization from a field of 21,000 oersted and an initial temperature of 1.3° K. The field was applied along the *a*-axis of the cobalt ammonium sulphate crystal, and was turned off slowly in a period of 4 minutes to avoid eddy current heating in the copper. The anisotropy of the γ-rays was measured in the usual way (Bleaney *et al.* 1954), and the temperature of the chrome alum was measured by the ballistic method.

The results of one experiment are shown in Fig. 1. It is seen that the anisotropy grows from zero, or almost zero, to about 5.5%, and then decreases as the whole sample warms up. If we assume that there is thermal equilibrium during the period while the anisotropy is decreasing (a debatable assumption which we do not wish to justify in this short communication) we can obtain values of anisotropy as a function of temperature. Such values are plotted in Fig. 2: the solid curve is the value of the anisotropy obtained from a paramagnetic Tutton salt (87% Zn, 12% Cu, 1% Co)$Rb_2(SO_4)_2.6H_2O$ (Bleaney *et al.* 1954). It is interesting to note

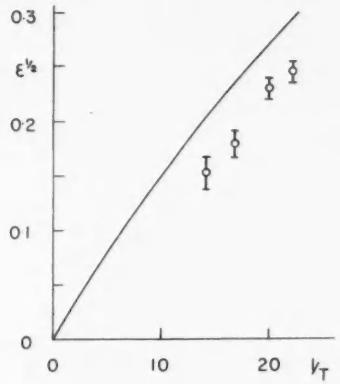

FIG. 2.

that the anisotropy is very nearly the same as is obtained in a paramagnetic salt. We can conceive of this if we admit that the electron "spin" of each ion is constrained to point along a definite crystal axis, the tetragonal axis of the crystalline field (Bleaney *et al.* 1954). The crystalline field and hyperfine coupling produce such a large anisotropy energy that the spin may point in either direction along this axis, but may not point at an angle to this axis. In the paramagnetic state, the direction of the spin of any one ion is decided at random, while in the antiferromagnetic case the direction is determined by the interaction. The anisotropy of γ-radiation does not depend on the direction of the electron spin.

Cobalt ammonium sulphate has been studied by Garrett (1951). According to his work, the crystal should have cooled to about 0.05° K immediately after demagnetization, and an anisotropy of 5.5% should have been noticed from the start. At the present time, we can offer no explanation why this is not so.

We wish to acknowledge the support of the National Research Council of Canada for this work. One of us (M.A.R.L.) is grateful for the award of an N.R.C. studentship during the tenure of which this work was carried out.

BLEANEY, B. *et al.* 1954. Proc. Roy. Soc. (London), A, **221**, 170.
GARRETT, C. G. B. 1951. Proc. Roy. Soc. (London), A, **206**, 242.
POPPEMA. 1954. Thesis, Groningen.

RECEIVED NOVEMBER 14, 1958.
DEPARTMENT OF PHYSICS,
UNIVERSITY OF BRITISH COLUMBIA,
VANCOUVER 8, B.C.

J. M. DANIELS
M. A. R. LEBLANC

Announcement on the International Yard and Pound

It would be appreciated if you would publish the enclosed announcement on the international yard and the international pound. The text is self-explanatory but it may be of interest to recall the following facts of local concern to Canada.

In 1951 "An Act Respecting Units of Length and Mass" (15 George VI, Chapter 31) defined the Canadian yard as 0.9144 meter, which is in exact agreement with the joint announcement. The same Act defined the Canadian pound as 0.45359243 kilogram which is slightly discrepant with the ratio being established for the International pound. This difference is insignificant in all measurements except those of the very highest precision. Nevertheless steps are being taken toward the amendment of the Canadian legislation to make the Canadian pound 0.45359237 kilogram and so legally equal to the International pound. The ratio 0.9144 was chosen because it leads to a yard which is approximately half-way between the present Imperial (United Kingdom) yard and the U.S. yard. It has the added advantage of making one inch exactly equal to 2.54 centimeters. The ratio used in the Canadian legislation of 1951 to relate the Canadian pound to the International kilogram was the originally accepted ratio between the pound and the kilogram. Through the years the Imperial (United Kingdom) pound and the U.S. pound have become very slightly different and the ratio used in the joint announcement makes the International pound approximately the average between the Imperial pound and the U.S. pound.

ANNOUNCEMENT

The Directors of the following standards laboratories:

Applied Physics Division, National Research Council, Ottawa, Canada
Dominion Physical Laboratory, Lower Hutt, New Zealand
National Bureau of Standards, Washington, United States
National Physical Laboratory, Teddington, United Kingdom
National Physical Research Laboratory, Pretoria, South Africa
National Standards Laboratory, Sydney, Australia

have discussed the existing differences between the values assigned to the yard and to the pound in different countries. To secure identical values for each of these units in precise measurements for science and technology, it has been agreed to adopt an international yard and an international pound having the following definitions:

the international yard equals 0.9144 metre;
the international pound equals 0.453 592 37 kilogramme.

It has also been agreed that, unless otherwise required, all non-metric calibrations carried out by the above laboratories for science and technology on and after July 1, 1959, will be made in terms of the international units as defined above or their multiples or submultiples.

Received December 16, 1958.
L. E. Howlett
Division of Applied Physics,
National Research Council,
Ottawa, Canada.

NOTES TO CONTRIBUTORS

Canadian Journal of Physics

MANUSCRIPTS

General.—Manuscripts, in English or French, should be typewritten, double spaced, on paper 8½×11 in. **The original and one copy are to be submitted.** Tables and captions for the figures should be placed at the end of the manuscript. Every sheet of the manuscript should be numbered. Style, arrangement, spelling, and abbreviations should conform to the usage of recent numbers of this journal. Greek letters or unusual signs should be written plainly or explained by marginal notes. Characters to be set in boldface type should be indicated by a wavy line below each character. Superscripts and subscripts must be legible and carefully placed. Manuscripts and illustrations should be carefully checked before they are submitted. Authors will be charged for unnecessary deviations from the usual format and for changes made in the proof that are considered excessive or unnecessary.

Abstract.—An abstract of not more than about 200 words, indicating the scope of the work and the principal findings, is required, except in Notes.

References.—References should be listed **alphabetically by authors' names,** unnumbered, and typed after the text. The form of the citations should be that used in current issues of this journal; in references to papers in periodicals, titles should not be given and only initial page numbers are required. The names of periodicals should be abbreviated in the form given in the most recent *List of Periodicals Abstracted by Chemical Abstracts*. All citations should be checked with the original articles and each one referred to in the text by the authors' names and the year.

Tables.—Tables should be numbered in roman numerals and each table referred to in the text. Titles should always be given but should be brief; column headings should be brief and descriptive matter in the tables confined to a minimum. Vertical rules should not be used. Numerous small tables should be avoided.

ILLUSTRATIONS

General.—All figures (including each figure of the plates) should be numbered consecutively from 1 up, in arabic numerals, and each figure referred to in the text. The author's name, title of the paper, and figure number should be written in the lower left corner of the sheets on which the illustrations appear. Captions should not be written on the illustrations.

Line drawings.—Drawings should be carefully made with India ink on white drawing paper, blue tracing linen, or co-ordinate paper ruled in blue only; any co-ordinate lines that are to appear in the reproduction should be ruled in black ink. Paper ruled in green, yellow, or red should not be used. All lines must be of sufficient thickness to reproduce well. Decimal points, periods, and stippled dots must be solid black circles large enough to be reduced if necessary. Letters and numerals should be neatly made, preferably with a stencil (**do NOT use typewriting**) and be of such size that the smallest lettering will be not less than 1 mm high when the figure is reduced to a suitable size. Many drawings are made too large; originals should not be more than 2 or 3 times the size of the desired reproduction. Whenever possible two or more drawings should be grouped to reduce the number of cuts required. In such groups of drawings, or in large drawings, full use of the space available should be made; the ratio of height to width should conform to that of a journal page (4¾×7½ in.), but allowance must be made for the captions. **The original drawings and one set of clear copies (e.g. small photographs) are to be submitted.**

Photographs.—Prints should be made on glossy paper, with strong contrasts. They should be trimmed so that essential features only are shown and mounted carefully, with rubber cement, on white cardboard, with no space between those arranged in groups. In mounting, full use of the space available should be made. **Photographs are to be submitted in duplicate;** if they are to be reproduced in groups one set should be mounted, the duplicate set unmounted.

REPRINTS

A total of 50 reprints of each paper, without covers, are supplied free. Additional reprints, with or without covers, may be purchased at the time of publication.

Charges for reprints are based on the number of printed pages, which may be calculated approximately by multiplying by 0.6 the number of manuscript pages (double-spaced typewritten sheets, 8½×11 in.) and including the space occupied by illustrations. Prices and instructions for ordering reprints are sent out with the galley proof.

Contents

Printed in Canada *by* University of Toronto Press